FREDERICO VASCONCELLOS GUATIMOSIM

# Influence of temperature on the mechanical behaviour and performance of foamed asphalt stabilized layers

São Paulo
2023

FREDERICO VASCONCELLOS GUATIMOSIM

# Influence of temperature on the mechanical behaviour and performance of foamed asphalt stabilized layers

Ph.D. Dissertation presented to the Escola Politécnica of the Universidade de São Paulo for the degree of Doctor of Science.

São Paulo
2023

FREDERICO VASCONCELLOS GUATIMOSIM

# Influence of temperature on the mechanical behaviour and performance of foamed asphalt stabilized layers

**Corrected version**

(Original version can be found in the unit that houses the Post Graduate Program)

Ph.D. Dissertation presented to the Escola Politécnica of the Universidade de São Paulo for the degree of Doctor of Science.

Research Area:
Transportation Engineering

Advisor: Prof. Kamilla Vasconcelos, Ph.D.

São Paulo
2023

Este exemplar foi revisado e corrigido em relação à versão original, sob responsabilidade única do autor e com a anuência de seu orientador.

São Paulo, ______ de ____________________ de __________

Assinatura do autor: ________________________

Assinatura do orientador: ________________________

Catalogação-na-publicação

Guatimosim, Frederico
Influence of temperature on the mechanical behaviour and performance of foamed asphalt stabilized layers / F. Guatimosim -- versão corr. -- São Paulo, 2023.
181 p.

Tese (Doutorado) - Escola Politécnica da Universidade de São Paulo. Departamento de Engenharia de Transportes.

1.Espuma de Asfalto 2.Reciclagem a Frio 3.Rigidez 4.Influência da Temperatura 5.Deformação Permanente I.Universidade de São Paulo. Escola Politécnica. Departamento de Engenharia de Transportes II.t.

# ACKNOWLEDGEMENTS

First and foremost, I would like to express my gratitude for my family and their continuous and unconditional support. My family is my bedrock, the foundation that allow me to achieve all the goals I set out to accomplish. I would like to thank my parents Henrique and Thereza Christina for raising me with the best education, with honesty and integrity. The journey so far wouldn't have been as pleasant and joyful without my sister with her words of encouragement and loving care. I'd like to thank my grandmother, Maria Thereza for the patience, life lessons and unshakeable belief in me. I would like to express my gratitude for my aunt Flavia, whom I have as a role model for life. Your everyday lessons and love are much cherished and a drive for my achievements. To my uncle Rodrigo, I would like to give special thanks, for the career guidance and countless lessons. My career road would have been much bumpier was it not for your help, motivation, and partnership.

The dedication for the research wouldn't have been possible without the help from Anselmo, my uncle Renato, and all my Copavel colleagues.

I would also like to express my appreciation for Prof. Kamilla Vasconcelos, my supervisor and friend, who has guided me along long years of research, with harsh and comforting words, whenever they were needed.

I would like to thank all my colleagues and the personnel from the Laboratory of Pavement Technology of University of São Paulo for their valuable support during my research. I'd like to specially thank Diomária, Edson, Robson, Erasmo and André Kazuo for all the help, discussions, instructions and insights along the process.

To all the colleagues from Ecorodovias, Arteris and CCR concession groups, I can only thank you for all the support with the trial sections, field monitoring and laboratory tests. A special thanks to Valeria Faria, Luis Miguel, Marcia, Geraldo, Cleto e José Carlos from CPR Laboratory.

At last, I'd like to thank Prof. Kim Jenkins and Prof. Allan Carter for the help, discussions and kind attention, that helped guide and shape this research.

# RESUMO

O crescimento da popularidade de técnicas de reciclagem a frio de pavimentos asfálticos foi motivado nas últimas décadas por suas características sustentáveis. A estabilização com espuma de asfalto é uma das técnicas em crescimento, produzindo uma mistura de comportamento granular, ao mesmo tempo em que exibe coesão devido ao ligante asfáltico adicionado e é suscetível à temperatura e frequência de carregamento. Este estudo tem como objetivo analisar a influência da temperatura no comportamento mecânico e no desempenho em campo de materiais estabilizados com espuma de asfalto. É apresentado uma revisão de diferentes métodos para o projeto de mistura e de estruturas com camadas estabilizadas com espuma de asfalto, mostrando que não há consenso sobre os procedimentos de projeto de mistura, nem para a abordagem usada para a previsão de desempenho. O comportamento mecânico é avaliado com FWD e testes de laboratório para cinco diferentes seções teste, com a realização de ensaios de caracterização do material, avaliação da cura ao longo do tempo e acompanhamento de sua resposta mecânica em pista. O efeito da variação de temperatura na rigidez do material é avaliado através de resultados de FWD e medições de temperatura in situ. O comportamento mecânico e o desempenho também são avaliados por meio de ensaios de Módulo de Resiliência, Módulo Dinâmico, ensaio Monotônico Triaxial e ensaios de deformação permanente de carga repetida. Os ensaios de caracterização em laboratório confirmaram a dependência do estado de tensões e comportamento viscoelástico enquanto os ensaios de deformação permanente mostraram influência tanto do estado de tensão quanto do efeito da temperatura, com pequenos incrementos de temperatura resultando em redução significativa no desempenho do material. O efeito da variação de temperatura nas respostas do material, avaliado através da análise mecanicista, é perceptível, mas a associação dessas respostas com o modelo de desempenho para deformação permanente levou a resultados contrários àqueles obtidos nos ensaios de laboratório.

**Palavras-chave**: Reciclagem a frio; Espuma de asfalto; Rigidez; Influência da Temperatura, Deformação Permanente.

# ABSTRACT

The growth in popularity of cold recycling of asphalt pavements has been motivated in the last decades for its sustainable characteristics. Foamed asphalt stabilization is one of the growing techniques, producing granular-like material behaviour, while also exhibiting cohesion due to the added asphalt, and being susceptible to temperature and loading frequency. This study aims to analyse the influence of temperature on the mechanical behaviour and the field performance of foamed asphalt stabilized materials. A comprehensive study of different methods used for mixture and structural design of foamed stabilized materials is presented, showing that there is neither consensus on the procedures for mixture design, nor on the approach used for the performance prediction. The material mechanical behaviour is evaluated using FWD data and laboratory tests for five different trial sections, with material characterization, evaluation of material curing over time and its mechanical response during service being presented. The effect of temperature variation on the stiffness of foamed asphalt stabilized material is evaluated using FWD data and in situ temperature measurements. The mechanical behaviour and performance are also evaluated using Triaxial Resilient Modulus Test, Monotonic Triaxial Test, Dynamic Modulus and permanent deformation tests. The laboratory tests show how foamed asphalt stabilized materials present both stress dependency and viscoelastic behaviour. The permanent deformation tests showed influence of both the stress state and the effect of temperature, with small temperature increments resulting in significant reduction in material performance. The effect of temperature is also evaluated through mechanistic analysis with the effect of temperature on material responses being noticeable, but the association of this responses with the existing performance model for permanent deformation led to divergent results when compared to the previous laboratory tests.

**Keywords**: Cold Recycling, Foamed Asphalt, Temperature dependent, Stiffness, Permanent Deformation.

# FIGURES LIST

# TABLES LIST

# TABLE OF CONTENTS

# 1 INTRODUCTION

Cold recycling of asphalt pavements has had a significant growth in recent years, highly motivated for its sustainable characteristic, but also due to its cost-effectiveness and increasing reliability. As the recycled material can be treated in different ways and used for both new pavement structures and rehabilitated sections, cold recycling has become a viable road paving option for a wide variety of conditions and applications.

The perspective of saving resources while optimizing production and operation has disseminated the technique, with different approaches and procedures being adopted in the mixture composition and structural design around the world.

The list of benefits generated by the use of cold recycling instead of traditional paving methods such as virgin aggregates and new material resources is well documented, and was well exposed by Stroup Gardiner (2011): (1) reduction on the use of new natural resources; (2) reduction on the amount of materials generated for disposal; (3) reduction on fuel consumption for both material production and transportation; (4) reduction on greenhouse gases emissions; (5) operational improvement through minimizing lane interdiction times; (6) elimination of overlay procedures, addressing deficiencies without the need of geometric adjustments to the road.

The recycled aggregate can be produced from a wide variety of sources, from Reclaimed Asphalt Pavement (RAP) to reclaimed granular layers, Construction Demolition Waste (CDW), crushed Cement Treated Base (CTB) and other reclaimed material.

Since this recycled aggregate is a product of deteriorated pavement layer, it often needs grading correction and additives to achieve the desirable performance standard.

Portland Cement, hydrated lime and bitumen are the most common agents used for cold recycling and stabilization of aggregates, and the choice of each one, as well as their proportions directly affect the behaviour of the final product. When Cement is used as additive for cold recycling, bonds are created between the aggregates by the hydrated crystals, providing an increase of the mix stiffness and brittleness, at the expense of reduced flexibility. Cement can be used as a complement to asphalt emulsion or foamed asphalt, accelerating the emulsion break and improving the mechanical properties of the mix, especially at the early stages (Yan et al. 2017). Cement also acts as active filler during the foaming process, improving asphalt dispersion throughout the mix (Schwartz and Khosravifar, 2013).

When asphalt binder is added, as it is highly viscous at ambient temperatures, it is usually used for cold stabilization in the form of asphalt emulsion or foamed asphalt. As asphalt is added, the material tends to gain cohesion, flexibility, and have a more viscoelastic behaviour.

## 1.1 RESEARCH PROBLEM IDENTIFICATION

The mixture composition of foamed asphalt stabilized materials has multiple possibilities, and therefore can produce different materials. Depending on the proportions and characteristics of different sources of aggregates, the added content and combination of the binding agents used, and stabilization process applied, the resulting recycled materials can have different mechanical behaviour.

Cardone et al. (2015) defined that cold recycled materials using foamed asphalt stabilization are either Bitumen Stabilized Materials (BSM) or Cement-Bitumen Treated Materials (CBTM). Due to the active filler being limited to 1%, BSM presents a stress-dependent behaviour, while CBTM might incorporate a higher cement/bitumen ratio, that will result in a more cohesive and stiff material.

Figure 1 presents how the material mechanical behaviour changes as either bitumen or cement are added to the mixture. The higher the bitumen content, more the mixture characteristics will approach that of an Asphalt Concrete. The more cement is added, the more the mixture will behave as cement treated material.

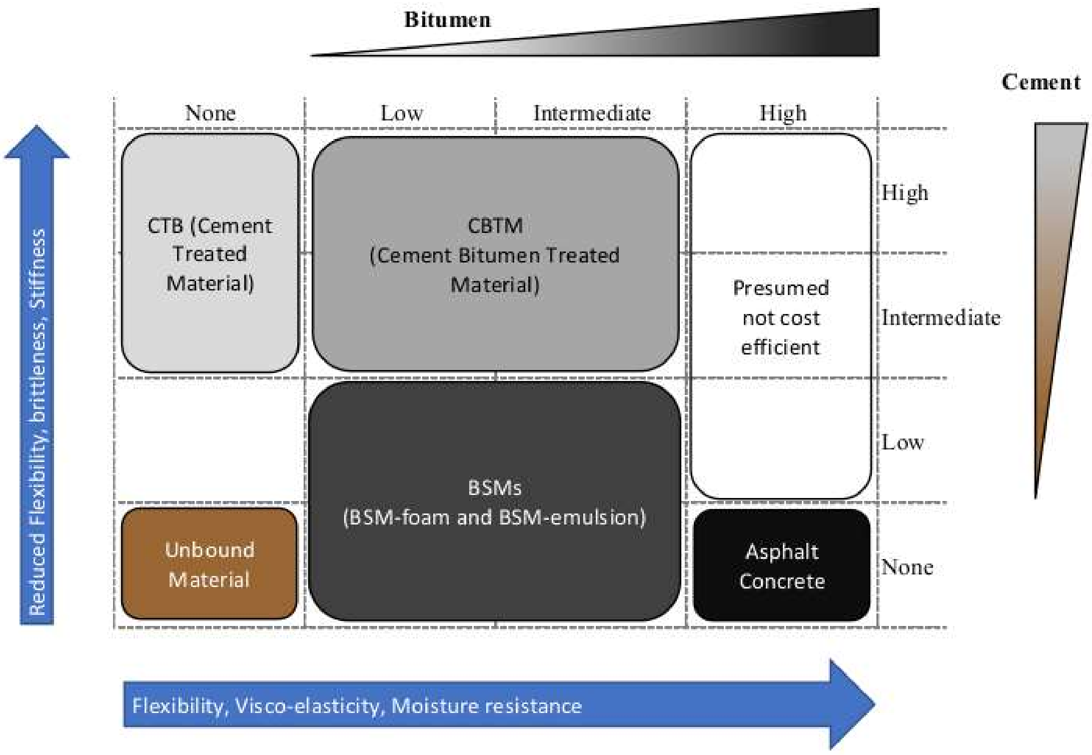


**Figure 1. Combination of cement and bitumen at different contents (adapted from Grilli et al. 2012).**

Although the effect of each additive is well documented, opinions diverge on mixture design procedures, and material composition (Brovelli and Crispino, 2012). As countries have diverse cultures and uneven availability of resources, cold stabilized materials are treated differently in terms of pavement design and construction.

Bitumen is not only added as a binding agent in recycled mixtures, but also as part of the RAP added as the aggregate. Although oxidized, the presence of asphalt involving the stone aggregates in the RAP may have impact on the viscoelastic behaviour of the recycled material, changing how the aggregates and bitumen binder interact within the mixture (Diefenderfer and Link, 2014).

Although BSMs are considered to present granular material behaviour, they still exhibit some cohesion due to the added asphalt, and its viscoelasticity makes it susceptible to temperature and loading frequency changes. This fact has been explored in BSM research associating it to HMA, but considering the material particularities, and its application in a country with high temperatures amplitude and different climate conditions, such as Brazil, the effect of changing temperatures on these materials become relevant.

Brazilian standards for foamed asphalt mixtures do not completely address the mixture and the pavement structural designs, using references based on national experience and international manuals from the 1990s and early 2000s. As a result, the technique is not well known across the country, nor is used in large scale. A study on how temperature can influence foamed stabilized mixtures behaviour and performance would give an important contribution for the growth of its application.

## 1.2 OBJECTIVES

The main objective of this study is to analyse the influence of temperature on the mechanical behaviour of foamed asphalt stabilized materials, allowing better understanding of its field mechanical performance and how it can be used in the design of pavement structures.

The specific objectives of this thesis are:

- Present a comprehensive literature review of the design of foamed asphalt stabilized mixtures and pavement structures as they are conducted around the world today.
- Evaluate the mechanical behaviour of foamed asphalt stabilized pavement in the field.
- Determine foamed asphalt material sensitivity to temperature change.
- Evaluate the influence of the temperature sensitivity of foamed asphalt materials on its mechanical response and permanent deformation performance.
- Analyse the structural behaviour of foamed stabilized materials in pavement structures and how that affects its service life performance.

## 1.3 DISSERTATION OUTLINE

This dissertation is organized in 7 chapters, developed in a format to allow chapters 2 to 6 to become separate papers, as described below:

Chapter 1 – Introduction of the studied subject, with the presentation of the research problem, objectives, and how the study is organized.

Chapter 2 – Pavement design of foamed asphalt stabilized mixtures. A comprehensive study of different methods adopted to design foamed stabilized mixtures and the life-performance of pavement layers.

Chapter 3 – Field evaluation of high level roads with foamed asphalt stabilized base layers. Presentation of different trial sections, its material characterization, material curing over time and its performance under service, using FWD data and laboratory evaluation.

Chapter 4 – Foamed stabilized material in situ temperature sensitivity. Using FWD monitoring and in situ temperature measurements on the pavement structure, this chapter present a study to determine material stiffness temperature sensitivity, and how it affects pavement behaviour.

Chapter 5 – Laboratory assessment of temperature effect on material performance. Using laboratory tests to characterize a BSM foamed asphalt mix, in terms of its material resistance to permanent deformation.

Chapter 6 – The Effect of temperature in the mechanistic analysis of foamed asphalt stabilized pavement structures. Using three different approaches for mechanistic analysis, foamed asphalt pavements are analyzed to evaluate the significance of the impact of temperature on pavement design and performance during service.

Chapter 7 – Final Considerations. Discussion of the research conclusions, the attainment of its objectives and suggestions for further research.

# 2 PAVEMENT DESIGN OF FOAMED STABILIZED MIXTURES

## 2.1 INTRODUCTION

Since the early 1910’s, experiences with pavement recycling have been recorded in the United States (Zelaya, 1985 apud Castro, 2003), while the first foam bitumen systems were recorded by Czanyi (1957 apud Macarone et al. 1993). Although the oil crisis in the 1970’s made the foaming technique less attractive due to the asphalt price rise (Macarone at al. 1994), Mobil Oil developed and improved different foaming systems since the 1960s into the early 1990s (Macarone at al. 1993), solving most of the clogging and pressure problems that delayed the expansion of the technology.

The first foam bitumen recycling project is attributed to Mobil Oil in the Australia during the 1960s (Austroads, 2018), although some authors indicate that it would have been conducted by the French company Jean Lefebvre in 1981 (Goacolau et al., 1996 apud Castro, 2003).

Since then, the technology associated with the foaming process has evolved substantially, with machinery becoming increasingly efficient, avoiding the clogging and early problems that delayed its development.

Foamed mixtures can have different behaviour and performance, ranging from granular materials to high quality asphalt materials (Plati et al. 2010), hence many different approaches have been taken to describe its mechanical behaviour. Some procedures have drawn similarities between it and Hot Mix Asphalt (HMA), especially when using Reclaimed Asphalt Pavement (RAP) as primary aggregate source, due to the nature of the mix regarding its residual asphalt content. On the other hand, other procedures have tended to dissociate cold stabilized bitumen mixes from HMA, defining less rigorous performance parameters for such mixes.

The objective of this chapter is to provide a literature review on different methodologies applied around the world for the mix design and structural design of foamed stabilized materials, from Brazilian experiences to international standard procedures. This chapter presents different methods and procedures used for the design of foamed asphalt stabilized mixtures around the world, and the design of pavement structures containing these mixtures. In this sense, a comparison between the methodologies was done highlight the existing differences and its implications on the material mechanical behaviour.

## 2.2 LITERATURE REVIEW

### 2.2.1 Foamed Asphalt Mixtures in Brazil

Although there is no specific indication on how cold bitumen stabilized materials should be considered for structural design, there are different specifications for foamed bitumen stabilized layers in Brazil.

The Brazilian National Department of Transportation is a reference in all the country and has two different specifications for in plant (DNIT ES 169/2014) and in situ (DNIT ES 166/2014) recycling procedures, with foamed bitumen stabilized material parameters and characteristics defined within it. Regarding the material characteristics, both specifications indicate only the mixture grading limits, and the minimum resistance for Indirect Tensile Strength (ITS) test using Marshall compacted samples, cured for 72 hours at 40°C. The foamed material should reach a minimum ITS of 0.25 MPa for the dry condition and a minimum of 0.15 MPa for the soaked condition. There is no specified range for bitumen, cement or lime content, which makes the mix design based solely on ITS results and grading, independent of aggregate source and binder used.

The city of São Paulo has its own specification for in plant recycling of foamed asphalt layers (PMSP ETS-02/2009), where it defines a gradation curve, minimum ITS resistances, and detailed ranges for material gradation. The specified mixture is required to have at least 75% RAP, foamed asphalt incorporation from 2% to 4% and active filler (lime or cement) addition of 1% to 2% by weight. The minimum ITS values for both dry and soaked Marshall specimens is set as 0.28 MPa, and 0.20 MPa, respectively, with a minimum

Tensile Stress Retention (TSR) of 70% (relation between soaked and dry ITS resistances). The curing procedure defined is also different, requiring specimens to be kept for 72h at 60°C, instead of 40°C.

Some of the state transportation departments in Brazil have their own specifications and procedures, including the Department of Transportation of the State of São Paulo, and the Department of Transportation of the State of Paraná that have very similar procedures for in situ recycling of foamed asphalt materials (DER-SP ET-DE-P00/033-2006; DER/PR ES-P 32/05).

Both specifications present gradation limits and determine the same minimum ITS values for both dry and soaked Marshall specimens, 0.40 MPa, and 0.20 MPa, respectively. Also, the two specifications determine the recommended active filler addition percentage to be 1% and should not surpass 2%, while the optimum binder content for the mix design be between 2% and 4%.

Although there are multiple specifications, there is no specific standard or recommendation on how to consider foamed asphalt layers in pavement design.

The traditional flexible pavement design procedure in Brazil is based on the CBR Design Procedure. It was developed in the early 1960's and was updated in 1981, with the inclusion of a minimum asphalt layer thickness depending on the expected traffic (Balbo, 2007). The method uses an equivalent thickness approach, attributing different coefficients to each material, so a total thickness can be defined to protect the subgrade. Foamed asphalt mixes are not referred to in this method hence no coefficient is defined for such material.

More recently, the DNIT has adopted a mechanistic-empirical (ME) approach for its new projects, using the new national design method called MEDINA and its homonymous software (DNIT IS-247/2021). Since the new ME method is under continuous improvement, there has not been yet any clear indication as to how foamed asphalt mixtures and other recycled materials should be considered for pavement structural design. Since neither structural design parameters nor indications on how to analyse the distress and failure criteria are defined for foamed asphalt layers, all design parameters are left to the pavement design engineers' consideration.

### 2.2.2 Transportation Research Laboratory (TRL) – United Kingdom

The Design Manual for Roads and Bridges (DMRB) is the standard protocol adopted in all United Kingdom and is signed by the respective road authorities of England, Scotland, Northern Ireland and Wales. This manual defines in its Volume 7, Section 2, Part 3 (DMBR HD 26, 2006) the standard pavement structures that could be considered based on road relevance, traffic magnitude and pavement foundation class (related to the subgrade stiffness). The manual also defines that “alternative pavements”, the ones that include cold recycled layers such as foamed asphalt materials, should be designed according to TRL 611 (Merrill et al. 2004).

The design procedure TRL 611 (Merrill et al. 2004) was developed by the Transportation Research Laboratory (TRL) and is a comprehensive design guide for different cold recycled materials. It creates distinction among different recycled mixes defined as Quick Hydraulic (QH) to Slow Hydraulic (SH), Quick Viscoelastic (QVE) and Slow Viscoelastic (SVE), as presented in Figure 2.

Figure 2 shows different combinations of hydraulic binders (e.g., cement, hydrated lime, granulated blast furnace slag, fly ash) and asphalt binder, from unbound to fully bound materials. The materials are defined by their existing binding agent, as detailed below:

- QH when the only binder is cement;
- SH when the mix has a hydraulic binder but that one not being cement;
- QVE when the mix has both asphalt binder and hydraulic binder, including cement;
- SVE when the mix has both asphalt binder and hydraulic binder, excluding cement.

For bituminous bound mixtures, such as QVE and SVE, the minimum amount of bitumen, cement and lime content is 3.0%, 1.0% and 1.5% for in plant produced recycled mixtures and 4.0%, 1.0% and 2.5% for in situ produced mixtures.

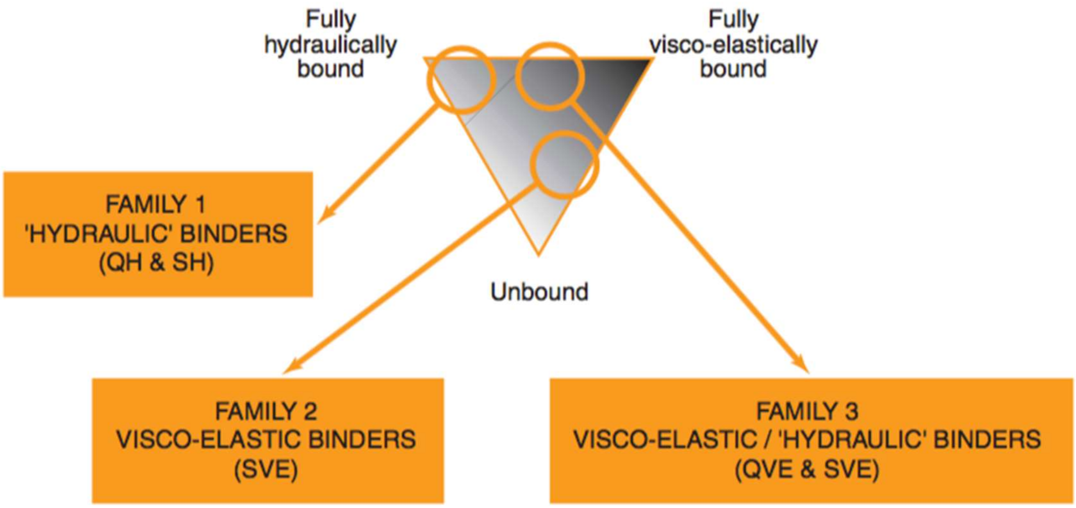


**Figure 2. Identification of material families (Merrill et al. 2004)**

The mixture design recommended by the TRL 611 guide was developed by Milton and Earland (1999), although other design methods can be used upon detailing and fulfillment of material requirements.

The bituminous bound recycled mixes, such as SVE and QVE, which can be foamed mixtures, are requested to comply to specific gradation limits and be tested for Indirect Tensile Stiffness Modulus (ITSM). The cured specimens must have ITSM of the order of 1900 MPa to 3100 MPa, resulting in a mixture classification B1 to B3, respectively. Curing is defined by Milton and Earland (1999) as 72 hours at 60°C but it is recommended by Merrill et al. (2004) that the curing process should be conducted for all mixture families at 20°C and 40° for 28 days so long-term stiffness can be assessed.

During the research that resulted in TRL 611 guide, Nunn and Thom (2002) pointed out that foamed bitumen stabilized mixtures are unlike standard HMA. However, it was shown that in plant produced foamed mixtures were susceptible to fatigue, and therefore could be treated in similar manner to HMA.

The TRL 611 addresses pavement design method to determine the pavement's structural need, in terms of its foundation condition, traffic level, and defines a minimum allowed thickness for the designed layer based on the recycled mixture classification, using design curves such as the one presented in Figure 3.

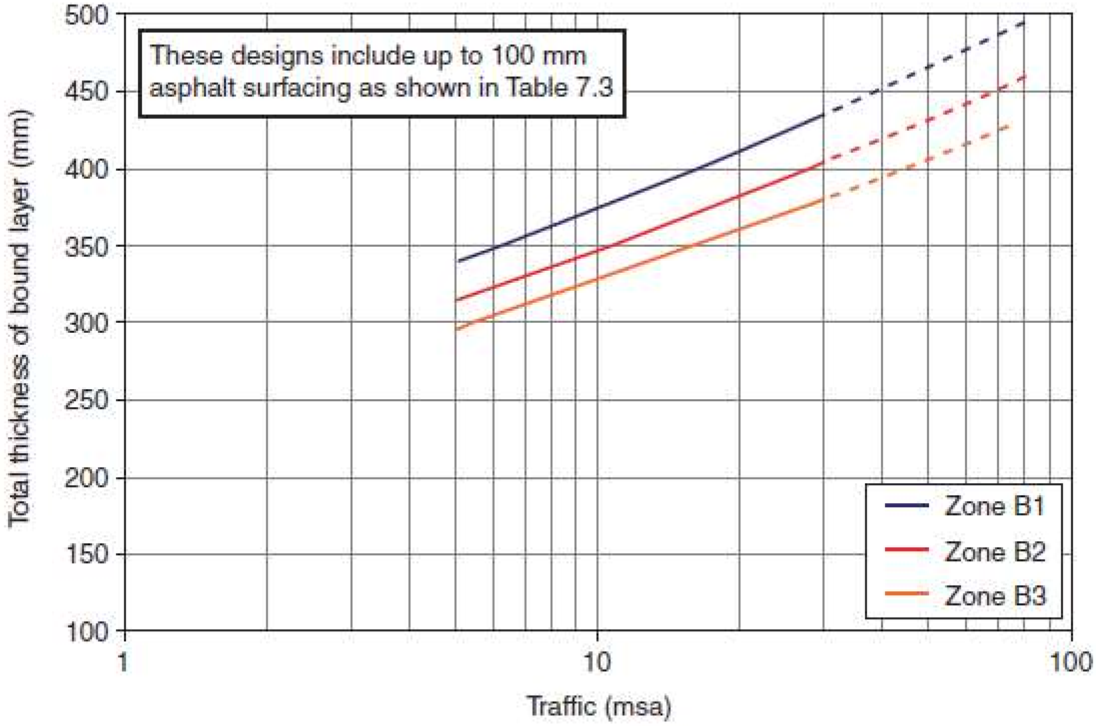


**Figure 3. Example of design curves for bitumen bound cold recycled material for a Foundation Class 1 according to Merrill et al. (2004).**

### 2.2.3 Austroads 2018 - Department of Transport and Main Roads (TMR), Queensland – Australia

The procedure developed by the Department of Transport and Main Roads of the Queensland Province, in Australia, uses Foamed Bitumen Stabilized materials with the incorporation of 3.0% to 4.0% of foamed bitumen and 1.0% to 2.0% of active filler, usually lime or hydrated lime, aiming for a higher fatigue performance, without compromising the mixture rut resistance (Ramanujam and Jones, 2007; TMR 2012).

The procedure has detailed information on the mixture composition and performance parameters, using Indirect Tensile Resilient Modulus (ITRM) as the usual method to characterize the material. The materials behaviour is considered according to have to two distinct phases, before cracking, as a cohesive layer, and after cracking, as a granular material would (TMR, 2012).

The minimum limits defined for ITRM are set between 2.500 and 4.000 MPa for dry condition and 1.500 and 2.000 MPa for soaked conditioned specimens, which are stiffness values that could be expected for HMA mixes.

For the design of pavement structures containing foamed asphalt layers, the material is evaluated in terms of its volumetric properties, its stiffness, and the tensile strain at the bottom of the layer. These parameters are considered in the equation (2.1), and they are related to the admissible number equivalent single axle of loads until the material fatigue (Austroads, 2011).

$$N_f = \left[\frac{6918\times(0.856V_b+1.08)}{S_{mix}^{0.36}\mu\varepsilon}\right]^5 \tag{2.1}$$

where: $N_f$ = the allowable number of equivalent single axle load repetitions until fatigue failure;

$V_b$ = foamed asphalt binder percentage by volume in the mixture;

$S_{mix}$ = mixture stiffness (ITRM) MPa;

$\mu\varepsilon$ = tensile strain at the bottom of the layer (microstrains);

In the post cracking phase, the material is expected to behave as a granular material, with a pre-defined expected resilient modulus of 500 MPa for any mixtures.

Based on the experiences using ITRM as a primary performance related parameter, Austroads developed the mixture design and structural design procedure (Austroads, 2018).

Extensive research was made to understand the details of the material characterisation and performance. The effect of moisture content, additive type and compaction method on the resilient modulus was studied, revealing how sensitive the material was to this parameter. As an example of this sensibility, it was estimated that for a 1% increase in density the material would increase modulus in 12% (Austroads, 2018).

Continuous monitoring of field performance allowed for comparisons and evaluation of the condition in which the material spends its service life, giving insights on how to improve the mix design procedures.

The Austroads Guide to Pavement Technology Part D (2019) details the mixture design procedure, including the definition of gradation limits, test protocols and performance standards, including different material requirements depending on the average Equivalent Single Axle (ESA) for the initial year of service, and long term traffic prediction. To better characterise the field performance during mixture design, the compaction, curing and testing procedure was slightly modified. All ITRM tests should be performed on 152mm diameter samples compacted with 50 blows of the 1.2kg Marshall hammer on each face of the specimen.

The ITRM tests were defined to be required with three different curing processes:

- After 3 hours curing at 25°C to determine the initial indirect tensile resilient modulus;
- After 3 days at 40°C to determine the cured indirect tensile resilient modulus;
- After 3 days at 40°C and 10 minutes soaked in a vacuum chamber at partial vacuum (95 kPa under local atmospheric pressure) to measure the soaked indirect tensile resilient modulus.

The mixture design is considered adequate if the ITRM tests achieve the minimum modulus presented in Table 1.

**Table 1. Minimum modulus values for ITRM tests (adapted from Austroads, 2018)**

| Layer | Average daily ESA in design year of opening | Min. initial ITRM (MPa) | Min. 'cured' ITRM (MPa) | Min. 'soaked' ITRM (MPa) | Min.retained modulus ratio |
|---|---|---|---|---|---|
| Base | < 100 | 500 | 2500 | 1500 | 0.40 |
| | 100 - 1000 | 700 | 3000 | 1800 | 0.45 |
| | > 1000 | 700 | 4000 | 2000 | 0.50 |
| Subbase | < 100 | 500 | 2500 | 1500 | 0.40 |
| | 100 - 1000 | 700 | 2500 | 1500 | 0.45 |
| | > 1000 | 700 | 2500 | 1500 | 0.50 |

For pavement structural design, the method adopts equation (2.1) as previously described. However, the mixture stiffness (Smix) was substituted by a Design Modulus of the Foamed layer (E),which is the result of ITRM test soaked modulus corrected for the weighted mean annual pavement temperature (WMAPT) (Fu and Harvey, 2007) as described in equation (2.2).

$$E = F_T \times S_{mix} \leq 2{,}500\ MPa \qquad (2.2)$$

where: $F_T$ = Temperature correction factor, as defined in Table 2;

**Table 2. Temperature correction factors for the design modulus of Foamed Asphalt Layers (adapted from TMR ,2012)**

| WMAPT (°C) | $F_T$ |
|---|---|
| ≤ 25 | 1 |
| 30 | 0.9 |
| 35 | 0.8 |
| 40 | 0.7 |

### 2.2.4 City of Canning – Australia

Since the beginning of the 2000's, extensive work and research have been done in the City of Canning on foamed bitumen stabilization (Leek, 2001). As a result, a report was published in 2010 reviewing the performance of in situ Foamed Bitumen Stabilized pavements (Leek, 2010).

In this report, a new fatigue model was presented to design and assess the performance of foamed bitumen layers, which are primarily used as pavement base layers. Flexural fatigue is defined as the primary mode of distress for the material, based on flexural beam fatigue tests results.

The mixtures used for the tests were all designed and prepared with similar binder contents, ranging from 3.5% to 4.0%, with the addition of around 1% of Portland cement or either hydrated lime or quicklime ranging from 0,8% to 2,0%.

Differently than the model presented for the Queensland TMR, no volumetric properties, nor the mixture stiffness are used in the fatigue model, even though the characteristics required for the materials used on both the Canning procedure and the Queensland procedure are similar. equation (2.3) presents fatigue life model as a function of the tensile strain.

$$N_f = \left( {}^{1558}/_{\mu\varepsilon} \right)^6 \qquad (2.3)$$

where: $N_f$ = the allowable number of load repetitions with strain level $\mu\varepsilon$, considering the material fatigue failure;

$\mu\varepsilon$ = tensile strain at the bottom of the layer (microstrains) applied by 80 kN axle load;

### 2.2.5 New Zealand Transport Agency – New Zealand

Contrary to the design methodologies practiced in the United Kingdom and Australia, the procedure adopted by the New Zealand Transport Agency (NZTA) does not consider fatigue as the main distress mode (Alabaster et al., 2013).

No specific procedure is defined for mixture design, with Indirect Tensile Strength and Unconfined Compressive Strength (UCS) suggested as parameters that should be defined by the structural designer (Auckland Transport, 2013).

It is important to observe that mixtures used have 2.7% to 3.0% of asphalt content, and around 1.0% of cement on its composition. In contrast, the other procedures previously described recommend a foamed asphalt content that can reach 4.0%, and up to 2.0% of active filler, resulting in high cohesion and stiffness (Austroads, 2011).

Alabaster et al. (2013) state that it is unclear whether the fatigue life occurs in the foamed asphalt stabilized materials, and therefore only the equivalent granular phase is accounted for the design. Once foamed material is considered as granular, the primary mode of failure is permanent deformation, and the mechanistic verification is done analysing the vertical strain on top of the subgrade with the Austroads subgrade strain criterion (Austroads, 2011), as shown in equation (2.4):

$$N_{pd} = \left({}^{9300}/_{\mu\varepsilon_v}\right)^7 \quad (2.4)$$

where: $N_{pd}$ = the allowable number of standard axle loads, considering material permanent deformation;
$\mu\varepsilon_v$ = the maximum vertical strain at the top of the subgrade;

For the mechanistic pavement design, it is recommended that foamed bitumen layer should be considered to have an Elastic Modulus of 800 MPa, with poison's ratio of 0.30 and that the analysis should consider the layer as anisotropic, with an elastic moduli ratio of $E_{vertical}=2E_{horizonal}$ (Austroads, 2011).

### 2.2.6 TG2 2009 – Structural Design Method – South Africa

In its first edition, published in 2002, the Technical Guideline 2 (TG2) presented a study based on a series of pavement structures using Bitumen Stabilised Materials (BSM), both emulsion or foamed bitumen, with trial sections subjected to Heavy Vehicle Simulator (HVS) accelerated testing (Asphalt Academy, 2002).

This research allowed for the development of material performance models, which considered its behaviour to be divided in two phases. These two phases, similar to what is considered for the Queensland procedure, are divided in (i) a cohesive phase, when the material is subject to fatigue failure, and (ii) an equivalent granular phase, when the materials primary mode of distress is permanent deformation (Asphalt Academy, 2002). As the performance model was being validated by the industry, questions were raised about its reliability on correctly predicting the real field performance. To answer these questions, new research was conducted, resulting in the in a newer version of the guide, published in 2009 (Austroads, 2011).

It was found that the mixtures that based the 2002 study were mostly designed with approximately 2.0% of cement, and that much of the cohesive behaviour that resulted in fatigue failure was a result of the high cement content. Although a higher cement content would give a higher mechanical resistance, it would also make the material stiffer, more brittle and less flexible, thus subject to fatigue failure. For that reason, the 2009 edition of the TG2 limited the active filler addition to 1.0%, guaranteeing that the asphalt non-continuous bonds would remain predominant in the BSM mixture. The BSM was then defined to behave as a granular material, because of the dispersed and fragile bitumen bonds, but with smaller susceptibility to moisture damage and higher cohesive strength (Asphalt Academy, 2009).

The guide recommends binder contents for foam and emulsion applications ranging from 1.5% to 3.0%, depending on whether it is a coarse well graded mixture or fine graded and soil stabilization. That represents a contrast when compared to common bitumen rates applied in Australia and the United Kingdom, indicating a divergence in the approach to the mixture design and therefore its structural behaviour.

The TG2 guide classifies BSM from higher to lower performance standpoint, as BSM 1, BSM 2 or BSM 3, depending on its material composition, characteristics, and mechanical properties. The mixture design procedure uses ITS tests to define bitumen binder content. The tests are conducted in 152 mm diameter specimens, compacted at Modified AASHTO compaction effort, with Proctor hammer blows or its own Vibratory Hammer procedure (Jenkins and Kelfkens, 2008). For the material classified as BSM 1, optimum binder content is then defined as the smaller bitumen content that provides the specimens with 225 kPa ITS for dry samples and 100 kPa for soaked samples. Curing should be done at 40˚C for 72h or until the specimens reach constant mass, then part of the specimens should be soaked for 24 hours at 25˚C.

The proposed structural design procedure is the Pavement Number Design method, which is defined as a knowledge-based structural design method. The Pavement Number (PN) is an index calculated for each designed pavement structure based on its material properties and thicknesses, so that a minimum required PN is achieved based on the traffic demands and the desired reliability. The graph presented in Figure 4 shows how PN is related to the reliability and the design traffic, being Category A 95% reliability, and Category B 90%. The design traffic is expressed in Million Equivalent Single Axles (MESA).

The knowledge-based procedure was based on three data sets (briefly described below), which provided historical information on pavement performance, and a proposition for pavement behaviour rules (Jooste and Long, 2007).

The Technical Recommendation for Highways Design Catalogue (CSRA, 1985) was the first data set, providing 17 selected pavement structure for Category A and B roads (reliability of 95% and 90%, respectively) defined for design traffics ranging from 1 to 30 MESA. These structures had been used extensively throughout the country and were used for climate factor calibration and the determination of material constants such as modular ratios and reference stiffness values.

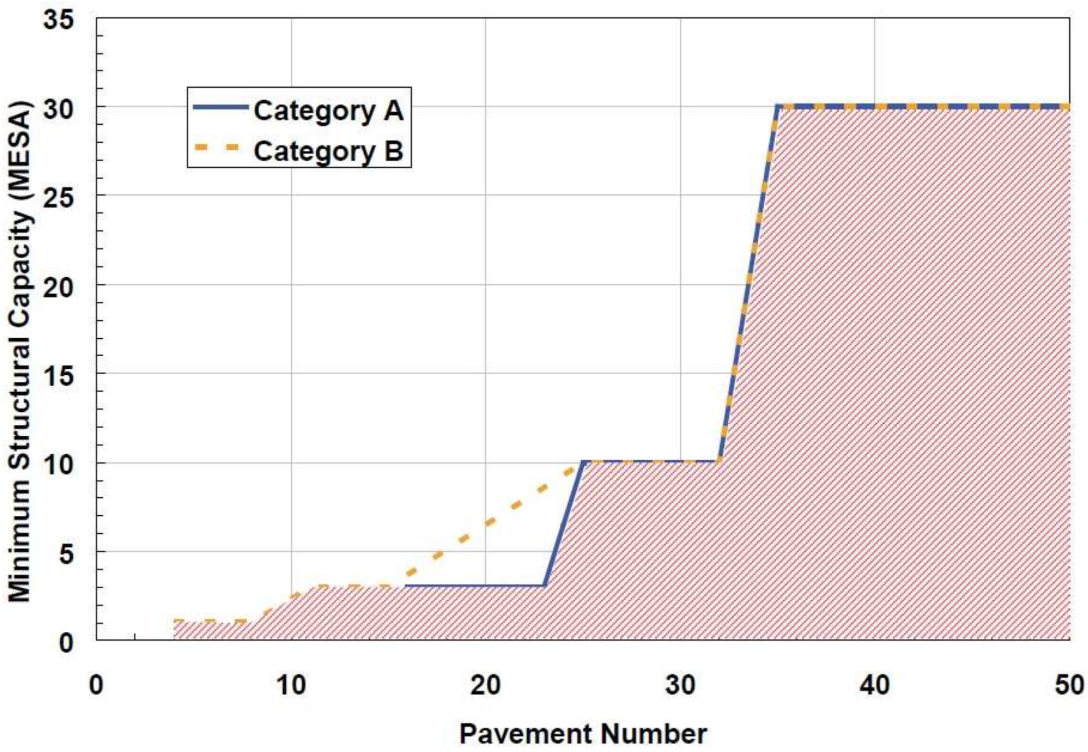


**Figure 4. Criteria for Determining Allowed Capacity from PN (Asphalt Academy, 2009)**

The information contained in the Long-Term Pavement Performance (LTPP) program for bitumen stabilized pavements was used as the second data set. The performance data provided historic insight into 25 roads for which long term performance of bitumen stabilized materials could be assessed, associating specific traffic ranges and climatic conditions to reliable in-service structures.

The third data set was based on the HVS test results conducted on 15 pavement configurations, including bitumen stabilized pavements, so that material performance and distress could be observed in real scale.

The information gathered from the three sets allowed for the definition of the Effective Long-Term Stiffness (ELTS) concept, in which the materials design stiffness is defined as the average of its long term in situ stiffness (Asphalt Academy, 2009). Based on the characteristic of the designed material and its underlying support layer, the realistic ELTS can be calculated. For cohesive materials, the influence of its support will have little impact on its initial stiffness, but a greater influence for the layers long-term performance and distress. To account for that, different modular ratios are considered for ELTS calculation, relating the layer stiffness to that of its support material. As a result, the ELTS of each layer is calculated as the product of the materials modular ratio and the underlying layers stiffness, limited to a pre-defined maximum ELTS value for each material type. The maximum defined ELTS for BSM 1 is 600 MPa, with materials classified as BSM 2 and 3 having smaller maximum ELTS.

Figure 5 shows a flow chart of the design procedure, indicating each step. For structural verification of a defined structure, the subgrade ELTS is defined first, based on its characteristics, climatic conditions, and designed pavement thickness (cover thickness). Then, ELTS can be calculated for each of the overlying layers from bottom to top considering its pre-defined maximum stiffness, its modular ratio and the stiffness of the immediate underlying layer.

Based on the layers ELTS and thickness, an individual Pavement Number (PN(i)) is calculated as the layer contribution. Each layer PN(i) is then summed to account for the structure PN, that is then related to the minimum structural capacity, defined in terms of traffic in MESA, using Figure 4. However, this design method is restricted to roads with design traffic smaller than 30 MESA.

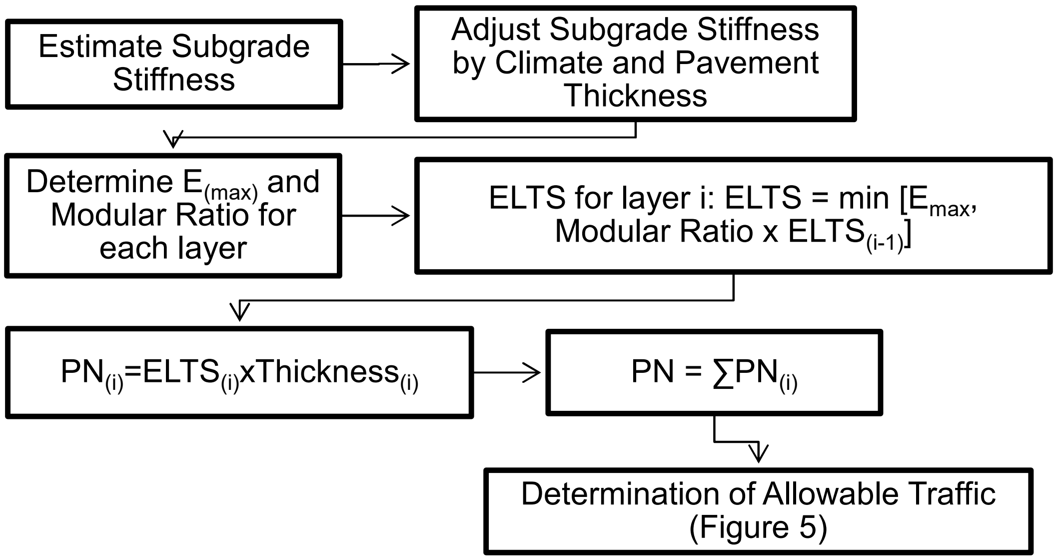


**Figure 5. Flow chart of the PN design methodology (adapted from Austroads, 2011)**

### 2.2.7 TG2 2020 AND SAPEM 2014 – South African Pavement Engineering Manual

Although the Pavement Number method can be used for the design of new BSM structures (SABITA, 2020), The South African Pavement Engineering Manual (SAPEM) presents the mechanistic pavement design approach. The Manual serves as a reference for all aspects of pavement engineering, subdivided in 14 chapters (SANRAL, 2014). Chapter 10 is called Pavement Design, and it discusses different aspects of the design process, from traffic evaluation to structural capacity determination and economic assessment.

It also describes The South African Mechanistic-Empirical Design and how BSM layers should be considered. The design method analyzes each layer composing the pavement, evaluating the material to assess its stresses and strains under loading at critical points, as shown in the pavement structure exemplified in Figure 6.

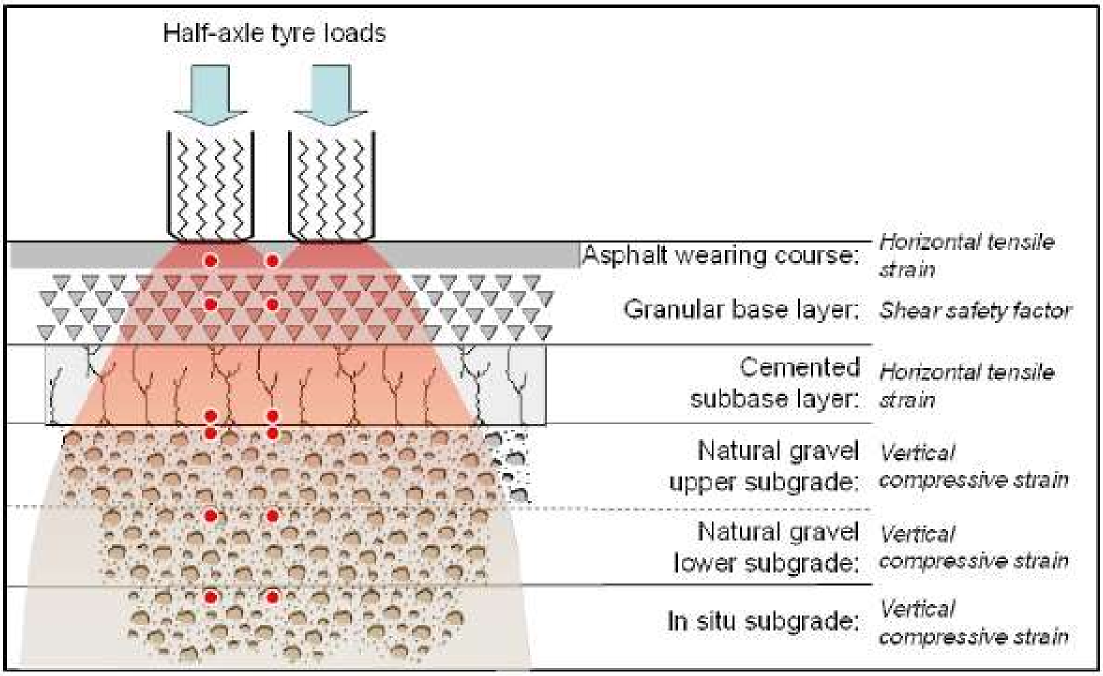


**Figure 6. Position of analysis for each layer and evaluation parameter (SANRAL, 2014)**

For BSM layer analysis, as it is considered to behave as a granular material, the stress state evaluation should be done similarly. Their primary criterion for failure criterion is permanent deformation, and for that assessment, a transfer function relating the allowable number of load repetitions to its stress state is used.

To analyze the stress state of the material under loading, the method uses a Stress Ratio, that can be represented in terms of the major principal stresses acting on the evaluated point of the layer. The Deviator Stress Ratio is derived from the Mohr Coulomb theory, allowing to draw a relationship between material shear parameters (cohesion and internal friction angle), and major principal stresses under loading (Theyse et al., 1996). The Stress Ratio can be calculated for BSM layers using equation (2.5):

$$DSR = \frac{(\sigma_1 - \sigma_3)}{\sigma_3\left[K\left(\tan^2\left(45+\frac{\phi}{2}\right)-1\right)\right]+2C\tan\left(45+\frac{\phi}{2}\right)} \qquad (2.5)$$

where: DSR = Deviator Stress Ratio;

$\sigma_1$ and $\sigma_3$ = Applied major and minor principal stresses;

C = Cohesion;

ϕ = Internal Friction Angle (degrees);

The stress ratio obtained from the analysis of the material under loading can be related to the allowable number of load repetitions using a transfer function. Although no transfer functions for BSM materials is presented in the SAPEM, two equations are commonly used in South Africa.

The first is referred to as the Loudon Transfer Function, which was developed from the Waterbound Macadam model proposed by Theyse et al. (2000) as a design tool based on the performance of numerous BSM pavement structures on five continents (Bierman, 2018). The test setup and procedure used to define the shear properties of the BSM mixture is defined my Mulusa (2009) and allows for the determination of Mohr Coulomb envelopes through Monotonic Triaxial Tests.

Although it was extensively used in South Africa, specially by Loudon International Consultants, this equation had not been published, hence minimal information being available about its calibration and verification. The Loudon Transfer Function is presented in equation (2.6):

$$N = 10^{(1.55+0.1(RD)+0.05(RetC)+0.1(PS)-2\ \ .333(SR))} \qquad (2.6)$$

where: N = the allowable number of load repetitions;

RD = relative density of the material, compared to its maximum density (%);

RetC = Retained Cohesion obtained from Monotonic Triaxial Tests (%);

*PS* = allowed plastic strain (%);

SR = deviator stress ratio as presented in equation (2.5);

The second transfer function is an update of the Loudon Transfer Function, with the substitution of the Relative Density term for the Modified AASHTO density term, adjustment and calibration of the transfer Function and the incorporation of a reliability term (Bierman, 2018). This transfer function was first introduced by Bierman (2018) and then published in the latest version of the TG2 (SABITA, 2020).

This transfer function calibration used data from fourteen pavement structures that composed the LTPP study, and a trial section from the N7 highway, near

Cape Town. The LTPP data was mainly comprised by pavement structures, and a series of FWD and rutting measurements, while N7 information additionally provided Monotonic Triaxial Tests and Triaxial Repeated Loading Tests.

Then, the calibrated function was adjusted based on existing data to predict the performance of BSM materials in a range of reliability of 95%, 90%, 80% and 50%. Equation (2.7) present the New Transfer Functions:

$$logN = A - 57.286(DSR)^3 + 0.0009159(P_{mod}.RetC) + 0.086753(PS) \qquad (2.7)$$

where: N = the allowable number of load repetitions;

$P_{mod}$ = material density in terms of its Modified AASHTO density (%);

RetC = Retained Cohesion obtained from Monotonic Triaxial Tests (%);

*PS* = allowed plastic strain (%);

DSR = deviator stress ratio as presented in equation (2.4);

A = Reliability adjustment term, as described in Table 3:

**Table 3. New BSM Transfer Function reliability factors (adapted from Bierman, 2018)**

| Reliability | A |
|---|---|
| 50% | 1.1369 |
| 80% | 1.0198 |
| 90% | 0.9312 |
| 95% | 0.8436 |

### 2.2.8 Foamed Asphalt materials in the United States Of America

Road authorities in the United States of America (USA) are very independent, which results in each Department of Transportation (DOT) adopting or creating its own specifications and procedures.

Schwartz and Khosravifar (2013) presented in a study for the Maryland DOT, a summary of 12 different road authorities specifications for foamed asphalt stabilized materials, including the Federal Highway Administration (FHWA), comparing gradations, curing procedures, compaction methods and minimum ITS values. The study showed that similar parameters were used for foamed asphalt material mixture design, including: (i) the Marshall compaction method; (ii) the curing procedure at 40°C for 72 hours, or until constant mass; and (iii) the use of ITS and TSR for optimum asphalt content determination.

Asphalt and active filler (cement or hydrated lime) contents are mostly determined by the results of ITS tests and the local authority's minimum strength requirements. These requirements can vary from 150 kPa to 345 kPa for ITS soaked, which associated with the minimum TSR values of 50% to 70%, can result in minimum ITS values of 300 kPa to 490 kPa for dry samples. The authors indicate that usual cement content is 1,0%, and that asphalt contents should range from 2,0% to 3,5%.

The most common method utilized in the USA for the design of pavement structures is the Structural Number method presented in the 1993 AASHTO Design Guide (Díaz-Sanchez et al., 2017), which is still being used by a number of DOTs even though AASHTO has released its new Mechanistic-Empirical method (Sabouri and Dave, 2023). This method uses empirical correlations between traffic loading, subgrade support condition, serviceability, and statistical reliability to determine the required Structural Number (SNreq). To calculate the Structural Number (SN) of a pavement, the structural contributions of all layers are summed, and the determined SN must be greater than SNreq. The contribution of each layer can be obtained by the multiplication of each layer thickness by a drainage and a structural coefficient that is defined based on its material, stiffness, and drainage capability.

This design method is still widely used, and foamed asphalt materials need a structural coefficient for the proper application of the design procedure. Díaz-Sanchez et al. (2017) indicate that layer coefficients for cold recycled mixtures are recommended to be between that of granular materials and asphalt concrete, which would result in a range from 0.15 $in^{-1}$ to 0. 35 $in^{-1}$. The Wirtgen Cold Recycling Manual (Wirtgen, 2012) indicates that these coefficients could vary from 0.18 $in^{-1}$ to 0.35 $in^{-1}$, depending on the ITS and shear resistance properties of each mixture. Romanoschi et al. (2003) have recommended a structural coefficient of 0.18 $in^{-1}$ for FDR mixtures stabilized with foamed asphalt, while Schwartz and Khosravifar (2013) indicated that for mixtures of soaked ITS between approximately 275 kPa and 350 kPa, the structural coefficient could vary from 0.30 $in^{-1}$ to 0.35 $in^{-1}$. Meanwhile Díaz-Sanchez et al. (2017) proposed a model for calculating the layer structural coefficient based on graphical correlations from the AASHO Road Test, based on the materials elastic modulus.

Da Costa (2016) compiled different structural coefficients for Foamed Asphalt (FA) stabilized layers in a table which was adapted, expanded, and is presented in Table 4. For some of the publications mentioned in Table 4, a “n.d.” is assigned if they did not disclose the contents of foamed asphalt or filler incorporated.

**Table 4. Structural coefficients for Foamed Asphalt stabilized layers (adapted from Da Costa, 2016)**

| Reference | Stabilizing agent | Structural Coefficient (in-1) |
|---|---|---|
| Wirtgen (2012) | Foamed Asphalt (FA) n.d.% | 0.18 - 0.35 |
| Bemanian et al. (2006) | - | 0.18 |
| Romanoschi et al. (2003) | 3.0% FA + 1.0% cement | 0.18 |
| Van Wijk (1984) | FA - n.d.% | 0.20 - 0.42 |
| Diefenderfer and Apeagyei (2011) | 2.7% FA + 1.0% cement | 0.21 - 0.33 |
| Marquis et al. (2003) | FA - n.d.% | 0.22 |
| | FA - n.d.% | 0.22 |
| | 2.5% FA + 1.5% cement | 0.23 |
| | 3.0% FA + 1.5% cement | 0.35 |
| Thompson et al. (2009) | 2.0% FA + 1.5% cement | 0.23 |
| | 2.5% FA + 1.0% fly ash | 0.25 |
| Van Wijk et al. (1983) | 7.15% FA | 0.26 - 0.37 |
| Schwartz and Khosravifar (2013) | FA + cement - n.d.% | 0.30 - 0.35 |
| Díaz-Sanchez et al. (2017) | 2.0% FA + 1.0% cement | 0.36 - 0.39 |

### 2.2.9 California Department of Transportation – CALTRANS

The California Department of Transportation is one of the pioneers in the application and research of foamed asphalt materials. The foamed asphalt stabilization technique is mainly used in California as a Full Depth Reclamation

(FDR) process, resulting in the rehabilitation of deep pavement layers (ARRA, 2001).

The current proceedings are based on the collaboration between CALTRANS and the University of California Pavement Research Center (UCPRC) in Davis and Berkeley, where a Guideline for Project Selection, Design and Construction was elaborated for FDR using Foamed Asphalt (Jones et al. 2009).

The guideline recommends practices and procedures for all aspects of the recycling process, from material sampling, to testing and construction. Gradations are specified along with material requirements defined to characterize and determine its suitability for FDR with foamed asphalt. The mixture design process involves the determination of foaming characteristics, optimum moisture content, active filler choice and content, and asphalt binder content. It also defines a procedure to evaluate temperature sensitivity of the foaming process, with the preparation and stabilization of specimens at aggregate temperatures of 5°C, 25°C and 30°C, to assess bitumen dispersion, and resulting ITS values, to determine minimum working temperatures on the field.

Asphalt binder content should be between 2.0% and 4.0%, and the determination should be performed using ITS tests on Marshall specimens cured for 72h at 40°C and 24h soaked at 20°C-25°C. The design binder content is defined as the one which results in specimens with ITS resistance 100 kPa higher than the ITS of average untreated control samples.

Foamed mixtures are also tested for ITS to determine the active filler contents, with a minimum 1.0% active filler required, while the maximum filler amount is limited to 2.0% for cement and 3.0% for hydrated lime.

The Highway Design Manual presents the design procedure for pavement structures (Caltrans, 2017). A Mechanistic-Empirical Design procedure is presented, but it is only being implemented in California for selected projects with 20 to 40-year design life, no method for the performance evaluation of foamed asphalt stabilized materials is presented, and the structural parameters for its consideration in design are not clearly defined. The common alternative procedure for pavement design in the Highway Design Manual is an empirical method, usually referred to as the Hveem or R-value method. It takes into consideration (i) Traffic Index (TI), (ii) California R-value (R), (iii) Gravel Equivalent (GE) and (iv) Gravel Factor (Gf).

The Traffic index is determined based on the design traffic as a measure of the cumulative number of axle loadings expected, as presented in Table 5. The R-value represents a measurement of the soil resistance to deformation under saturation and wheel loading condition and can be obtained through the California Test (CT) 301. The Gravel Equivalent index is the equivalent thickness of gravel that would prevent permanent deformation in the underlying layer or the entire structure. The GE for each layer can be determined based on the material and its thickness, while the entire pavement structures GE can be determined using equation (2.8).

$$\mathrm{GE} = 0.0032 \times \mathrm{TI} \times (100\text{-R}) \tag{2.8}$$

**Table 5. Conversion values for TI in terms of Equivalent Single Axle Loadings (ESAL) (adapted from Caltrans, 2017)**

| ESAL | TI | ESAL | TI |
|---|---|---|---|
| ≤ 4,710 | 5.0 | ≤ 6,600,000 | 11.5 |
| ≤ 10,900 | 5.5 | ≤ 9,490,000 | 12.0 |
| ≤ 23,500 | 6.0 | ≤ 13,500,000 | 12.5 |
| ≤ 47,300 | 6.5 | ≤ 18,900,000 | 13.0 |
| ≤ 89,800 | 7.0 | ≤ 26,100,000 | 13.5 |
| ≤ 164,000 | 7.5 | ≤ 35,600,000 | 14.0 |
| ≤ 288,000 | 8.0 | ≤ 48,100,000 | 14.5 |
| ≤ 487,000 | 8.5 | ≤ 64,300,000 | 15.0 |
| ≤ 798,000 | 9.0 | ≤ 84,700,000 | 15.5 |
| ≤ 1,270,000 | 9.5 | ≤ 112,000,000 | 16.0 |
| ≤ 1,980,000 | 10.0 | ≤ 144,000,000 | 16.5 |
| ≤ 3,020,000 | 10.5 | ≤ 186,000,000 | 17.0 |
| ≤ 4,500,000 | 11.0 | ≤ 238,000,000 | 17.5 |
| ≤ 6,600,000 | 11.5 | ≤ 303,000,000 | 18.0 |

Meanwhile, the Gravel Factor is a material property related to its strength when compared to gravel materials. The Gf is either tabled or calculated, in the case of HMA materials. Foamed Asphalt mixtures used in FDR procedures should be considered to have a Gf of 1.4 (Caltrans, 2012) which is the same considered for Asphalt Treated Permeable Base materials (Caltrans, 2017).

At the end, the sum of the products of each layer thickness and Gf has to be equal or bigger than the pavement structure GE, while each product must be equal or bigger than the GE of the underlying layers. The layer thickness (in feet) determination to account for the underlying layer protection can be performed using equation (2.9):

$$\text{Thickness (t)} = {}^{\text{GE}}/_{\text{Gf}} \tag{2.9}$$

### 2.2.10 Foamed Asphalt Materials in Canada

Although Canada has cold weather during most of the year, which makes it difficult for foamed asphalt stabilization, there are multiple specifications across the country on how this material should be designed and used.

The city of Edmonton, in the province of Alberta, on its Design and Construction Standards Manual (2015) details the procedure for FDR using foamed asphalt. The manual indicates a minimum bitumen content of 2.6% by mass, and a minimum addition of 1.0% cement, but no maximum content for neither of them. The specification also says that Marshall specimens should be compacted and tested for ITS for soaked and unsoaked conditions, specifying that soaked specimens must be placed under water for 24 hours at 25°C, but no other details are given about the curing procedure. It also does not indicate minimum values for the ITS tests, only specifying that TSR should be greater than 50%.

The Ontario Pavement Design and Rehabilitation Manual (MERO, 2013) refers to Foamed Asphalt as Expanded Asphalt Mix, and it defines a granular equivalency coefficient for both Cold Recycled (CR) and Full Depth Reclamation (FDR) mixtures stabilized with FA. The manual differentiates the techniques of CR and FDR, where the former focus on the stabilization of degraded asphalt layers, whereas the latter can include granular materials from the base and subbase. According to the Manual, a well graded crushed stone (Granular A) has a granular equivalency coefficient of 1.0, an HMA layer have coefficient of 2.0, and the foamed asphalt CR and FDR layers have granular equivalency coefficients of 1.8 and1.6, respectively.

The Ontario Provincial Standard Specifications (OPSS.PROV 331, 2015; OPSS.PROV 335, 2015) define that the design of foamed asphalt mixtures should be conducted according to the Wirtgen Cold Recycling Technology Manual (Wirtgen, 2012). It also determines minimum dry and soaked ITS values as 225 kPa and 100 kPa respectively, like the specified values from the Wirtgen Manual, which is based on the South African TG2 (Asphalt Academy,2009).

The majority of provinces in Canada uses AASHTO as the main method to determine overall pavement strength (C-SHRP, 2002). That includes Quebec, where the main software for structural design calculations, Chaussée 2, allows for the use of cold recycled mixtures in the design. The user guide for the software indicates that the thickness of cold recycled layer is usually between 85 mm and 110 mm and should be defined based on the thickness and conditions of the existing degraded asphalt layers. After defining the cold recycled layer thickness, the user can then calculate the required HMA thickness that should be placed on top of it, based on the remaining thickness of degraded HMA left under the recycled layer.

### 2.2.11 Foamed Asphalt Materials in Italy

Cold recycled materials with asphalt are widely used in Italy, with different research groups in the country invested in the development of the technique (Tebaldi et al., 2018; Graziani et al., 2018; Grilli et al., 2019; Preti et al., 2022; Gouveia et al., 2022).

The “Capitolato speciale d’appalto per la manutenzione straordinaria di pavimentazioni stradali” of San Marino (Casali and Grilli, 2021) presents a specification for cold in plant recycling of asphalt mixtures. This specification was developed for the use of asphalt emulsion but defines detailed requirements for all materials used in the recycled mixture, including the cement, asphalt emulsion and virgin aggregates and RAP. It indicates a gradation envelope for the recycled mixture that limits the amount of fines passing the 63µ sieve between 3% and 8%. The mix design procedure defines the use of gyratory compacted samples to be produced, cured for 3 days at 40°C and then tested for ITS and ITSM. A distinction between target mixtures is made regarding the type of road where it will be used, with a minimum ITS value of 0.30 MPa for local and secondary roads, and 0.40 MPa primary roads. It also demands that mixtures to be applied in primary roads should be tested for ITSM, to achieve a minimum modulus of 3.000 MPa, while mixtures for local and secondary roads do not require the ITSM test. The indicated content for the addition of asphalt emulsion is between 4.0% to 5.0% by mass of aggregates, while the indicated cement content is between 1.5% and 2.5%.

The ANAS Group also has its own specification for foamed asphalt stabilized mixtures, and although not a government institution, the group manages approximately 32,000 km of roads in Italy. Its pavement specification manual (IT.PRL.05.21 - Rev. 3.0) presents details for the mixture design and execution of foamed asphalt materials both in situ and in plant with mixture requirement differences between the execution methods. The specification for in situ recycling defines a finer gradation envelope material and higher contents of foamed asphalt and cement addition. It specifies the gradation for the in situ recycled mixture with the amount of fines passing the 63μ sieve between 5% and 10%, while the in plant mixture is restricted to 4% to 10%, with higher minimum values also defined for the other gradation sieves. As for the addition of binding agents, the foamed asphalt incorporation is recommended in rates between 2% and 4% by weight of mixture, while cement addition varies from 1.5% to 2.5% for in plant mixes 2.0% to 4.0% for in situ mixtures. The amount of foamed asphalt and cement incorporated should be defined by the results of ITS tests in gyratory compacted samples, cured at 40°C until constant mass. The desired ITS results for optimum binder incorporation are between 0.32 and 0.55 for in situ mixtures and 0.30 and 0.50 for in plant recycled mixtures. No indication is made in the specification regarding material stiffness or how it should be considered for pavement structural design.

Although techniques of material stabilization with foamed asphalt and asphalt emulsion are widely used, most of the cold recycled mixtures used in the country have high cement contents. This results in mixtures with high stiffness and mechanical resistance that can be identified more as cement bitumen treated materials (CBTM) than bitumen stabilized materials (BSM).

## 2.3 MIX DESIGN DISCUSSION

The different procedures present how the foamed stabilization technique is approached in distinct countries and transportation agencies around the world. While many aspects are common among procedures, mixture design tests, reference values and the approach to material behaviour for structural evaluation differ significantly.

From the analysis of the different methods used for mixture design, a few parameters have been identified for differing the most. These parameters will be analysed separately so that its influence on the mixture behaviour, and therefore the approach for structural design can be evaluated. The analysis will focus on the material gradation, foamed bitumen content, active filler type and content, curing and the mechanical tests used as reference to evaluate its impact on the final mixture produced by each Design Method.

### 2.3.1 Material Gradation

The particle size distribution is an important factor for material stability, compacity, moisture susceptibility and mechanical resistance under loading. Most of the procedures presented, have gradation limits defined so that the stabilized material can perform suitably to its application. Although the defined limits can be different in many aspects of particles size distribution, the focus here is on the amount fines, being the material passing the 75μ sieve, which is the material with higher specific surface, and responsible for bitumen dispersion through the mix, highly influencing the optimum binder content.

As described by Jenkins (2000), during the process of foamed asphalt stabilization, as the bitumen bubbles burst when they get in contact with the aggregates, the resulting droplets have just enough surface energy to heat and attach themselves to the fine particles. Through this process, the bitumen becomes dispersed around the mix creating a fine mortar which, after compaction will give cohesion, keeping the aggregates together.

In that sense, a minimum amount of fines, especially for the filler fraction, is instrumental for the adequate dispersion of the asphalt binder through the mix. The excess of fines, on the other hand may contribute to the increase of the aggregate specific surface area, which would increase moisture retention in the material. Fu et al. (2011) have pointed that the excess of fines in the foamed asphalt mixture could reduce its strength due to the formation of a continuous and unbound weak filler phase.

To account for that, and the effect of the specific surface increase, asphalt binder content would need to be increased as well, with the mortar representing a bigger fraction of the aggregate distribution. Although the bonds are dispersed through the mixture, the increase of the mortar fraction could result in cohesion gain, which under fatigue performance analysis would represent an improvement.

When analysed from the Failure Criteria point of view, both procedures from Austroads and the British TRL adopt fatigue as the primary failure criteria, while also defining higher fines and filler contents for the mixture gradation reaching up to 20% of fines, as presented in Table 6. On the other hand, Californian, Brazilian and South African mixture design limits are lower, while New Zealand mixture design limits the fines passing on the 75µ to 7%.

### 2.3.2 Active Filler Content

The definition of the active filler, as well as the amount defined for addition has a direct impact on material behaviour. The benefits of the active filler are related to its finer particles in the improvement of bitumen dispersion during the foaming process, but also to the reduction of moisture sensibility and the improvement of early life strength and stiffness.

As pointed by the TRL (Merrill et a. 2014), the effect of cement on stiffness is significant and occurs in a short curing period, while lime and other hydraulic binders may provide stiffness gain in a slower way. High incorporation rates of cement may result in a more cohesive behaviour, which may be related to fatigue life depending on the approach adopted for failure analysis. Betti et al. (2016)

also evaluated how different combinations of cement, lime and mineral filler affected the mixture stiffness, indicating that higher addition of either cement or lime will result in increased modulus, with one or the other resulting in similar effects.

In different study, Gouveia et al. (2021) evaluated the use of quicklime as active filler, comparing it to mixtures where Portland cement was used instead. The research showed that addition of quicklime in contents higher than 2% up to 5% did not result in significant change in material mechanical behaviour, while cement continually increased material ITS resistance and cohesion.

From the analysed design procedures, the higher cement addition rates did not exceed 2.0% for most specifications, with exception of Italian specifications, while hydrated lime could be found in applications of up to 3.0%. However, most procedures limit cement and other fillers application rate to assure that the bitumen bonds are the predominant binding mechanism of the mixture.

### 2.3.3 Foam Bitumen Content

One parameter that influences greatly the cold recycled mixtures is the bitumen content added during stabilization. As discussed, bitumen droplets from the foam process tend to have an affinity with the fine aggregate particles, and for that it should not be expected that the increase in bitumen addition in cold recycling would promote coating to the coarse aggregate particles.

Jenkins (2000) did a comprehensive study on the effect of aggregate gradation and bitumen dispersion on foamed asphalt mixtures, pointing out to the tendency of the binder to do not adhere to the coarse aggregates, instead attaching to the fine particles, creating mortar in the mixture.

If the binder content is too high but not enough filler is available, the binder will be concentrated in the fine fraction, and if there is not enough fines, it will attach to itself, creating lumps of bitumen instead of being evenly dispersed through the mixture. On the other hand, if an abundance of fines is available but not enough bitumen, a continuous and unbound mineral phase could be created, reducing the mixture strength (Fu et al. 2011).

When analysing the procedures around the world, it is possible to see a trend where the bitumen content incorporated is usually associated with the fine content allowed for the material gradation, as can be observed in Table 6, where the TRL and Austroads procedures have a finer gradation, with a greater allowable filler fraction and a higher usual bitumen content.

The Caltrans defines three possible bitumen contents, where 3.0% is the recommended content, while 2.0% could be adopted if no significant improvement is observed with the bitumen increase ratio. In case the addition of 3.0% foam bitumen is not satisfactory, 4.0% of bitumen binder could be applied.

For the South African procedure, foam bitumen stabilization is allowed for a wide variety of materials, including gravel soils, which would require higher bitumen contents for stabilization. For the most part, the procedure is used to stabilize crushed gravels and reclaimed asphalt pavement, resulting in low bitumen contents, close to 2.0%. The design procedure for the FHWA and the Canadian city of Edmonton are also procedures that allow for the stabilization of gravels and soils, due to its FDR characteristics. In this sense, higher bitumen contents may be necessary to achieve the minimum resistances.

The Brazilian specifications also indicate a wide range of recommended bitumen content, but the allowed amount of material passing the 75 µm sieve is also broad. It is possible to relate the lower fine content, to a tendency to produce low bitumen content foamed mixtures, when comparing the same required level of resistance.

**Table 6. Foamed Bitumen Mixture Design parameters for different procedures. Parameters defined as "n.d." indicate its non-definition within the specification.**

| Procedure | Foamed Bitumen Mixture Design | | | | |
|---|---|---|---|---|---|
| | Gradation - passing on 75µ sieve (g) | Active Filler Content (f) | Bitumen content (b) | Reference Tests | Curing |
| **Brazil - DNIT** | 5% ≤ g ≤20% | n.d. | n.d. | -$ITS_{dry}$ ≥ 250 KPa<br>-$ITS_{soaked}$ ≥ 150 KPa | -72h at 40°C (dry)<br>-72h at 40°C + 24h at 25° (soaked) |
| **Brazil – PMSP-SP** | 8% ≤ g ≤20% | 1.0% ≤ f ≤ 2.0% | 2.0% ≤ b ≤ 4.0% | -$ITS_{dry}$ ≥ 280 KPa<br>-$ITS_{soaked}$ ≥ 200 KPa | -72h at 60°C (dry)<br>-72h at 60°C + 24h at 25° (soaked) |
| **Brazil – DER-PR/SP** | 5% ≤ g ≤20% | 1.0% ≤ f ≤ 2.0% | 2.0% ≤ b ≤ 4.0% | -$ITS_{dry}$ ≥ 400 KPa<br>-$ITS_{soaked}$ ≥ 200 KPa | n.d. |
| **United Kingdom - TRL** | 5% ≤ g ≤21% | -1.0% ≤ Cement ≤ 1.5%<br>-Hydrated Lime ≥ 1.5% (ex situ)<br>-Hydrated Lime ≥ 2.5% (ex situ) | -b ≥ 4.0% (in situ)<br>-b ≥ 3.0% (ex situ) | -B1-ITSM ≥ 1,900 MPa<br>-B2-ITSM ≥ 2,500 MPa<br>-B3-ITSM ≥ 3,100 MPa | 28 days at 20°C and 40°C |
| **Australia - Austroads / TMR** | -8% ≤ g ≤16% for Initial daily ESA < 1,000<br>-5% ≤ g ≤20% for Initial daily ESA ≥ 1,000 | 1.0% ≤ f ≤ 2.0% | 3.0% ≤ b ≤ 4.0% | -Minimum initial ITRM<br>-Minimum Cured ITRM<br>-Minimum Soaked ITRM | -3h at 25°C<br>-3 days at 40°C<br>-3 days at 40°C + 10 minutes soaked in vacuum |
| **Australia - City of Canning** | n.d. | -Cement ≤ 1.0%<br>-2.0% ≤ Hydrated Lime ≤ 3.0% | 3.5% ≤ b ≤ 4.0% | n.d. | n.d. |
| **New Zealand - NZTA** | 0% ≤ g ≤7% | Cement around 1.0% | 2.7% ≤ b ≤ 3.0% | ITS and UCS | Defined by Designer |
| **South Africa - TG2** | 4% ≤ g ≤14% | f ≤ 1.0% | 1.5% ≤ b ≤ 3.0% | -$ITS_{dry}$ ≥ 225 KPa<br>-$ITS_{soaked}$ ≥ 125 KPa | -72h at 40°C (dry)<br>-72h at 40°C + 24h at 25° (soaked) |
| **South Africa - SAPEM** | refer to TG2 | refer to TG2 | refer to TG2 | refer to TG2 | refer to TG2 |

| Procedure | Foamed Bitumen Mixture Design | | | | |
|---|---|---|---|---|---|
| | Gradation - passing on 75μ sieve (g) | Active Filler Content (f) | Bitumen content (b) | Reference Tests | Curing |
| **USA – DOT Maryland** | 5% ≤ g ≤15% | n.d. | n.d. | -$ITS_{soaked}$ ≥ 345 KPa<br>-TSR ≥ 70% | -40°C until constant mass<br>-Soaking at 20 min at 25°C + 45 min at 55mm Hg + 10 min at 25°C |
| **USA – DOT Arizona** | 5% ≤ g ≤20% | n.d. | n.d. | -$ITS_{soaked}$ ≥ 310 KPa<br>-TSR ≥ 50% | -40°C until constant mass + 24h at 25°C soaked |
| **FHWA FP-14 FLH T-522** | n.d. | n.d. | 2.0% ≤ b ≤ 4.0%. | -$ITS_{soaked}$ ≥ 170 KPa<br>-TSR ≥ 60% | -60°C for 48°C<br>-Soaking at 260 to 660 mm Hg until 55-77% saturation + 24h at 25°C |
| **USA - Caltrans** | 5% ≤ g ≤15% | -1.0% ≤ Cement ≤ 2.0%<br>-2.0% ≤ Hydrated Lime ≤ 3.0% | 2.0% ≤ b ≤ 4.0% | $ITS_{b\%}$ - $ITS_{0\%}$ ≥100 KPa | 72h at 40°C + 24h at 25° soaked |
| **Canada – City of Edmonton** | 5% ≤ g ≤20%<br>(80μ sieve) | Cement ≥ 1,0% | b ≥ 2,0% | TSR ≥ 50% | Soaking at 25°C for 24h |
| **Canada Ontario** | 4% ≤ g ≤12% | f ≤ 1.0% | 1.5% ≤ b ≤ 3.0% | -$ITS_{dry}$ ≥ 225 KPa<br>-$ITS_{soaked}$ ≥ 100 KPa | -72h at 40°C (dry)<br>-72h at 40°C + 24h at 25° (soaked) |
| **Italy – San Marino** | Considering 63μ sieve:<br>3% ≤ g ≤8% - in plant | 1.5% ≤ Cement ≤ 2.5% | Asphalt Emulsion (e):<br>4.0% ≤ e ≤ 5.0% | -$ITS_{dry}$ ≥ 300 KPa<br>-ITSM ≥ 3,000 MPa | 72h at 40°C |
| **Italy – ANAS Group** | Considering 63μ sieve:<br>4% ≤ g ≤10% - in situ<br>5% ≤ g ≤10% - in plant | 2.0% ≤ Cement ≤ 4.0% -in situ<br>1.5% ≤ Cement ≤ 2.5% -in plant | 2.0% ≤ b ≤ 4.0% | -In situ: 320 kPa ≤ ITS ≤ 550 kPa<br>-In plant: 300 kPa ≤ ITS ≤ 500 kPa | 40°C until constant mass |

### 2.3.4 Mixture Design tests

When we analyse the foamed asphalt mixture design procedures from a test protocol standpoint, two tests can be highlighted, the Indirect Tensile Strength Test (ITS) and the Indirect Tensile Resilient or Stiffness Modulus Test (ITRM or ITSM). Both the ITRM and the ITS are used to determine the influence of the foam bitumen on the material strength, and how water presence affects its behaviour.

The ITRM and ITSM are performed to assess the material elastic response to tensile loading, determining an Elastic Modulus that can be used for pavement design consideration, while determining the minimum bitumen addition to achieve a determined application threshold.

On the other hand, the ITS test takes the material to failure under indirect tensile strength, verifying the ultimate stress the sample can withstand before its rupture. The test itself does not provide input for the mechanistic design of pavement structures, however, it can be associated with how much cohesion is provided by the asphalt binder, and how successful it is on reducing moisture susceptibility.

### 2.3.5 Curing Procedures

Regardless of the test protocols adopted, foam mix stabilization requires curing to attain an increase of material stiffness and mechanical resistance. According to Twagira (2010), curing is a process where the existing bonds between the bitumen binder and the mineral aggregates increases the materials´ strength and stiffness. The decrease in material moisture during the curing process induces a reduction of the lubrication between aggregates, which results in a higher friction among particles, hence an increase in strength (Lynch, 2013). The curing process of the foamed asphalt recycled layer in the field can be attributed to a series of effects such as the temperature gradient, the relative humidity, drainage, wind speed, and the contribution of the adjacent pavement layers.

Since cold recycling can use a wide variety of sources for the aggregates, along with all the field variables that influence the curing process, its length may differ greatly for different job sites. Some materials achieve full strength within short periods of time (such as a month), while it can be verified that curing may continue even after an entire year under service (Mulusa, 2009; Lynch, 2013; Martinez et al. 2013).

To accelerate and simulate the long curing process of the field material in laboratory, each mix design procedure adopts a different curing protocol for the test samples. The differences between the curing procedures may result in different responses of the material under testing. While past experiences have used curing temperatures of over 50°C (Fu and Harvey, 2007; Milton and Earland, 1999) most procedures have defined 40°C as the maximum temperature for curing of foamed asphalt cold recycled mixes, as higher temperatures may soften the bitumen present in the mixture, changing binder distribution through the material and affecting its mechanical behaviour.

It is interesting to note that the Curing procedure adopted by the TRL takes 28 days at 25°C and 40°C, while the other procedures are usually limited to 3 days. After constant mass is obtained during the curing process, no increase in strength should be observed from the asphalt binder standpoint. However, the active filler present on the mix, usually cement or lime may continue to provide strength and stiffness for longer periods.

The early cure procedure defined in the Austroads mixture design, with the sample resting for 3 hours at 25° before testing provides a valuable insight on the material early behaviour, when a new or rehabilitated road is opened for traffic. However, as moisture can significantly impact material mechanical response, the slow curing at 25°C may produce specimens of varying moisture contents, which can yield high variability results. Alternatively, the use of 40°C as curing temperature allows for faster curing until constant mass, providing a simple standard condition for design and characterization tests to be performed.

## 2.4 STRUCUTRAL DESIGN DISCUSSION

As each procedure has its own particularities regarding the mixture design, the same happens for the evaluation of pavement structures with foam bitumen materials. The material characteristics defined during mixture design and the approach adopted when evaluating the material have direct impact on the method chosen to analyse and design the pavement structure and the performance of the foam bitumen layer.

A summary of the structural design methods and the related parameters is presented in Table 7. The Brazilian, Californian and the Canadian (Ontario) design procedures use an equivalent granular approach to protect the underlying layers, both considering the gravel reference factor as 1.0. While the $G_f$ defined for the Caltrans method is 1.4, no precise coefficient is defined for the DNIT Method, while the Canadian specification define the structural equivalency between 1.6 and 1.8.

The wide adoption of the 1993 AASHTO design method may explain why the structural coefficient presents such a broad range of values, as different mixture compositions and local resistance requirements will result in different structural contributions.

The methods from Austroads, Canning and the TRL all define fatigue as the primary mode of failure of the foamed bitumen layer. It can reflect the mixture design method used, with higher fine contents, as well as higher addition of active filler and asphalt binder, creating more cohesive mixtures.

The ITRM test also provides a measure of material stiffness that can be used as an input for mechanistic design, with values that are commonly higher than 2,000 MPa, indicating highly cohesive mixtures. Both Canning and the Austroads procedures use tensile strain on the bottom of the foamed layer as the primary performance parameter.

**Table 7. Foamed Bitumen Structural Design characteristics for different procedures**

| Procedure | Foamed Bitumen Structural Design | | | |
|---|---|---|---|---|
| | Method | Design Parameters | Performance Model for the Layer? | Layer Failure Mechanism |
| **Brazil - DNIT** | Empirical (CBR based) | Gravel equivalent (n.d.) | no | n.d. |
| **Brazil - DER-PR** | n.d. | n.d. | no | n.d. |
| **United Kingdom - TRL** | Deterministic | Material Class. B1-B3 | no | Fatigue |
| **Australia - Austroads / TMR** | Mechanistic Empirical | $S_{mix}$ (ITRM corrected) - around 2,000 MPa | yes | Fatigue |
| **Australia - City of Canning** | Mechanistic Empirical | n.d. | yes | Fatigue |
| **New Zealand - NZTA** | Mechanistic Empirical | E=800 MPa; μ=0.30 | yes | Permanent Deformation |
| **South Africa – Pavement Number** | Empirical (Pavement Number) | ELTS ≤ 600 MPa | no | Permanent Deformation |
| **South Africa – TG2** | Mechanistic Empirical | ELTS ≤ 700 MPa | yes | Permanent Deformation |
| **United States - Various** | AASHTO 1993 | $0.18 \leq a \leq 0.38$ ($in^{-1}$) | no | n.d. |
| **United States - Caltrans** | R-value Method | Gf = 1.4 | no | n.d. |
| **Canada - Ontario** | Catalog - Empirical (Granular Base Equivalency) | CR = 1.8<br>FDR = 1.6<br>Granular = 1 | no | n.d. |
| **Italy – San Marino** | Mechanistic Empirical | E ≥ 3,000 MPa | no | n.d |

On the other hand, the methods from New Zealand and South Africa limit material stiffness to 800 MPa and 700 MPa, respectively. These procedures indicate that the foam material is going to behave as a granular material with higher cohesion for the most part of its service life, with limited applicability of the classical fatigue theory for a non-continuously bound material such as foam bitumen layers (Jenkins, 2012).

The New Zealand transfer function used to predict the performance of foam bitumen pavements evaluates the maximum vertical strain on top of the subgrade, not directly assessing the performance of the foamed asphalt layer. As for the South African prediction models, both transfer functions evaluate the stress state of the foam bitumen layer on critical points, using mixture shear properties as input parameters allowing for detailed analysis of material performance.

The approach used in each pavement design can also be associated with how the foam bitumen material is treated during mixture design. As discussed, the lower fine fraction content, associated to the lower rate of bitumen and active filler addition result in less cohesive mixtures.

## 2.5 PARTIAL CONCLUSIONS

Based on different procedures for mixture and structural design of pavements containing foamed asphalt layers, a few observations were made, as follows:

- Some of the procedures investigated limit cement and other active filler addition to preserve bitumen as the binder responsible for the main behavioral characteristics of the mix, although no consensus exists on maximum rates.
- As the fine fraction of aggregate gradation has an instrumental role on the dispersion of bitumen droplets and the mix stabilization, the allowed content of fines can directly affect the material performance, as well as bitumen binder consumption.

- As bitumen and fines are added to the mixture, the mortar gains cohesion, although the non-continuous nature of the mixture is preserved.
- The structural design procedure, with respect to the failure criterion standpoint, is directly associated with the mixture design, test protocols and curing procedures considered. The final mixtures can be considerably different for each procedure.

# 3 FIELD EVALUATION OF HIGH LEVEL ROADS WITH FOAMED ASPHALT STABILIZED BASE LAYERS

## 3.1 INTRODUCTION

The use of foamed bitumen stabilized layers for pavement rehabilitation has been increasingly growing in the last decade. It has been propelled by the advances in cold recycling technology, as well as a global effort to reduce environmental impacts through the adoption of more sustainable and efficient materials, procedures and techniques.

The stabilization technique can be applied to either virgin aggregates, or recycled material, such as Reclaimed Asphalt Pavement (RAP) and Crushed Cement Treated Bases (CCTB), producing materials that can be used for pavement base and subbase layers (Schwartz and Khosravifar, 2013).

The stabilizing process consists of the dispersion of bitumen binder into an aggregate mix in the form of foam, produced by the combination of pressurized binder, water and air (Jenkins, 2000). The addition of active fillers such as hydrated lime and Portland cement is common, with the possibility of its content being limited to 1,0% when producing a Bitumen Stabilized Material (BSM) or reaching up to 4,0% for Cement Bitumen Treated Materials (CBTM). The foaming and stabilization process can be performed in mobile plants or in place, which provides logistical flexibility, while reducing transportation costs, fuel consumption and environmental impacts (Stroup-Gardiner, 2011).

During the foam bitumen stabilization process, water is added to mix, to assist in the dispersion of the bitumen droplets, but also to help in the material compaction once its laid. The presence of water, as well as the addition of active fillers induce the curing process to the material, in which moisture content diminishes while stiffness and material cohesion increase (Cardone et al., 2015; Crispino and Brovelli, 2011; Khosravifar et al., 2015; Plati et al., 2010). To facilitate the curing process of the applied layer, lane closures are indicated before the execution of any overlying layer application (Jones et al., 2009).

Due to the nature of the non-continuous bonds created during the cold stabilization process, the foam bitumen stabilized materials are less resistant and durable than hot mix asphalt (HMA), and for that matter are usually considered for pavements of low traffic volume roads.

High traffic volume roads demand quality materials that can withstand vehicle loading, reducing pavement deterioration and the need for maintenance. Another issue for these roads is the difficulty to perform rehabilitation procedures that involve lengthy curing processes and therefore long lane interdiction periods.

This chapter presents five trial sections rehabilitated using foam bitumen stabilization, located in three high traffic volume highways in Brazil. The sections have been monitored for multiple years, and this chapter evaluates its performance and the technique's applicability to high traffic volume roads.

## 3.2 TRIAL SECTIONS

In this chapter, the five trial sections monitored will be presented to provide insight about each road's relevancy, the location of the trial sections (as presented in Figure 7) and the characteristics of the foamed stabilized pavement structure.

### 3.2.1 SP-070 Trial section

Section 1 is in Highway SP-070, under the toll concession Ecopistas. The SP-070 is a road that connects the city of São Paulo, the biggest in Brazil, with the east of the state, the nearby cities as Guarulhos, and the industrial area located in the Paraíba Valley.

The section is comprised of two segments on the third lane (heavy traffic lane), on the west track of the highway, coming into the city of São Paulo (Guatimosim et al. 2018). Due to its proximity to the city, the section is subject to traffic jams, with a projected number of ESALs for 10 years of more than 100 million.

After milling and replacing the deteriorating HMA layer on top of a cracked Cement Treated Base (CTB), the concession decided to perform a base recycling procedure including the removal of the CTB and laying of a 340 mm foamed bitumen stabilized layer, covered by a 20 mm-thick Gap Graded asphalt mix, as shown in Table 1. The whole procedure in this section, from lane interdiction, through milling, laying of the new layers, road marking painting and lane opening was performed in one-night shift on August 31st, 2013 (Guatimosim, 2015).

### 3.2.2 BR-381/SP Trial Sections

Trial sections 2, 3 and 4 are located on highway BR-381, near to the city of Extrema, under toll concession Autopista Fernão Dias. The highway connects the city of São Paulo to Belo Horizonte, Brazil’s sixth most populated city (IBGE, 2018). The three sections were built in the heavy traffic lane of the south track of the highway heading to São Paulo, with a projected traffic for the next 10 years of 140 million ESALs. The sections are in a 1,000-meter segment that contains eight different pavement sections that have been continuously studied and monitored since December 2014.

Section 2 was the first to be built, in 2014, with 250 mm-thick of a foamed bitumen recycled base layer, covered by 125 mm-thick HMA layer (Kuchiishi et al., 2018a). Although the binder contents used during the recycling process of this base layer were higher than the ones typically used in other sections, it was considered that it would be interesting to evaluate the behaviour of this section in comparison to the others, since it resembled the binder contents used in other parts of the world, such as Australia (Austroads, 2018) and Italy (Graziani et al. 2018b).

Section 3 was part of a second research phase, and was built in July of 2014, with 250 mm-thick foamed bitumen recycled base layer, covered by 30 mm-thick Gap Graded asphalt mix surfacing (Kuchiishi et al., 2018a).

Section 4 was also built in July of 2014 as a part of the research second phase, where 250 mm-thick foamed bitumen stabilized Graded Crushed Stone (GCS) was laid and covered by 30 mm-thick of the same Gap Graded asphalt mix surfacing of Section 3 (Kuchiishi et al., 2018a).

### 3.2.3 BR-116/SP Trial Section

Section 5 is in Highway BR-116, under the toll concession CCR Nova Dutra. The highway is the main road connecting São Paulo and Rio de Janeiro, the country's two biggest cities, with an industrial and heavily populated area in between. The estimated number of expected equivalent single axles for the next ten years for that section is greater than 60 million.

The section was built on the far-right automatic toll lane, destined for commercial heavy vehicles, where the vehicles must slow their speed from around 80 km/h to 40 km/h to pass the toll gates. The section used to be a road shoulder before being turned into an additional lane for the automatic toll. For that reason, the existing pavement structure was highly degraded and had to be rehabilitated. The existing base was milled, and a 300 mm recycled base was placed on top of the remaining granular layers, with a 30 mm Gap Graded surface layer being executed on top, similarly to what was executed in the other sections.

### 3.2.4 Climate Considerations

As the foam stabilized material is significantly affected by the field curing (Khosravifar et al. 2015), and weather conditions are in important factor on this process (Plati et al. 2010), it is important to make a few observations regarding the climate conditions surrounding the test sections.

Although Sections 2, 3 and 4 are in the same segment of BR-381 Highway, Section 1 and Section 5 are located not more than 100 km away from each other as it can be seen in Figure 7, in an area of similar macroclimate conditions.

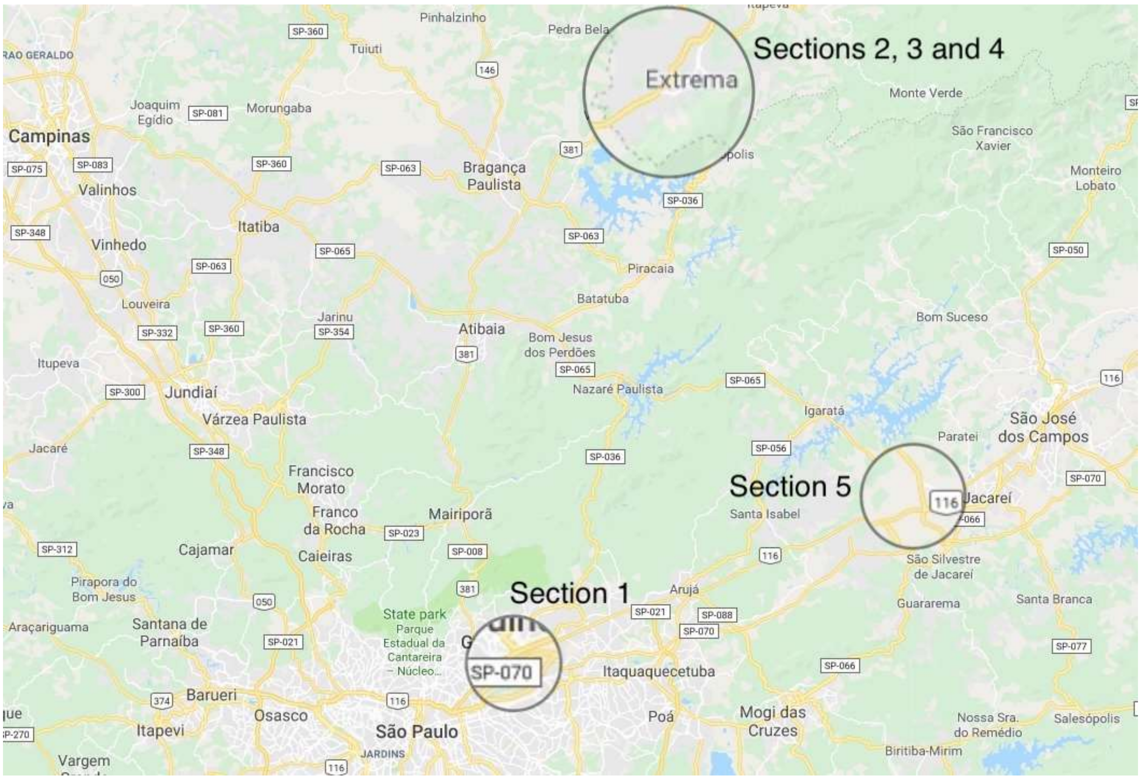


**Figure 7. Location of the trial sections**

In that sense, the weather condition for all segments is alike, with a rainy season from October until March, where it can rain 200 mm a month, and the dry spanning from April until September, with rainfall as low as 30 mm a month.

All year long, average air-temperature ranges from around 18°C on dry season to 22°C on the rainy season. In that sense, it is possible to see how the foamed asphalt layers stiffness changes with the season, and moisture presence due to rainfall increase.

The climate data from only one meteorological station was available for this study, the Mirante de Santana Station, which is in São Paulo, located around 15 km from section 1. As a reference for the determination of the climate conditions for the trial sections, LTPP InfoPave Climate tool was used to provide Modern-Era Retrospective Analysis for Research and Applications (MERRA) data. Using the LTPP Climate Tool, it was identified that Sections 2, 3 and 4 were located in the same grid cell (predefined square area of 50 km x 60 km), while sections 1 and 5 were located in a different cell. The square area defined by the grid cell means that the program considers the same climate condition for the entire area.

Figure 8 provides an insight into the annual climate for the trial sections by showcasing the total monthly precipitation and average temperature for the year of 2017 as an example. All data related to the weather conditions obtained by the Meteorological Station and the LTPP Climate Tool are presented in the appendix section. It

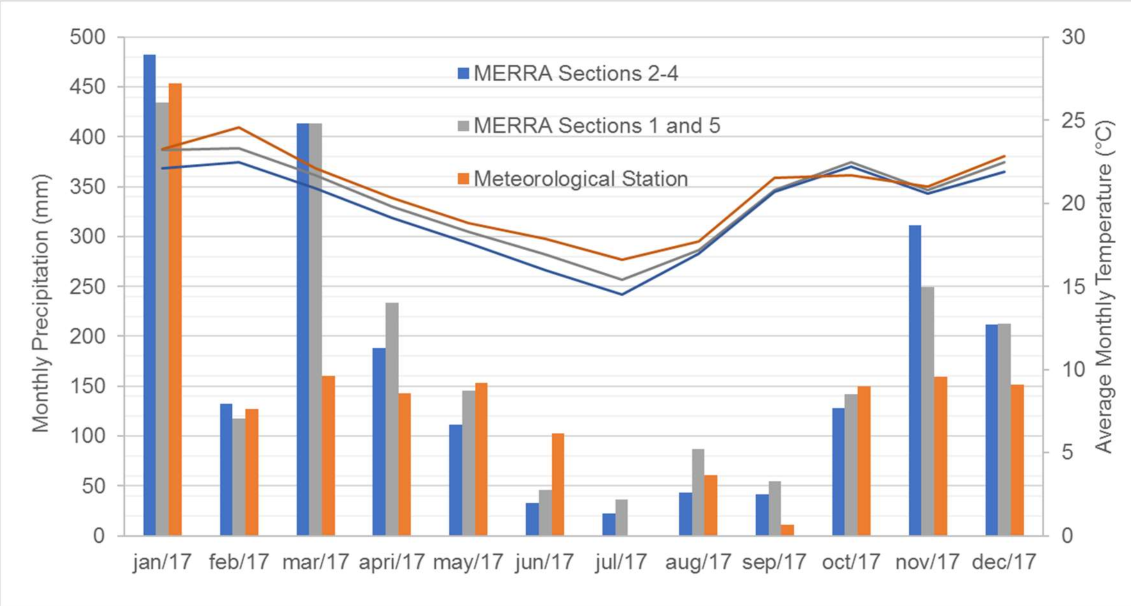


**Figure 8. Comparison between LTPP Climate Tool and data and Meteorological Station Data in terms of precipitation (bars) and temperature (lines).**

As it can be seen, the climate data gathered from the LTPP Climate Tool and the meteorological station produced similar results, indicating that there are no significant differences between the climate conditions for the 5 trial sections.

### 3.2.5 Trial Section Pavement Structures

Based on the rehabilitated trial sections, Table 8. Test section details and Pavement structure composition. presents a summary of each section's pavement structure, length, and location. The pavement structure here presented was divided in three major components, being the surface layer, whether dense HMA or Gap Graded, the foam stabilized layer and a remaining substructure, which is any existing pavement layer between the stabilized base and the subgrade.

**Table 8. Test section details and Pavement structure composition.**

| Pavement Layers | Unit | Section 1 | Section 2 | Section 3 | Section 4 | Section 5 |
|---|---|---|---|---|---|---|
| HMA Layer | mm | - | 125 | - | - | - |
| Gap Graded Surfacing | mm | 20 | - | 30 | 30 | 30 |
| Foam Stabilized Base | mm | 340 | 250 | 250 | 250 | 300 |
| Remaining Substructure | mm | 40 | 50 | 50 | 50 | 20 |
| Highway | - | SP-070 | BR-381 | BR-381 | BR-381 | BR-116 |
| Section Length | m | 260 | 95 | 95 | 95 | 200 |
| Expected Traffic for 10 year design period | ESAL | 100 million | 140 million | 140 million | 140 million | 60 million |

As mentioned, a thin Gap Graded asphalt layer was used as surfacing on Sections 1, 3, 4 and 5. Although these layers are designed for an air void content of 5.0%, the voids in the field can be around 7.0% with communicating pores, facilitating the curing and water exit from the foamed layer underneath. The execution of the hot mix also helps curing as water from the upper portion of the foamed layer tends to evaporate immediately as the surface layer is being placed on top of it. At last, due to higher structural deformability in the first stages of the curing process, these thin layers may serve as sacrifice temporary layers, until pavement deformation decreases, while working almost in a compression state, with low tensile strains.

## 3.3 STABILIZED LAYER CHARACTERIZATION

### 3.3.1 Mixture Characteristics

Depending on the availability of materials at the time of the rehabilitation procedures, each foam stabilized mix was designed with a different composition. Section 1 was part of a rehabilitation campaign, and had its recycled layer made out of the distressed CTB and RAP milled in previous days. The mix was designed based on the Asphalt Academy (2009) procedure, and contains 2,2% of asphalt binder, with the addition of 1% hydrated lime as active filler.

The recycled mix produced for Section 2 used stockpiled RAP with the addition of virgin aggregates, mostly Stone Crusher Dust (SCD) to achieve a desired grading curve. This material mix design aimed for higher resistances to guarantees a good performance of the section, and contained 3,0% of asphalt binder, with the addition of 2,0% of cement.

As for Sections 3 and 4, material composition was defined with the intent of comparing the recycled foam bitumen stabilized RAP material (with the addition of SCD) and a foam bitumen stabilized GCS layer. Both mix designs were made using the Wirtgen (2012) and Asphalt Academy (2009) procedures, resulting in asphalt binder contents close to 2% and the addition of 1% hydrated lime.

To limit lane interdiction time on section 5, so that the toll lane could be reopened, the recycled mixture was made on a mobile Wirtgen KMA 200 mix plant using stockpiled RAP material. To allow for an adequate gradation and a minimum amount of material passing the 75µ sieve, 15% of SCD was added, with the remaining 85% coming from the Concessions RAP stockpile deposits. Since the amount of material required to rehabilitate the entire section was small, foam stabilization was performed all at once, and the material stockpiled. The rehabilitation was conducted on the course of the two subsequent days, with works being carried daily from 8 AM to 5 PM, when the rehabilitated section was opened to traffic. Since the material had to be stockpiled, hydrated lime was used as active filler, avoiding the strict time windows imposed using cement. The mix design followed the Wirtgen (2012) and Asphalt Academy (2009) procedures, resulting in a 2.3% foamed asphalt binder content.

The composition and mix design characteristics for each foam stabilized layer are detailed in Table 9.

**Table 9. Stabilized layer mixture characteristics per section**

| Mix Composition | Units | Section 1 | Section 2 | Section 3 | Section 4 | Section 5 |
|---|---|---|---|---|---|---|
| RAP | % | 33.0 | 68.0 | 89.0 | - | 85.0 |
| Crushed CTB | % | 66.0 | - | - | - | 15.0 |
| Virgin SCD | % | - | 30.0 | 10.0 | - | - |
| Virgin GCS | % | - | | - | 99.0 | - |
| Portland Cement | % | - | 2.0 | - | - | - |
| Hydrated Lime | % | 1.0 | - | 1.0 | 1.0 | 1.0 |
| Foamed Bitumen Content | % | 2.2 | 3.0 | 2.2 | 2.0 | 2.3 |
| Maximum dry bulk density | kN/m³ | 20.30 | 20.60 | 19.14 | 21.68 | 20.20 |
| Optimum Moisture Content | % | 7.3 | 6.5 | 7.8 | 5.3 | 5.4 |

As a result of the materials mix design for each section resulted in different material compositions and grading curves. The material gradation for section 1 was obtained from Guatimosim (2015), the gradation for section 2 is presented by Andrade (2016), while the gradations for sections 3,4 and 5 were developed throughout this research and can be found detailed in the appendix section. All grading curves are presented in Figure 9, with the Wirtgen (2012) gradation envelope plotted as a reference.

It can be noted that except for the Virgin Graded Crushed Stone stabilized material used in Section 4, all the other mixes have reclaimed material as primary aggregate in their compositions, resulting in a low percentage (around 5%) of fines passing the 75 µ sieve for the final mix. Reclaimed material such as RAP, and milled CTB often result in lumps where small particles are kept together by the existing binder, for that reason those materials can present a coarser gradation (Loizos et al. 2012). To obtain a higher content of fines in these mixes Stone Crusher dust is usually used, as was the case of the mixes from sections 2, 3 and 5.

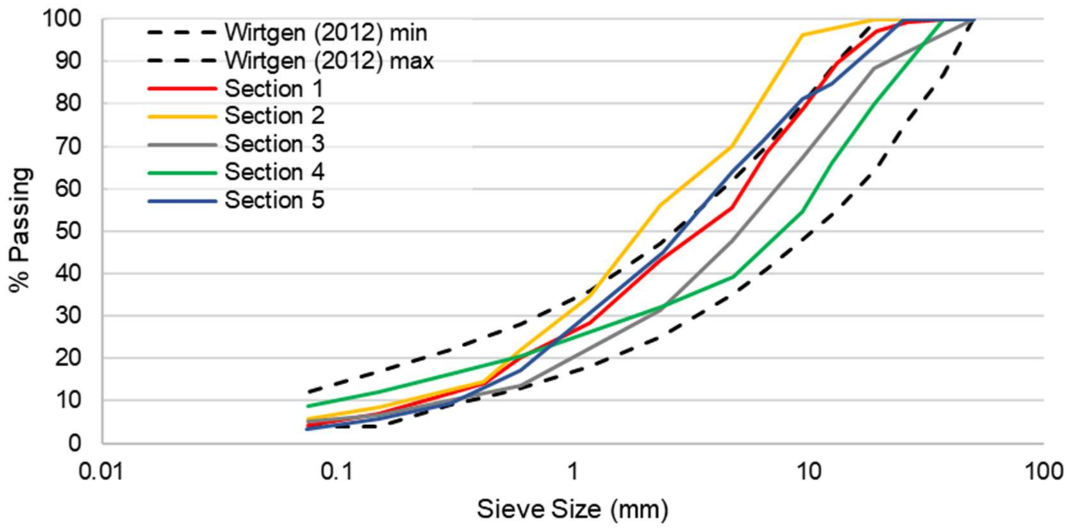


**Figure 9. Mix Gradation for each Trial Section Foamed Layer**

As observed by Bonfim (2011) the reclaimed aggregate can present different characteristics depending on the milling speed, milling drums, and bit used. Additionally, West (2010) stated that a finer gradation could be a result of aggregates breaking by the impact of the milling bits. For section 1, an adjustment to the process was made, reducing the milling speed for the CTB layer, producing more fines.

### 3.3.2 Laboratory Testing

During the execution of the trial sections with hydrated lime, the stabilized material was collected, sealed in plastic bags and transported to the laboratory in the University of São Paulo. The material with Portland Cement was reproduced in laboratory using a Wirtgen's WLB10 and WLM30 Foaming and Mixing unit respectively. There, the materials were tested to verify the design parameters for quality control and tested for Triaxial Resilient Modulus (TxRM) in order to access the material stiffness after the complete curing.

Table 10 presents the regression coefficients of the TxRM tests conducted by Guatimosim et al. (2018) and Kuchiishi et al. (2018b) for the foam stabilized materials used in Sections 1, 2, 3 and 4.

Samples from section 1 were cured for 7 days as part of a larger set of tests to evaluate the change in stiffness during curing. It was chosen because it represented the curing period at which the resilient modulus seemed to have stabilized during curing. The 25°C temperature was defined to allow a slower moisture decrease in specimens (Guatimosim, 2016).

Specimens from sections 3 and 4 were cured for 7 days at 40°C to provide enough time for the cure of the hydrated lime used as active filler. The samples from Section 2 were cured at 40°C for 28 days, to guarantee the total hydration of the cement added (Kuchiishi, 2019), which may have resulted in an incremented stiffness. The TxRM tests were performed according to DNIT ME 134/10 standard, with specimens of 100 mm diameter and 200 mm height been subject to cyclic loads, with periods of 0.1 second of load and 0.9 seconds of rest. All samples were compacted using vibratory compaction hammer (adapted Bosch GSH 11VC) according to (Jenkins and Kelfkens, 2008) until achieving AASHTO T-180 Modified density.

The effect of the confining pressure on the resilient modulus of the tested specimens can be noted on Figure 10, reproduced from the regression coefficients presented inTable 10. Although the confining pressure model may not be the best model to describe material behaviour, it does allow for the assessment of the effect of the confining pressure on material modulus.

**Table 10. Triaxial Resilient Modulus Regression Coefficients (confining pressure model).**

| Sample | Curing Method | k1 | k2 | $R^2$ | Reference |
|---|---|---|---|---|---|
| Section 1 - S 1 | 7 days at 25°C | 1597.9 | 0.164 | 0.55 | Guatimosim et al. (2018) |
| Section 1 - S 2 | 7 days at 25°C | 1684.0 | 0.156 | 0.70 | |
| Section 1 - S 3 | 7 days at 25°C | 1822.7 | 0.207 | 0.90 | |
| Section 2 - S 1 | 28 days at 40°C | 1574.5 | -0.087 | 0.23 | - |
| Section 2 - S 2 | 28 days at 40°C | 1960.0 | 0.034 | 0.20 | |
| Section 3 - S 1 | 7 days at 40°C | 1329.7 | 0.154 | 0.56 | Kuchiishi et al. (2018b) |
| Section 3 - S 2 | 7 days at 40°C | 1694.9 | 0.260 | 0.87 | |
| Section 4 - S 1 | 7 days at 40°C | 1909.3 | 0.370 | 0.89 | |
| Section 4 - S 2 | 7 days at 40°C | 2253.2 | 0.411 | 0.90 | |
| Section 5 - S 1 | Extracted sample | 1682.4 | 0.075 | 0.66 | - |

The recycled foam bitumen stabilized material from Section 1 had a higher modulus than that of Sections 3 and 4. As they all have similar asphalt binder contents and the same amount of hydrated lime was added as active filler, the difference identified between the three materials may be related to the presence of unhydrated cement in the recycled CTB and to its grading characteristics, providing better packing and aggregate arranging, and therefore an increased resistance to deformation.

As for Section 2, it can be noted that it has a higher stiffness and a smaller slope, indicating a less stress dependent behaviour. That behaviour could be associated with the higher content of asphalt binder and cement in the mix, and the stiffness obtained from its hydration process.

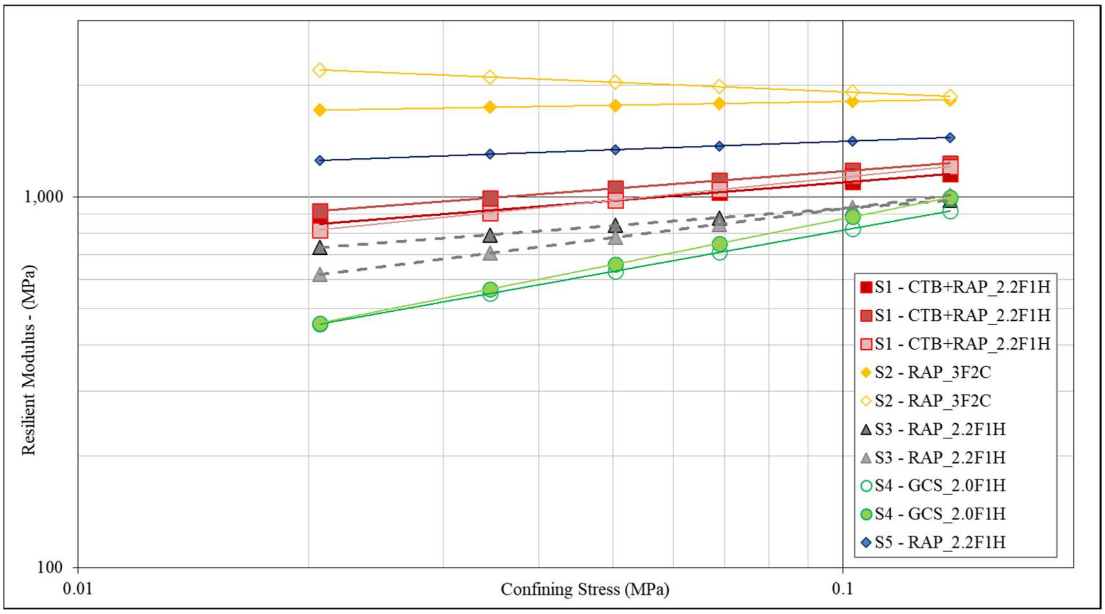


**Figure 10. Triaxial Resilient Modulus plotted according to Table 10 regression coefficients.**

The resilient modulus results for Section 5 are higher than those obtained for sections 1, 3 and 4, but differently than for other sections, the tested specimen was obtained from a field extracted core sample, that was cured for more than a year in the field under traffic loading. For that reason, due to advanced curing conditions and densification by traffic loading, the resulting material stiffness was higher than laboratory compacted specimens used for other sections.

## 3.4 MONITORING OF THE TRIAL SECTIONS

### 3.4.1 Structural Evaluation

During the research period, several Falling Weight Deflectometer (FWD) tests were performed, to access the evolution of the curing process of the in-service stabilized layers, and to monitor the pavement performance for each trial section.

The average deflection bowls were calculated for each of the trial sections for a series of FWD measurements. Figure 11 presents the evolution of the deflection bowls for Section 1, throughout 9 years of monitoring. After the first two measurements, it is possible to clearly observe an accommodation of the deflection bowl, maintaining relatively stabilized deflection curve since the 13$^{th}$ month after rehabilitation, and after 9 years of service. It is also possible to highlight the deflection decrease for the deflectometers closer to the weight drop, indicating the stiffening of the recycled layer.

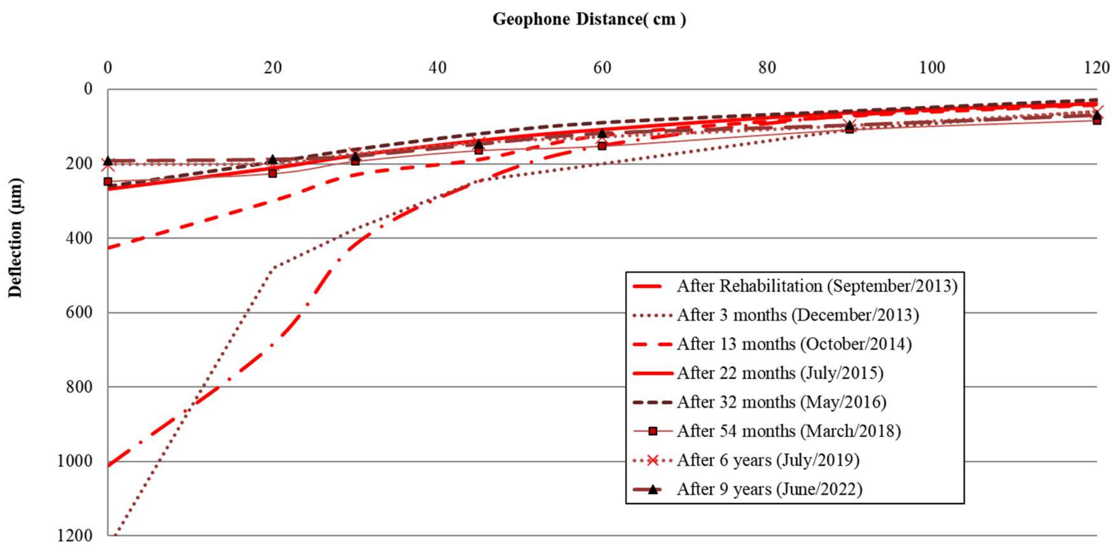


**Figure 11. Average Deflection Basin evolution – Section 1.**

It is important to note that after the first five years of service, Section 1 was subject to the application of a Micro surfacing layer, that was applied over the entire road platform due to contractual obligations and functional rehabilitation services to the adjacent lanes. This micro surfacing layer was placed directly over the gap graded wearing course and has an approximate thickness of 12 mm.

The evolution of the deflection bowl for Section 2 is presented in Figure 12, and it can be noted how small the deflections are, in general. With the existence of a 125 mm HMA layer, the maximum deflection variation with time can be a result of both the aging of the asphalt layer and the stiffening of the recycled base layer. It is interesting to point that the test from September 2016 has a higher deflection than the previous test for all deflectometers, indicating a possible seasonal effect, with the saturation of the structure and overall increase in deflection.

The deflections bowls for Section 3 are presented in Figure 13 and indicate a stabilization of the subgrade resilient modulus, with almost no variation through all monitoring period. It is also possible to observe that the deflections from deflectometers offset from 0 cm to 45 cm oscillate a lot for the first FWD tests, but seem to converge to a flatter curve, as shown in the two latest tests.

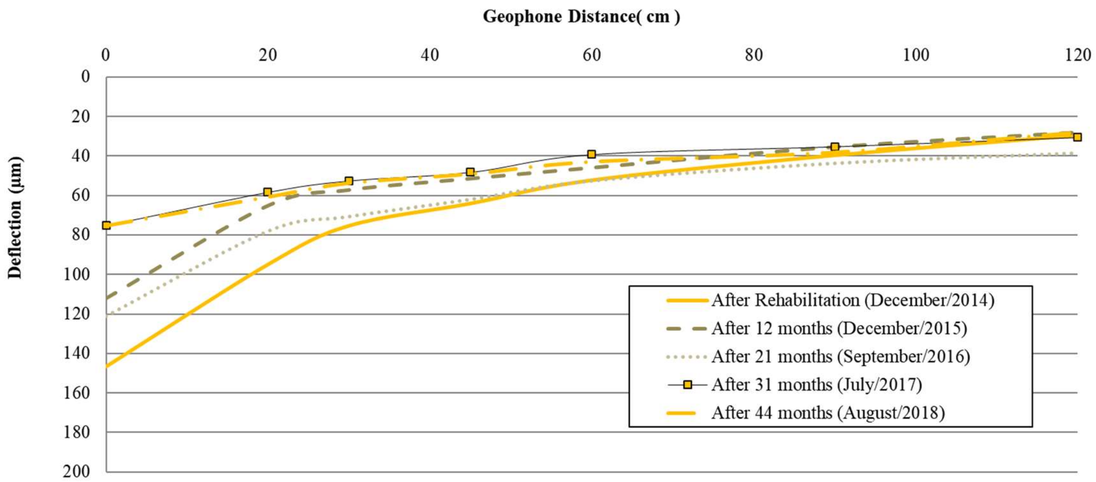


**Figure 12. Average Deflection Bowl evolution – Section 2.**

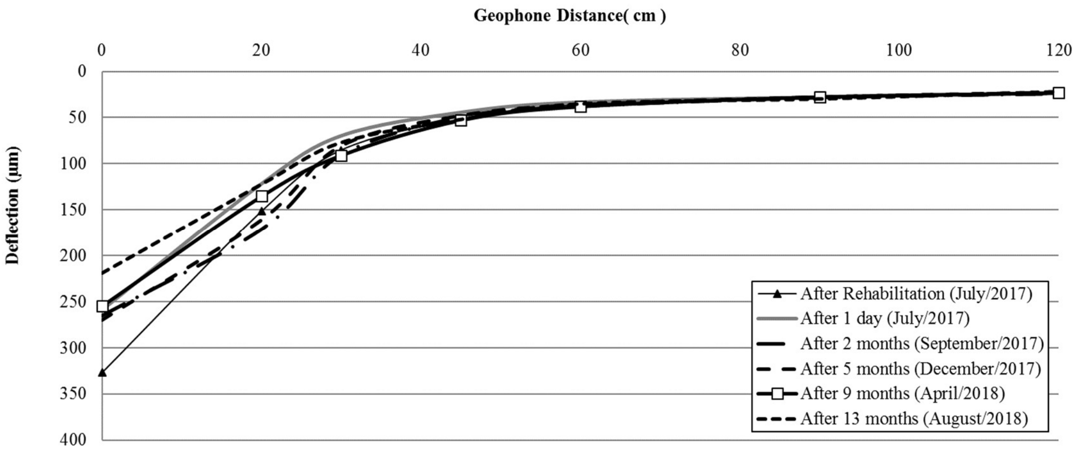


**Figure 13. Average Deflection Bowl evolution – Section 3.**

Figure 14 presents the evolution of the deflection bowls for Section 4. Although the first tests indicated a decrease in deflections, later tests indicate a lot of variation, including an increase on the maximum deflection. This could indicate the deterioration of the recycled layer, with a loss of cohesion due to excessive shear stress.

Figure 15 shows the average deflection bowl evolution during six months for the trial section 5. The deflection bowls from the FWD measurements made on Section 5 show how significant the reduction of the maximum deflection has been, in a period of six months It can also be noted how the deflection contribution from the lower layers is small, indicating that the stiffness gain comes from the upper portion of the pavement, and its 300 mm foam stabilized layer. Even after the first six months, the stabilized base still impacted the deflection bowls on the measurements made with 12 and 21 months, indicated by the decrease in deflection on the geophones closer to the loading point.

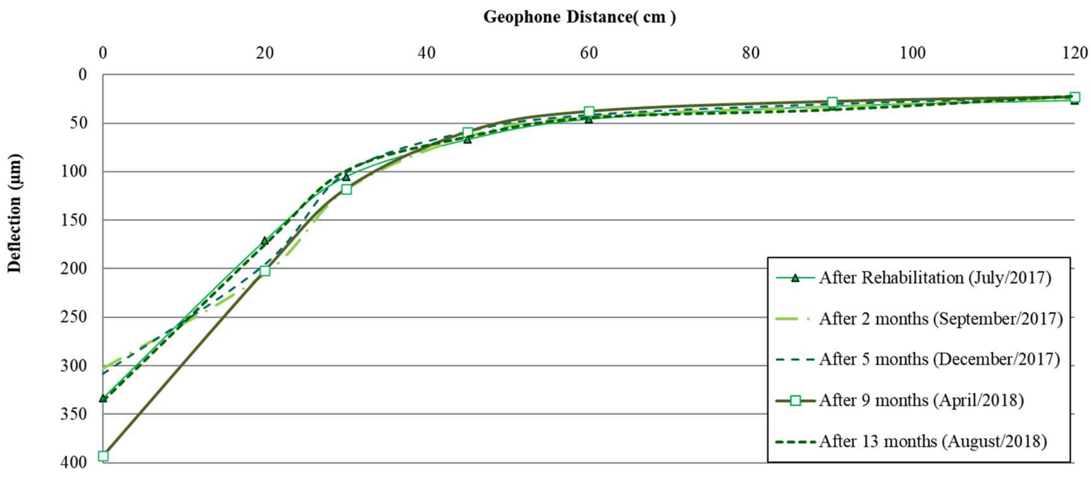


**Figure 14. Average Deflection Bowl evolution – Section 4.**

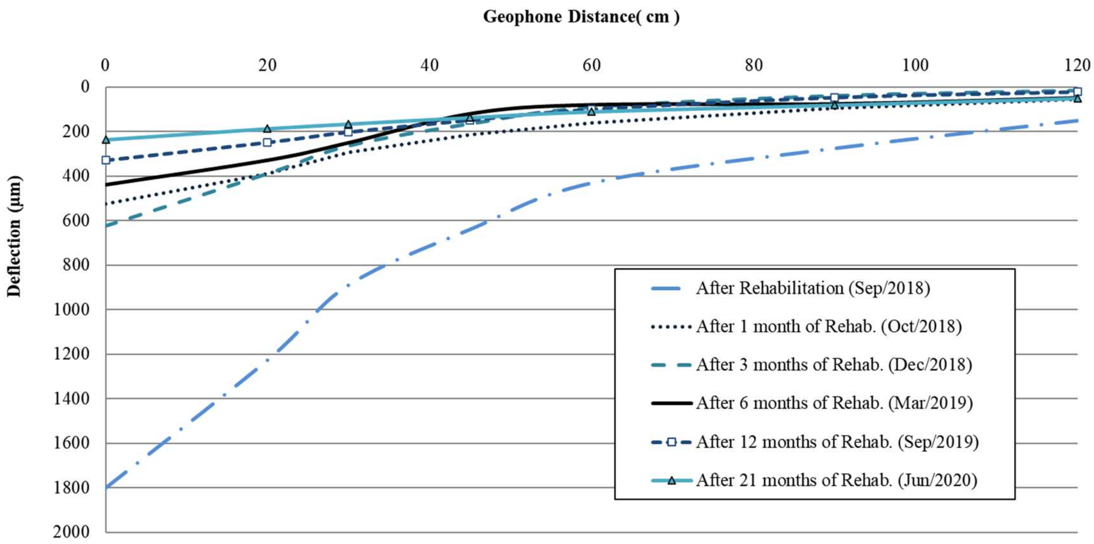


**Figure 15. Average Deflection Bowl evolution – Section 5.**

When we observe the evolution of the maximum deflection (geophone located at the load application point) for section 1 and 5, it can be noted how high they were right after the rehabilitation of the sections, and the considerable reduction observed with the curing.

### 3.4.2 Backcalculation

The FWD results obtained from the monitoring of the trial sections were backcalculated to infer the Resilient Modulus of the layers composing each section. All backcalculations were performed using the linear elastic software Elmod, from Dynatest Consulting Inc. For the backcalculations, each deflection bowl was analyzed individually, and then the average resilient modulus was calculated and presented for the layers.

To isolate the behaviour of the foam stabilized layers, all underlying layers were considered as part of a semi-infinite Remaining Substructure. For Sections 1, 3, 4 and 5, as the Gap Graded surfacing is too thin, it was not considered to be relevant to the structural behaviour. For Section 2, the 125 mm thick HMA layer was considered in the backcalculation analysis.

The results of the analysis for Section 1 presented on Figure 16 show how the remaining substructure modulus is relatively stable, with small seasonal variations. It also can be noted that the foam stabilized layer’s stiffness has reached a steady plateau after approximately two years, and aside some seasonal variation shows no sign of degradation after 9 years.

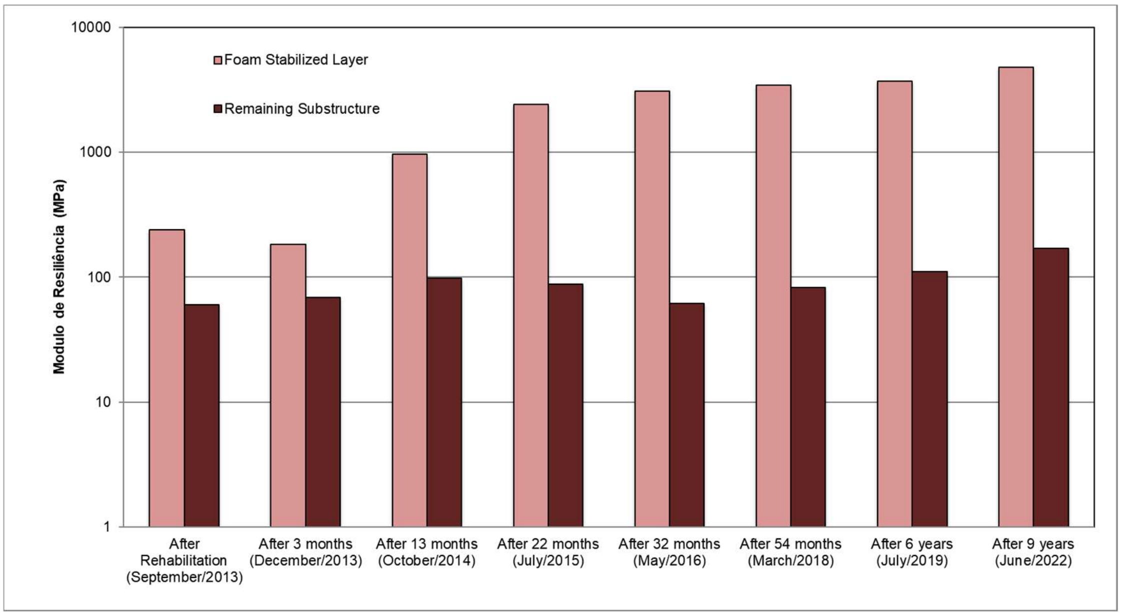


**Figure 16. Backcalculated Resilient Modulus Section 1.**

Figure 17 presents the analysis for Section 2. The resilient modulus of the stabilized layer is much higher than that found in Section 1, probably related to higher amount of asphalt binder and Portland cement in the mixture. It can be seen that the structure seems to have stabilized after the first year, with variations on the HMA modulus, probably related to the temperature effect at the time of the test on binder viscosity.

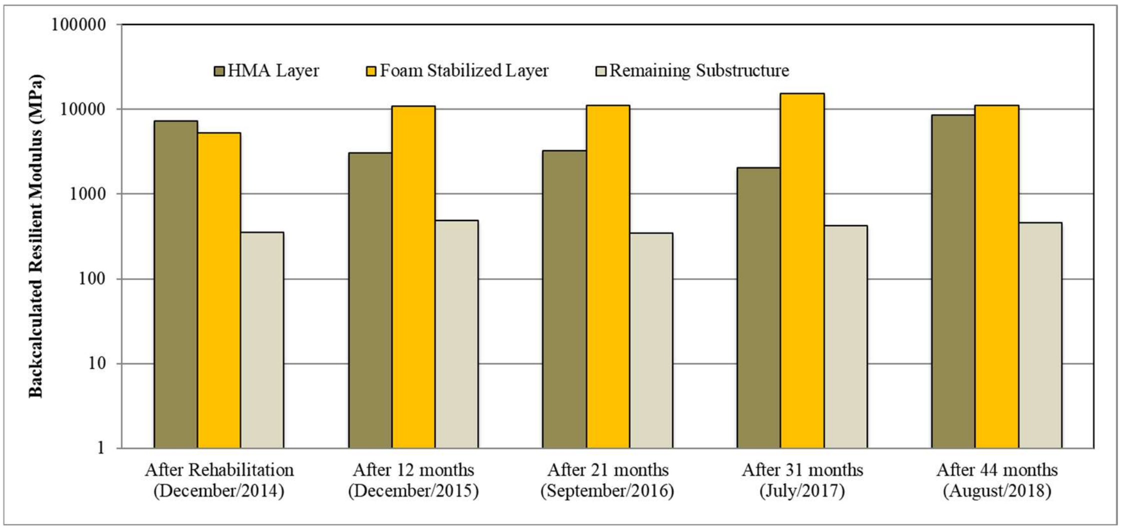


**Figure 17. Backcalculated Resilient Modulus Section 2.**

The results for Section 3 are presented in Figure 18 and show a moduli variation for both the stabilized layer and the remaining substructure, suggesting a seasonal effect. The moisture effect both on the stabilized layer and on the subgrade can be relevant. BSM materials can behave as granular materials with high cohesion, with stress dependency. The stabilized layer's Resilient Modulus is, nonetheless increasing, and no stabilization of the material stiffness was observed.

Figure 19 presents the results of the backcalculation for the foam stabilized layer in-service in Section 4 along with the remaining substructure. Similar to the results from Section 3, the stabilized material resilient modulus is oscillating a lot, with values diminishing by 30% from one survey to the other. After December/2017 it seems to have stabilized, following the tendency verified by the modulus of the remaining substructure, which might indicate a seasonal moisture variation.

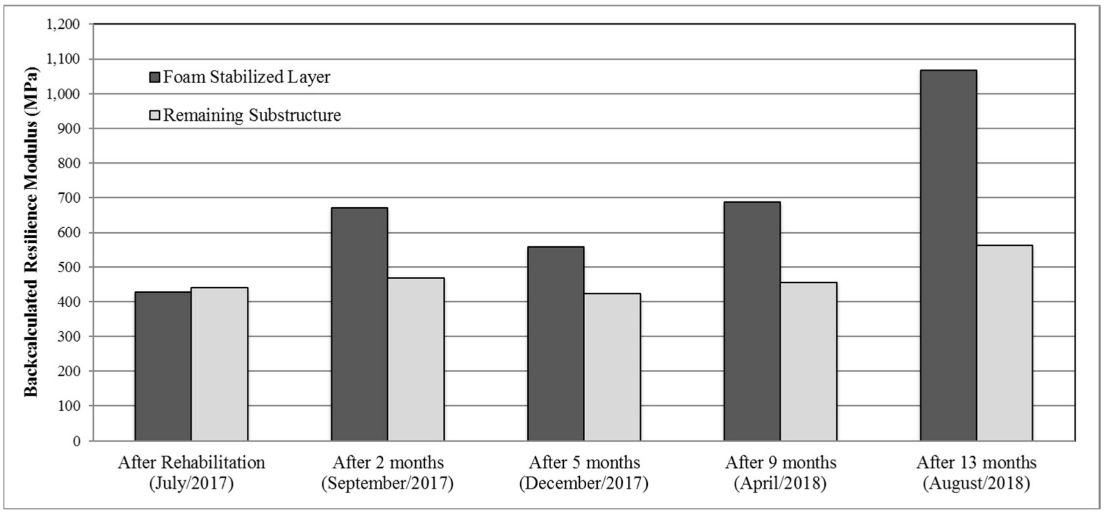


**Figure 18. Backcalculated Resilient Modulus Section 3.**

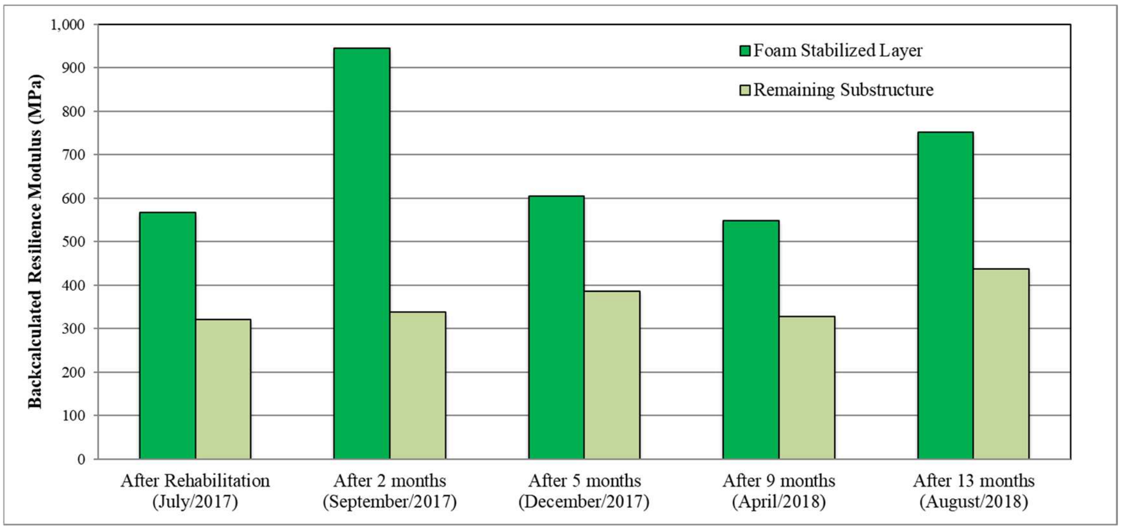


**Figure 19. Backcalculated Resilient Modulus Section 4.**

The backcalculation results for the pavement segment of section 5 is presented in Figure 20. The foam stabilized layer stiffness has increased significantly with a small decline from months 1 to 3, while increasing greatly from months 3 to 6. The observed decline can be a result of seasonal variation, with a possible increase of moisture in the base layer leading to higher deformations. It is important to note that although the months of December to March are a period of high precipitation, it is also summertime, resulting in high temperatures for lengthy periods. The high insolation and elevated temperatures during these three months have most likely contributed for the curing of the layer and its stiffness increase.

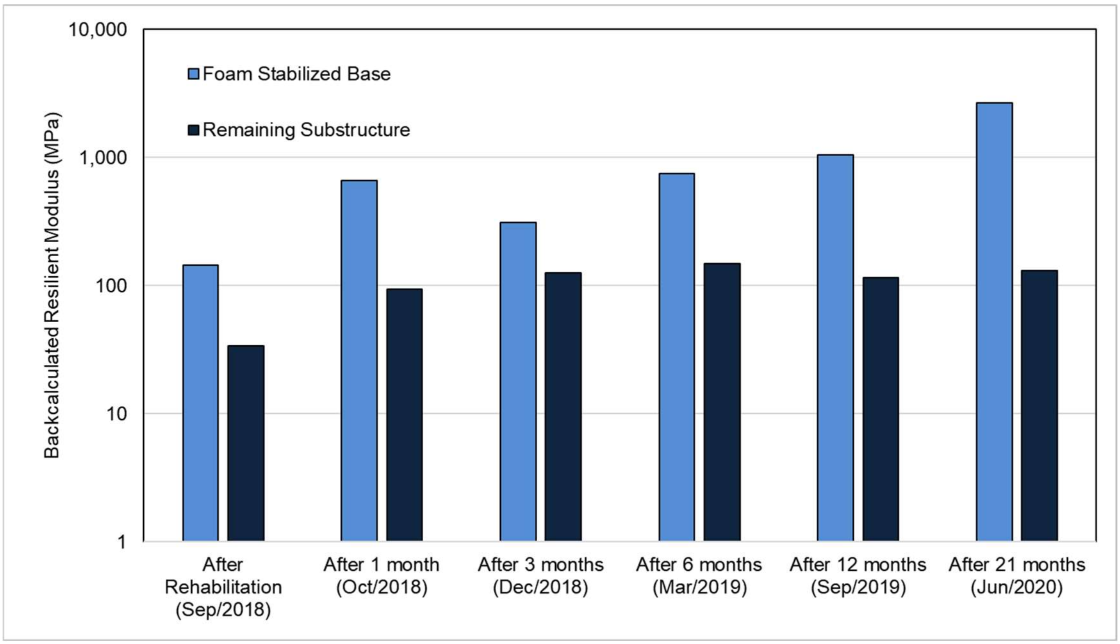


**Figure 20. Backcalculated Resilient Modulus Section 5.**

Even after the initial 12 months, it is interesting to note that the material still has gained stiffness into its second year, with a noticeable reduction in the modulus variability, indicating an uniformization of the section behaviour.

## 3.5 PARTIAL CONCLUSIONS

The analysis of the FWD monitoring showed how the sections performed during the monitoring period, which in the case of section 1 has been ongoing for 9 years, while supporting the high traffic demand of these major highways.

The five sections are located in three different highways that are managed by different concession groups, which each have different FWD monitoring spacing and frequency procedures. Since sections 2, 3 and 4 are the smallest (100 m each), to get FWD results from monitoring campaign require small spacing (10 to 20 meters) that cannot be achieved through routine more spaced tests (every 100 m). For that reason, new data has not been gathered since 2018. In the case of section 5, the rehabilitated lane is part of a toll plaza, where all lanes are not required to be tested. For that reason, these sections do not have such updated results as Section 1. According to the three managing concessions, all 5 sections are performing well, with no scheduled rehabilitation works.

Considering that, sections 1, 2 and 5 are the ones that are performing the best, as they are older with no visible deterioration, such as cracking of the asphalt surface layers, and good structural capacity based on the FWD analysis.

The asphalt wearing course on all sections was constructed immediately after the laying of the stabilized layer and the deflection right after rehabilitation was high, close to 1,000 microns for sections 1 and 5. Even under these conditions the material was able to cure and achieve stable performance with time.

The resilient modulus obtained both in the laboratory and in the backcalculation analysis presented similar results, with Section 5 with higher stiffness than sections 1, 3 and 4 in decreasing order, while Section 2 stiffness is the highest for both analysis. The high stiffness verified for the stabilized layer of section 2 can be attributed to the high incorporation rate of foamed asphalt (3.5%) and cement (2.0%), when compared to mixtures from other sessions (around 2% foamed asphalt and 1% cement). Sections 1, 3 and 5 were all rehabilitated with mixtures containing RAP, with similar resilient modulus test results, except for section 5, which tested specimens were extracted from the field instead of being laboratory made. The test results from section 3 were the lowest from all sections, while being the only mixture made with virgin crushed aggregate.

One important observation is that Section 4 started to show signs of fatigue cracking of the asphalt surface 3 months after the rehabilitation of the section. Since then, the section has been monitored by the concession with no further no signs of evolution of the degradation been reported. As a “sacrifice” wearing course for a trial section, allowing traffic over the recycled base layer while it is curing, the Gap Graded layer could present fatigue failure early, when deflections are high and the base doesn’t yet provide adequate support. Although the surface layer may be compromised, the analysis performed indicate that the base layer is still in good condition.

However, pavement deformability and how fast curing takes place influence directly on the surfacing service life. The trial section structures had to be open to traffic immediately, and it has taken them 6 to 12 months for the pavement to cure, while pavement deformability measured through surface deflections during this period were moderately high. In this sense, it is critical that the design of the asphalt wearing course receive special considerations such as the use of modified binders, improving its performance during the curing period.

Although it was not possible in the evaluated trial sections, a different approach would be to allow the base material to cure before laying the wearing course. During this period the material would gain stiffness, due to moisture evaporation, and if possible, material densification through traffic loading. This would accelerate the material curing and early traffic consolidation, allowing the wearing course to be laid on top of better support, and already correcting any early deformation the base may present (Lewis and Collings, 1999; Feisthauer et al. 2013; Jones et al. 2009).

Pavement design for Sections 3 and 4 adopted similar moduli for the base layer, but as seen on the results of the TxRM tests, the material used on the base layer of Section 3 has slightly higher stiffness. This may have been the difference factor accelerating the fatigue cracking in section 4.

The five sections have shown with the data collected until 2022, that foamed bitumen stabilization can be used as a good alternative for the base course of pavements subjected to high traffic volume.

# 4 IN SITU TEMPERATURE SENSITITVITY OF FOAMED STABILIZED ASPHALT LAYER

## 4.1 INTRODUCTION

The growth of cold recycling techniques in the last two decades has been highly motivated by the possibility of saving resources, limiting environmental impacts and the inherent performance benefits of the technique. Road maintenance results in a high annual production of waste asphalt materials that can be used for pavement rehabilitation and construction of new structures through cold recycling (Godenzoni et al., 2018). Foamed bitumen stabilization is one of the techniques of cold recycling that has grown the most in recent years, with successful applications in different countries such as New Zealand (Saleh and Herrington, 2003) South Africa (Collings et al., 2004; Jooste and Long, 2007; Bredenhann and Jenkins, 2015), Australia (Ramanujam and Jones, 2007; AUSTROADS, 2015), USA (Fu et al. 2008; Bang et al., 2011; Jones et al., 2014; Khosravifar et al., 2015), Italy (Betti et al., 2017; Cardone et al., 2015), Greece ( Loizos et al., 2012) and Brazil (Martinez et al., 2013; Andrade et al., 2016., Guatimosim et al., 2018).

Through the process of foam stabilization, the injection of air and water into hot bitumen forms bitumen bubbles, that in contact with the aggregate burst into bitumen splinters that disperse through the aggregates (Campher, 2015). During the bitumen dispersion through the mix, the bitumen droplets tend to adhere to and coat the finer grains, resulting in a bitumen-bound filler binding the coarser aggregates (Mulusa, 2009). Because of the stabilization process and the bitumen dispersion mechanism, the foamed mixture can be characterized as a non-continuously bound material, with a high content of voids, partial coated aggregates and a mortar phase providing an improved cohesion (Collings and Jenkins, 2011).

Although the material is not continuously bound as the Hot Mix Asphalt (HMA), some of the viscoelastic behaviour of these mixes can also be identified in foamed mixes (Collings and Jenkins, 2011; Kuchiishi et al. 2019). Due to the presence of the bitumen, and its rheological properties, foamed stabilized materials exhibit the temperature-dependent behavior (Fu and Harvey, 2007). As studies show that mixes containing high reclaimed asphalt pavement (RAP) content present temperature dependent behaviour, not only the bitumen binder from foam stabilization, but also the mix composition can affect the temperature sensitivity (Dal Ben, 2014). That creates a challenge for the evaluation of the temperature dependency, as cold recycled mixtures tend to exhibit great variability from one project to another.

When analyzing the in-situ performance of foamed stabilized layers, the assessment of temperature sensitivity is particularly important, as the material stiffness will vary with different environmental conditions, which cannot be controlled on field studies. Assessing the effect of temperature on stiffness makes it possible to analyze Falling Weight Deflectometer (FWD) field data, isolating temperature induced stiffness variation from the effect of material moisture and curing on the foamed asphalt layer.

Based on an existing trial section, located on highway BR-116/SP in Brazil (Gutierrez et al. 2019), the temperature sensitivity of the foamed asphalt layer was analyzed using FWD tests along with daytime temperatures, assessing temperature change and also stiffness variation through backcalculation. The objectives of this study were to: (i) determine the foamed asphalt material sensitivity to temperature change, (ii) compare the results with existing studies, and (iii) suggest a parameter for backcalculated moduli correction using temperature data.

## 4.2 LITERATURE REVIEW

The lack of a standard model that reliably describes how sensitive foamed asphalt materials are to temperature changes has to do with the immense variability on the nature and content of the different aggregates and binders involved in the process. Although this evaluation can be performed in a controlled environment such as the laboratory, the conditions to which the material is subject in the field are more complex. The stage of the curing process, the moisture content, the temperature gradient, and the existing pavement layers are some of the field variables.

The aggregate composition of the foamed asphalt stabilized layer is also a defining parameter on the layer sensitivity to temperature. Dal Ben (2014) investigated the laboratory temperature conductivity on foamed asphalt bases with different combinations of RAP and virgin aggregate, with higher temperature conductivity related to higher RAP contents.

Attempts have been made to capture the in situ sensitivity of foamed asphalt mixtures to temperature change (Fu and Harvey, 2007; Plati et al., 2010; Betti et al., 2017; Gandi et al., 2019), using different models. Plati et al. (2010) presented a model to estimate the foamed asphalt layer modulus at a reference temperature using equation (4.1), a laboratory estimated function developed by Loizos and Papavasilisou (2007).

$$E_{FB}\,(20°C) = E_{FB}\,(T) \times 1.037^{(T-20)} \tag{4.1}$$

where: $E_{FB}$ (20°C) = Estimated Modulus at 20°C in (MPa);

$E_{FB}$ (T) = Modulus at the measured temperature in (MPa).

T = Measured Temperature in (°C).

Before that, Fu and Harvey (2007) used different backcalculated modulus results from extensive FWD surveys, conducted in two different years over two days each, testing pavements at different temperatures throughout the day. Surface temperature measurements were made using infrared sensors, and then mid-layer temperature was calculated using BELLS2 equation (Fernando and Liu, 2001). The model used to normalize the stiffness to a reference temperature in that research is the one presented in equation (4.2).

$$E_{FB}\,(T0) = 10^{\alpha\,(T-T0)} \times E_{FB}\,(T) \tag{4.2}$$

where: $E_{FB}$ (T0) = Estimated Modulus at the reference temperature in (MPa);

T and T0 = Measured and Reference Temperatures in (°C);

$\alpha$ = Temperature sensitivity coefficient.

The temperature sensitivity coefficients calculated by the authors were 0.030 and 0.016, for the deflections measured in 2003 and 2005, respectively. The authors point out that it could indicate that as the foamed stabilized layer gets older, and the rheology of the existing binder changes as it oxidizes and becomes stiffer, the material temperature sensitivity decreases.

Similarly to what was done by Fu and Harvey (2007), Betti et al. (2017) also used FWD data to calculate temperature sensitivity coefficients. In this study, the analysis was performed for six sections containing different RAP mixes, with different amounts of foamed bitumen (FB), cement (C), lime (L) and mineral filler (MF) ranging from 2.0-3.0%, 0.0-2.5%, 0.0-3.0% and 0.0-3.5%, respectively. For the determination of the temperature sensitivity coefficient ($\alpha$), the FWD results for each section were used with temperature data gathered with a thermometer placed through a hole drilled on the pavement, so that the temperature sensitivity coefficient could be determined through linear regression. The equation model used for temperature correction was a generalized version of the one adopted by the Asphalt Institute for temperature correction of HMA layers, presented in equation (4.3), using $\alpha = 1{,}47362 \times 10^{-4}$ (Harichandran et al., 2000):

$$E_{FB}\,(T0) = 10^{\alpha\,(T^{\wedge}2\,-\,T0^{\wedge}2)} \times E_{FB}\,(T) \tag{4.3}$$

For each mix, a different $\alpha$ was calculated, as presented in Table 1, along with the recycled mixtures compositions and the modulus of the foamed stabilized material adjusted to 20 °C. It is interesting to observe that the total amount of filler addition to all mixtures was the same, 4.5%, and mixture 3B was the one with the most Mineral Filler added, and the one with smaller $\alpha$. That might indicate that fillers such as lime and cement induce a higher temperature sensitivity, possibly due to a better dispersion of the foamed asphalt during the stabilization process, but no conclusions were obtained on that matter.

Also, it is noteworthy that the coefficients obtained in this analysis were two to seven times smaller than the coefficient recommended by the Asphalt Institute for HMA moduli correction.

**Table 11. Mix compositions, modulus at reference temperature after 9 months of curing and temperature sensitivity coefficient calculated (adapted from Betti et al., 2017)**

| Mixture | FB (%) | C (%) | L (%) | MF (%) | E (MPa) at 20 °C | α |
|---|---|---|---|---|---|---|
| 3A | 2.0 | 1.0 | 2.0 | 1.5 | 1615 | $0.57 \times 10^{-4}$ |
| 3B | 2.0 | 1.0 | 0.0 | 3.5 | 1654 | $0.19 \times 10^{-4}$ |
| 5C | 3.0 | 2.5 | 2.0 | 0.0 | 1789 | $0.43 \times 10^{-4}$ |
| 5D | 3.0 | 2.5 | 0.0 | 2.0 | 1722 | $0.30 \times 10^{-4}$ |
| 5E | 3.0 | 0.0 | 2.0 | 2.5 | 1608 | $0.32 \times 10^{-4}$ |
| 5F | 3.0 | 0.0 | 3.0 | 1.5 | 1258 | $0.38 \times 10^{-4}$ |

When comparing the models developed or used in the three studies, it can be noted that the one proposed by Plati et al. (2010) and shown in Equation (1) does not allow for any curve adjustment depending on the mix, while the other two models shown in Equations (2) and (3) depend on an α coefficient that represents the studied mix temperature sensitivity as an input. That makes the models used by Fu and Harvey (2007) and Betti et al. (2017) more versatile, as you can use a specific temperature sensitivity coefficient for the studied mix.

## 4.3 TRIAL SECTION

The trial section used in this study is a 200-meter section located in an automatic toll lane of highway BR-116/SP, under the toll concession CCR Nova Dutra, as shown in Figure 1. The highway is the main road connecting São Paulo and Rio de Janeiro, two big cities, with an industrial and heavily populated area in between. The estimated number of expected AASHTO equivalent single axles for the next ten years for that section is greater than 60 million.

The section was built on the far-right automatic toll lane, destined for heavy commercial vehicles, where the vehicles must slow their speed from around 80 km/h to 40 km/h to pass the toll gates. The section site was previously the road shoulder that was adapted into an additional lane for the automatic toll. For that reason, the existing pavement structure was highly degraded and had to be rehabilitated. The existing surface and base course were milled, and a 300 mm recycled base was placed on top of the remaining granular layers, with a 35 mm Gap Graded surface layer on top. The final pavement structure was composed of 35 mm of Gap Graded surface Course, 300 mm of foamed asphalt base, on top of a remaining 200 mm of existing granular layer.

The foamed asphalt mix was composed by 85% of RAP, with 15% of stone crusher dust used for adjustment of the material grading, 2.3% of foamed asphalt and an additional 1.0% of hydrated lime as active filler. The designed mix achieved 2060kg/m³ maximum bulk density with a Modified Proctor compaction effort, and optimum moisture content of 5.4%. The rehabilitation was performed in September of 2018, with the section being monitored through the following two years with FWD tests.

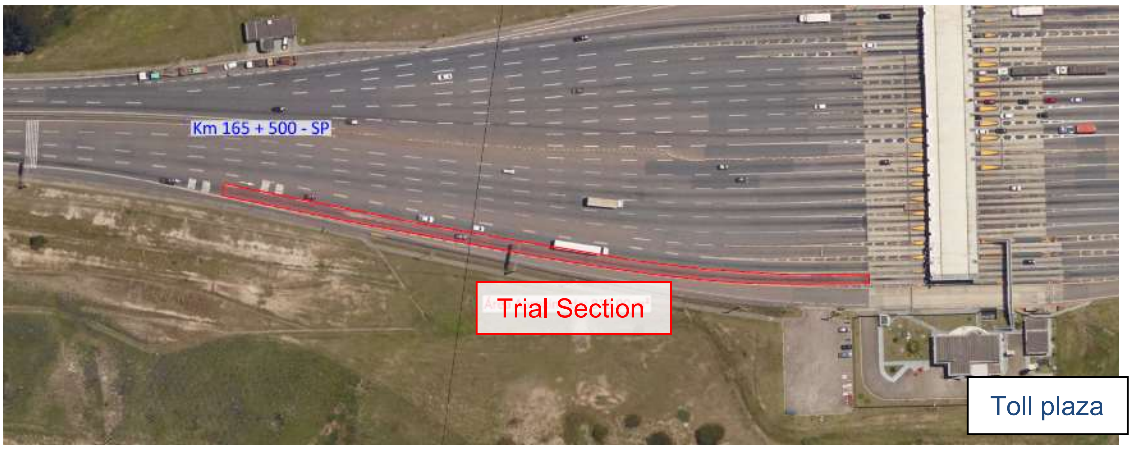


**Figure 21. Trial section position on BR-116/SP.**

## 4.4 FWD TESTS AND TEMPERATURE MEASUREMENTS

### 4.4.1 FWD Monitoring

Pavement monitoring has been performed using deflection data obtained from FWD tests on the rehabilitation day, and also done at 1, 3, 6, 12 and 21 months after the rehabilitation day. The FWD equipment used for these surveys was a KUAB 50, with a sequence of 2 drops of 40 kN load on a 300 mm diameter plate used for each measurement. Throughout these months, pavement deflection has decreased significantly, because of material curing and layer stiffness gain.

The curing in foamed stabilized layers is a process where the bonds between aggregates and the dispersed asphalt binder increase the material stiffness, as moisture contents decrease (Twagira, 2010), reducing lubrication between the particles, and increasing shear strength (Lynch, 2013). Moisture decrease happens due to a combination of factors including porosity of foamed asphalt material, temperature gradient, relative humidity and wind speed, which all directly impact the evaporation rate, but also because of drainage, and mechanical friction as grains are forced against each other under loading, expelling water from the contact area.

As environmental conditions cannot be controlled in the field, water ingress can happen because of rainfall, resulting in a long period until the foamed material achieves a more stable cured condition. As observed by Kuchiishi et al. (2019) using triaxial resilient modulus tests, after the initial curing period, a new increase in moisture can result in a loss of stiffness, but some of it is retained, not returning to its pre-curing condition. In this sense, while some sections may achieve full strength within short periods such as a month (Mulusa, 2009), curing can undergo periods longer than a year (Lynch, 2013; Collings et al. 2015).

The rehabilitation segment is a confined lane, meaning that the adjacent pavements have different layers and material configurations. This section was designed as a more permeable structure compared to the one in the adjacent inner lane, so that drainage would be possible. The outer adjacent lane is the road shoulder, with primarily granular structure and an HMA surface layer, which allows subsurface drainage while limiting surface permeability.

As the foamed asphalt base cured in service, the maximum deflections through the segment decreased, as shown in Figure 2. The deflection bowls presented in the graph correspond to the 90th percentile highest deflections amongst measurements made in each FWD survey. It can be observed how the deflections decreased significantly in the first month, increasing slightly after 3 months, reaching the lowest values on the 21st month. The slight increase between the 1st and 3rd months is probably due to the rainy season, as the average temperature on both surveys were around 22°C.

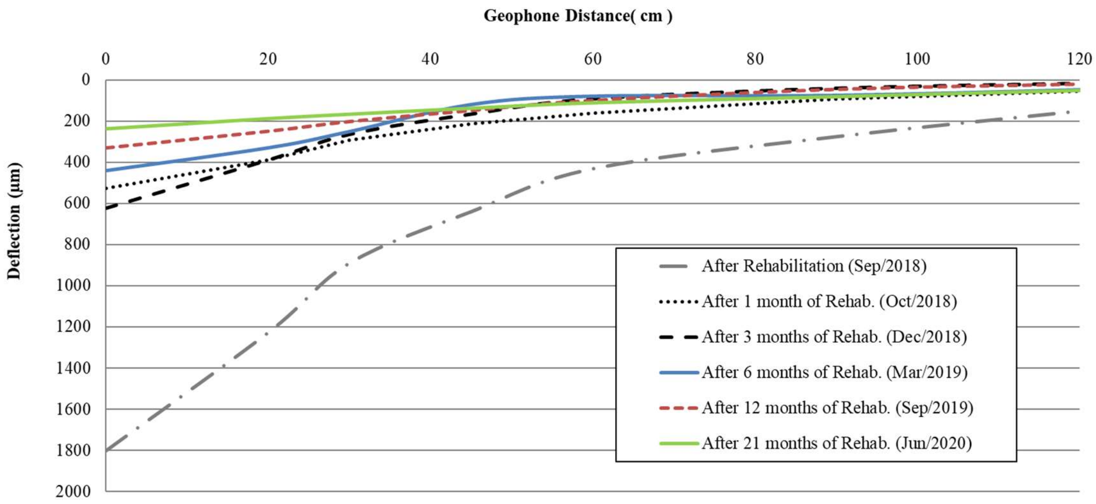


**Figure 22. Trial section 90th percentile deflection bowls, at different moments of the curing process.**

Although great variability was observed for the deflections on the first FWD survey (Figure 3), as time allowed the material to cure, a reduction in the maximum deflection dispersion throughout the section was observed, as shown in Figures 3 to 8. The graphs show the deflection bowls obtained by tests every 20 meters along the trial section, in different moments in time and with pavement surface temperatures ranging from 21°C to 27° C. This initial variability can be attributed to the difference in support within the section, as indicated by the backcalculated resilient moduli of the support structure, that ranged from 34 MPa to almost 300 MPa. As the previously existing distressed pavement was rehabilitated and the foamed asphalt base material cured, the permeability conditions improved, and moisture reduced in the entire structure, allowing for higher resilient moduli being measured for the foamed asphalt base and the underlying layers.

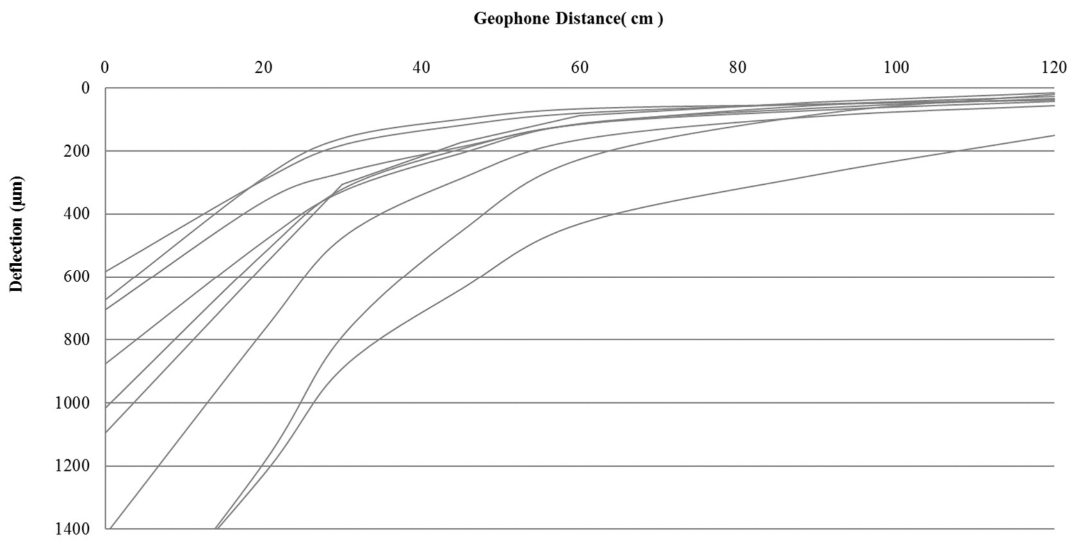


**Figure 23. Deflection bowls along the trial section with the day after rehabilitation (Sep/2018). Pavement surface temperature was between 21°C and 22°C.**

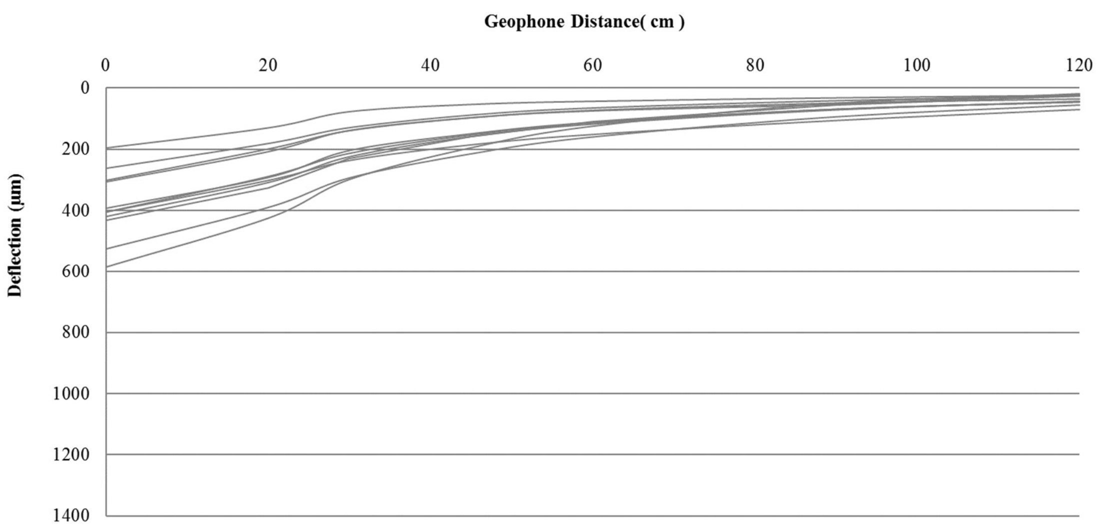


**Figure 24. Deflection bowls along the trial section one month after rehabilitation (Oct/2018). Pavement surface temperature was around 21°C.**

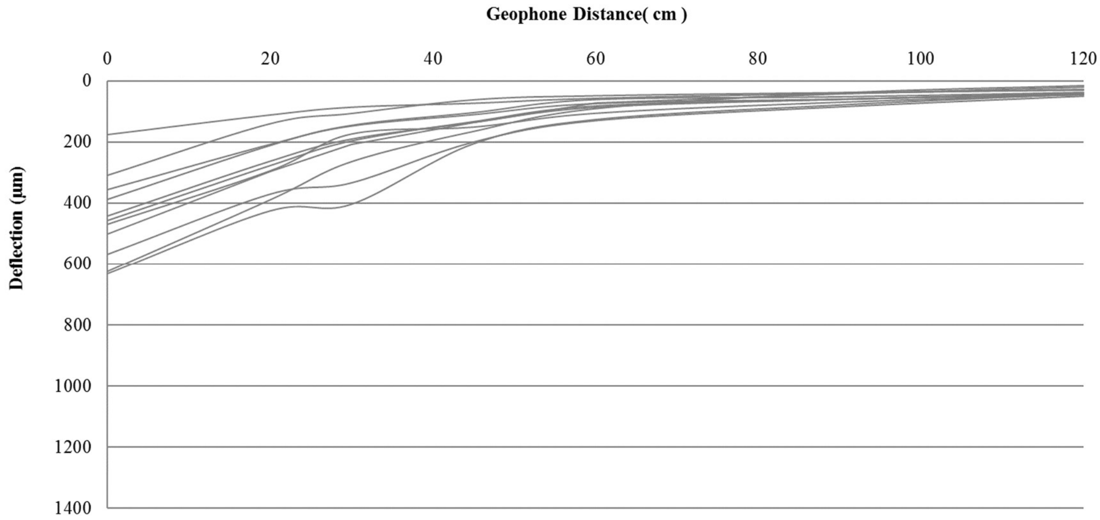


**Figure 25. Deflection bowls along the trial section three months after rehabilitation (Dec/2018). Pavement surface temperature was around 22°C.**

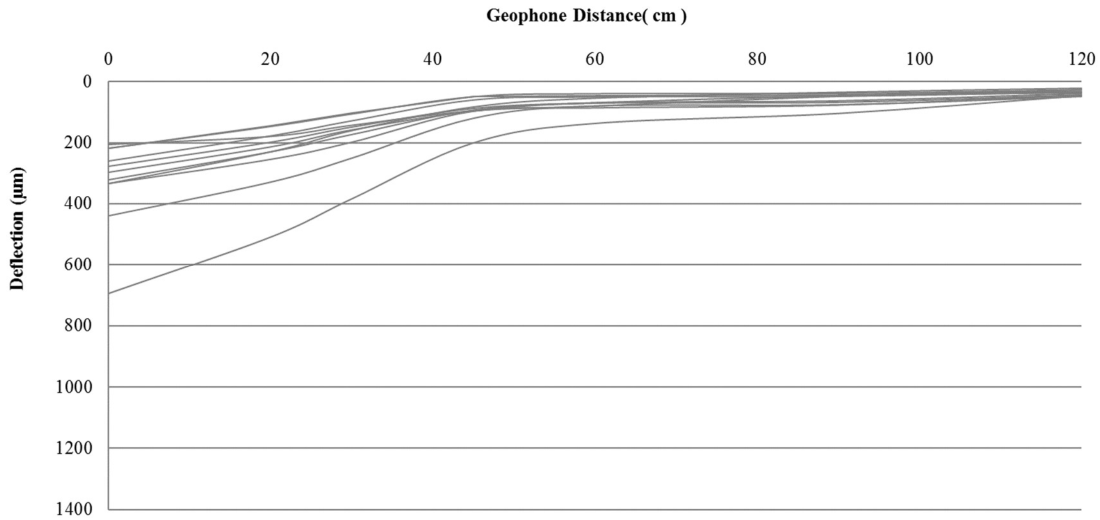


**Figure 26. Deflection bowls along the trial section six months after rehabilitation (Mar/2019). Pavement surface temperature was between 26°C and 27°C.**

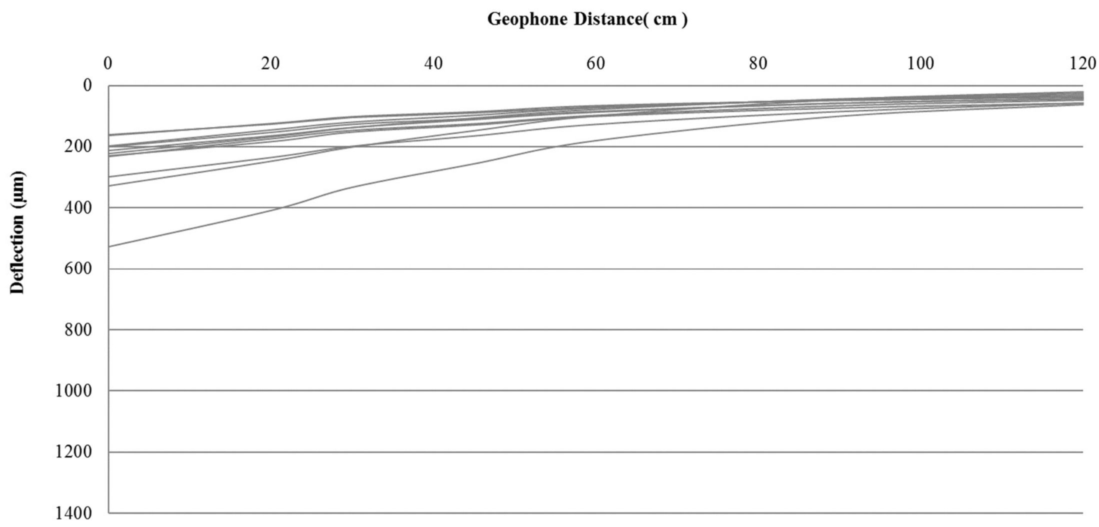


**Figure 27. Deflection bowls along the trial section twelve months after rehabilitation (Sep/2019). Pavement surface temperature was between 22°C and 23°C.**

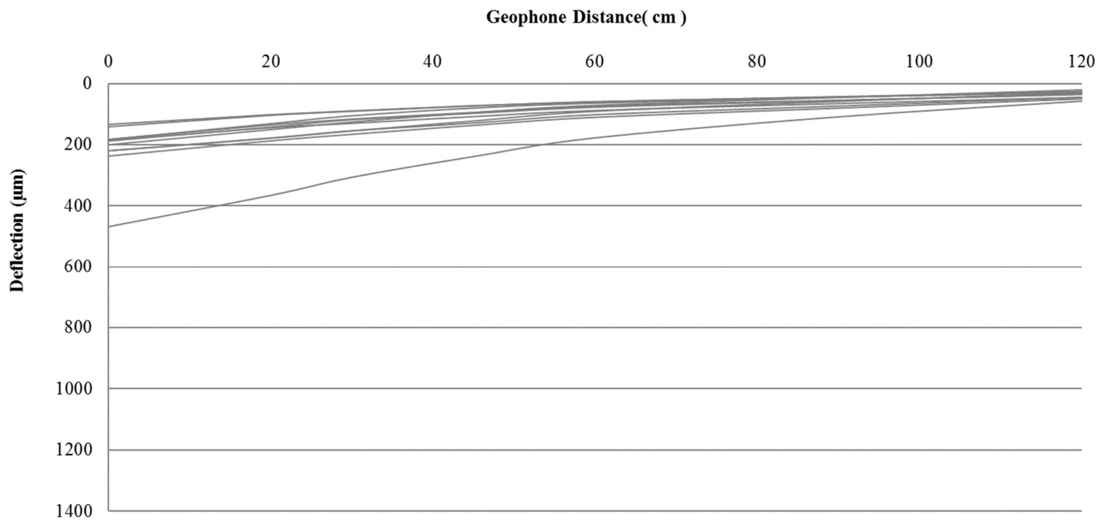


**Figure 28. Deflection bowls along the trial section twenty-one months after rehabilitation (Jun/2020). Pavement surface temperature was approximately 25°C.**

### 4.4.2 **Instrumentation and Temperature Monitoring**

During the FWD campaign in March 2019 (Figure 9 (a)), after 6 months of rehabilitation (end of the rainy season in this Brazilian region), an extended FWD survey was performed, with deflections been measured in the entire section at different times during the day to evaluate how the material stiffness changes as temperature changes. The deflection measurements were obtained at the center of the lane and the outer and inner wheel paths.

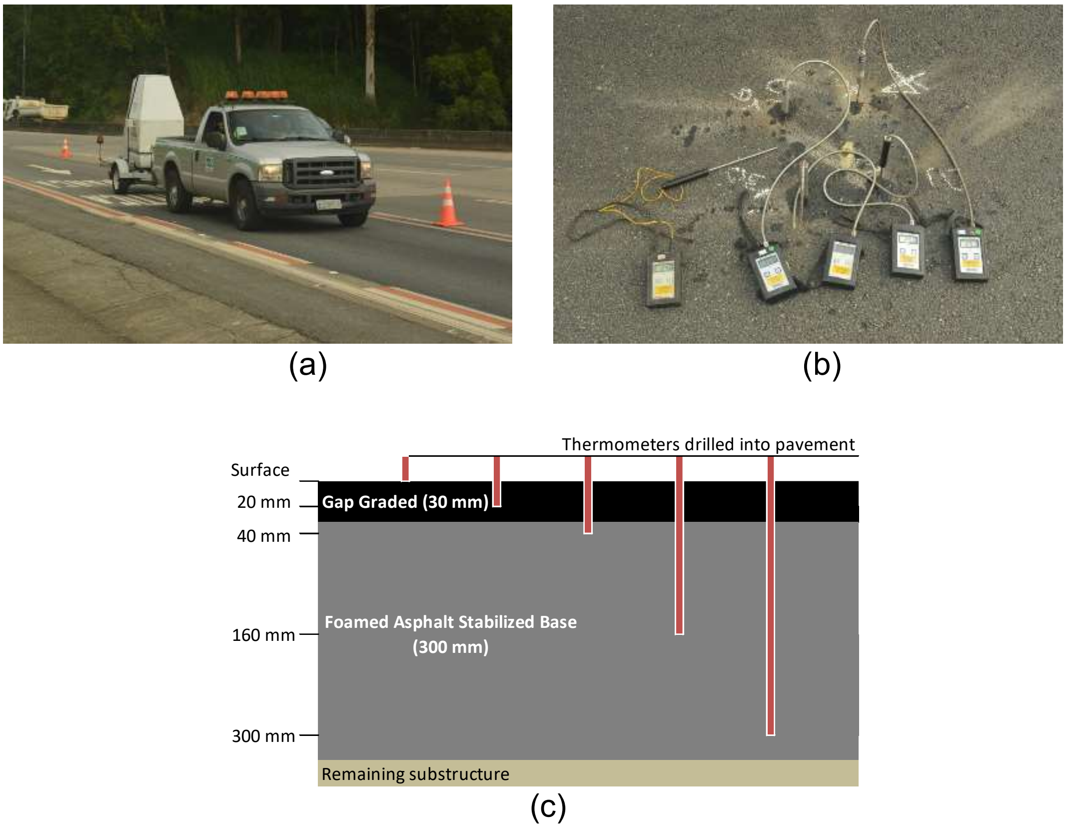


**Figure 29. (a) FWD equipment on the trial section; (b) thermometers positioned at the drilled holes to measure pavement temperature, (c) Thermometer positioning schematic.**

Holes were drilled to different depths in the pavement to assess the pavement temperature gradient as shown in Figures 9(b) and 3(c). Temperature was measured hourly, at the surface, and at depths of 20 mm, 40 mm, 160 mm and 300 mm, in the middle of the asphalt layer, the top, middle and bottom of the foamed base, respectively, so that a temperature gradient could be determined. The drilled holes were filled with liquid Vaseline, so that the inserted thermometers would have sufficient contact area to adequately assess the temperature. After insertion, the thermometers were left for approximately 15 minutes until temperature stabilization, so that it could be registered.

The same protocol of temperature gradient assessment and FWD testing during the day was later repeated for the monitoring surveys with 12 months and 21 months. The measured temperatures for the three surveys (6, 12 and 21 months after rehabilitation) are shown in Table 2, separated by the time of the measurement and the pavement depth.

**Table 12. Temperature measured at different day times and depths on the evaluated section in degrees Celsius (°C).**

| Pav. Depth (mm) | Time of day - 6 months after rehabilitation | | | | | | | | | | | |
|---|---|---|---|---|---|---|---|---|---|---|---|---|
| | 7:15 | 8:15 | 9:15 | 10:15 | 11:15 | 12:15 | 13:15 | 14:15 | 15:00 | 16:00 | 17:00 | 18:00 |
| Air | 19 | 22 | 25 | 28 | 29 | | 31 | 30 | | | | |
| 0 | 24 | 29 | 35 | 40 | 45 | | 50 | 51 | | | | |
| 20 | 26 | 27 | 34 | 37 | 42 | | 44 | 47 | | | | |
| 40 | 26 | 26 | 30 | 28 | 37 | | 31 | 47 | | | | |
| 160 | 28 | 28 | 29 | 29 | 31 | | 38 | 38 | | | | |
| 300 | 31 | 31 | 34 | 30 | 30 | | 30 | 25 | | | | |
| Pav. Depth (mm)) | Time of day - 12 months after rehabilitation | | | | | | | | | | | |
| | 7:00 | 8:00 | 9:15 | 10:20 | 11:13 | 12:00 | 13:00 | 14:02 | 15:30 | 16:00 | 17:00 | 18:00 |
| Air | | 18 | 18 | 19 | 19 | | | 20 | 20 | | | |
| 0 | | 20 | 20 | 22 | 21 | | | 23 | 22 | | | |
| 20 | | 18 | 19 | 21 | 21 | | | 23 | 22 | | | |
| 40 | | 18 | 19 | 19 | 19 | | | 21 | 21 | | | |
| 160 | | 21 | 20 | 21 | 21 | | | 22 | 22 | | | |
| 300 | | 24 | 23 | 23 | 23 | | | 23 | 24 | | | |
| Pav. Depth (mm) | Time of day - 21 months after rehabilitation | | | | | | | | | | | |
| | 7:30 | 8:24 | 9:24 | 10:30 | 11:24 | 12:00 | 13:00 | 14:00 | 15:00 | 16:00 | 17:00 | 18:00 |
| Air | 16 | 17 | 19 | 20 | 21 | 22 | 23 | 27 | 28 | 27 | 24 | 23 |
| 0 | 18 | 19 | 21 | 25 | 23 | 25 | 25 | 27 | 34 | 32 | 30 | 26 |
| 20 | 19 | 20 | 21 | 23 | 24 | 27 | 26 | 27 | 35 | 34 | 32 | 28 |
| 40 | 20 | 19 | 20 | 23 | 23 | 24 | 24 | 26 | 32 | 32 | 32 | 30 |
| 160 | 22 | 23 | 22 | 21 | 23 | 22 | 21 | 22 | 25 | 26 | 29 | 27 |
| 300 | 24 | 23 | 23 | 23 | 23 | 23 | 23 | 24 | 23 | 25 | 26 | 26 |
| | | | | | | | | | | | | |
| Scale (°C) | 50 | 47 | 44 | 40 | 37 | 34 | 31 | 28 | 24 | 21 | 18 | 15 |

It is noteworthy that the temperature on the bottom of the BSM layer, at 300 mm depth suffers small variation during the day. The temperature at the surface, however, presents a higher amplitude, as a result of direct sunlight heating the asphalt layer. As it can be noted for the survey with 6 months of the rehabilitation, early in the morning, the temperature at the bottom of the foamed asphalt base layer is as high as 30 °C, which can be an indication of how long it takes for the pavement temperature to reduce, and the influence of previous days average temperatures, as considered in the BELLS2 model Fernando and Liu (2001).

During the day the temperature of the foamed asphalt material is constantly changing, trying to reach an equilibrium between the fast-changing surface layer temperature and the steadier bottom of the base layer temperature. The survey within 21 months of the rehabilitation shows how in the morning the surface temperature is colder than the bottom temperature, creating a clear gradient. As the day advances, though, the surface layer is heated by sunlight, increasing its temperature, and the foamed asphalt layer slowly heats from the top down, creating a situation where the temperature is colder in the middle of the layer from around 10:00 until 14:00. Afterwards, by the end of the afternoon, the gradient is clear again, with the top of the foamed layer warmer than its bottom.

The variability of measured deflections was high throughout the section, as shown in Figure 10. The graph shows deflections on three different points along the section, representing the lowest, average, and maximum values of maximum deflection, measured early in the morning and late in the afternoon. The average pavement temperature at 7 AM was around 21 °C, rising to 29 °C by 5 PM.

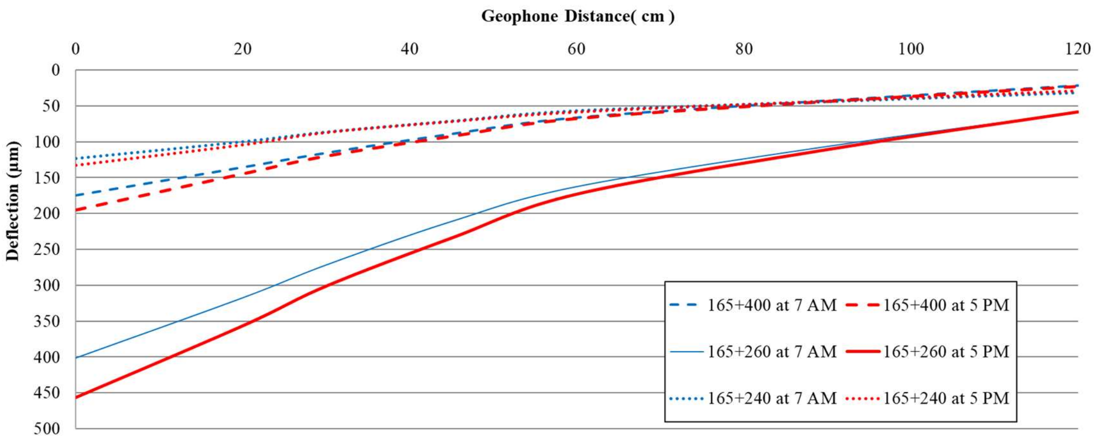


**Figure 30. Deflection bowls for minimum, average and maximum values of individual maximum deflection, at different times of the day**

It is interesting to observe how the increase in the temperature of the foamed asphalt base and the Gap Graded wearing course affect the overall deflection, with a lower impact for stiffer pavements. It is also noteworthy that within the same pavement, section deflections can vary significantly, probably affected by compaction, moisture and other localized boundary conditions.

### 4.4.3 Resilient Moduli Backcalculation

The FWD deflection bowls were used to backcalculate the resilient modulus of the foamed asphalt stabilized layer and the support layer. All backcalculations were performed using the linear elastic software Elmod, from Dynatest Consulting Inc. For the backcalculations, the deflection bowls measured were all analyzed individually, and then the average resilient modulus was calculated and presented for the layers. To isolate the behaviour of the foam stabilized layers, all underlying layers were considered as part of a semi-infinite remaining substructure. The Gap Graded surfacing on top of the Foamed asphalt base is 35 mm thick and was considered as the first layer, followed by the 300 mm foamed asphalt stabilized layer and the remaining substructure as the final third layer.

Temperature correction for the Gap Graded resilient modulus was performed using the temperature at 20 mm depth and equation (4.3), with $\alpha = 1.47362 \times 10^{-4}$, as proposed by Harichandran et al. (2000). As the survey performed at 21 months from rehabilitation had the greatest number of FWD tests and temperature measurements, the results of the average backcalculated resilient modulus for each hour of the day for this survey are presented on Figure 11. It can be noted some variation of the HMA and Foamed Asphalt base stiffness indicated by the error markers, that could be related to the variation of the support and material consolidation conditions, although no significant differences were observed between the tests performed in the middle of the lane and in either wheel path. Similar to granular materials that exhibit stress dependent behaviour, the low support stiffness results in less confinement of the foamed stabilized base, yielding a lower resilient modulus.

It can also be observed how the slope indicating the decrease in stiffness for the wearing course is greater than that of the foamed asphalt base, decreasing from around 5,200 MPa to 3,000 MPa, whereas the modulus of the base is reduced from around 3,100 MPa to 2,600 MPa. That could be a result of the effect of the higher asphalt binder content on the hot mix wearing course.

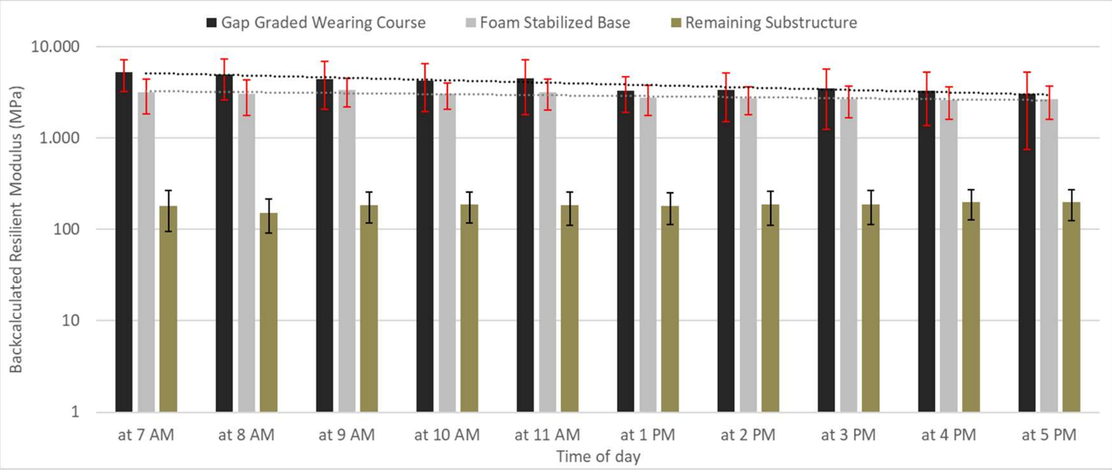


**Figure 31. Average backcalculated Resilient Modulus after 6 months of rehabilitation for the section points evaluated at different ambient temperatures.**

## 4.5 ASSESSMENT OF IN SITU TEMPERATURE SENSITIVITY

To measure and quantify the temperature sensitivity of foamed asphalt bases, a coefficient (α) was calculated, in terms of the backcalculated layer moduli and the pavement temperature at the time of the test, using equation (4.3). The analysis was performed using the FWD data collected during different time of the day, and the temperatures measured inside the pavement, for each longitudinal position of the section.

Since much variability was observed along the section, the calculation of α was done individually for each test position, separated both transversely (center of the lane, left and right wheel path) and longitudinally, to provide an improved regression reliability. The difference in moduli observed for the different positions even within the same section could be related to the material performance being influenced by localized boundary conditions such as compaction, material variability and moisture. Since the backcalculation was performed considering the entire foamed asphalt base as one layer, the temperature used for this analysis was the average between the measurements at 40mm, 160mm and 300 mm depth during the FWD survey.

The linear regression was calculated based on the model presented in equation (4.3), used by Betti et al. (2017) for foamed asphalt layers and by the Asphalt Institute (Harichandran et al., 2000) for HMA. Figure 12 shows two examples of the linear regression analysis for different points in the test section. Within the same trial section, the quality of the linear regression fits presented significant variability, which may be associated with the FWD plate positioning, temperature measurements, material variability and other analysis simplifications.

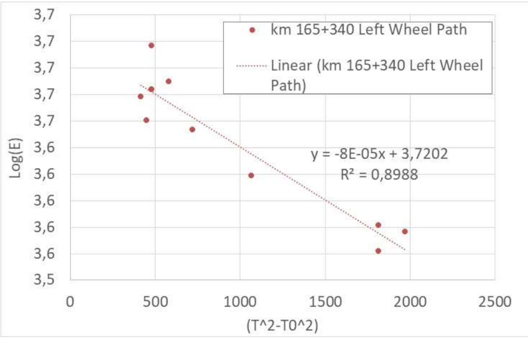


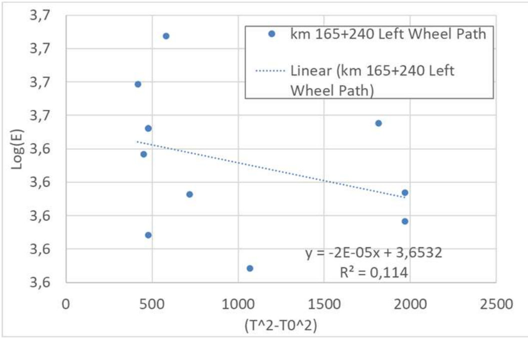


(a) (b)

**Figure 32. Graphs (a) and (b) show two examples of linear regression analysis for two different test positions.**

Figure 13 presents the results of the regression analysis for the entire section, considering three different FWD surveys, showing the sensitivity coefficients and the $R^2$ resulting from the regression analysis.

It can be observed that there is a significant dispersion of the calculated values for α between the three FWD surveys, and within the same survey. The α values obtained from the most recent survey show a higher concentration of values between $0.40 \times 10^{-4}$ and $0.70 \times 10^{-4}$ associated with a higher $R^2$. This concentration could be an indication of a convergent value for the cured material. For the surveys performed at 6 and 12 months after rehabilitation, the curing of the layer could be a factor increasing the dispersion of the results obtained.

One other factor that could have influenced the results obtained using the FWD data from 12 months after rehabilitation is the small variation of temperature recorded in that survey. For the calculation of α, all difference in the backcalculated resilient modulus for a given point is attributed to be a result of the effect of the temperature on the material stiffness. However, that is not the case, as moisture, positioning of the FWD plate during tests, material composition, and support conditions are all factors that can affect the deflection bowls, and therefore the entire analysis. In that sense, a wider temperature variation is desired for field assessment, so that the impact of temperature on material stiffness is amplified and the effect of other variables are reduced in the analysis.

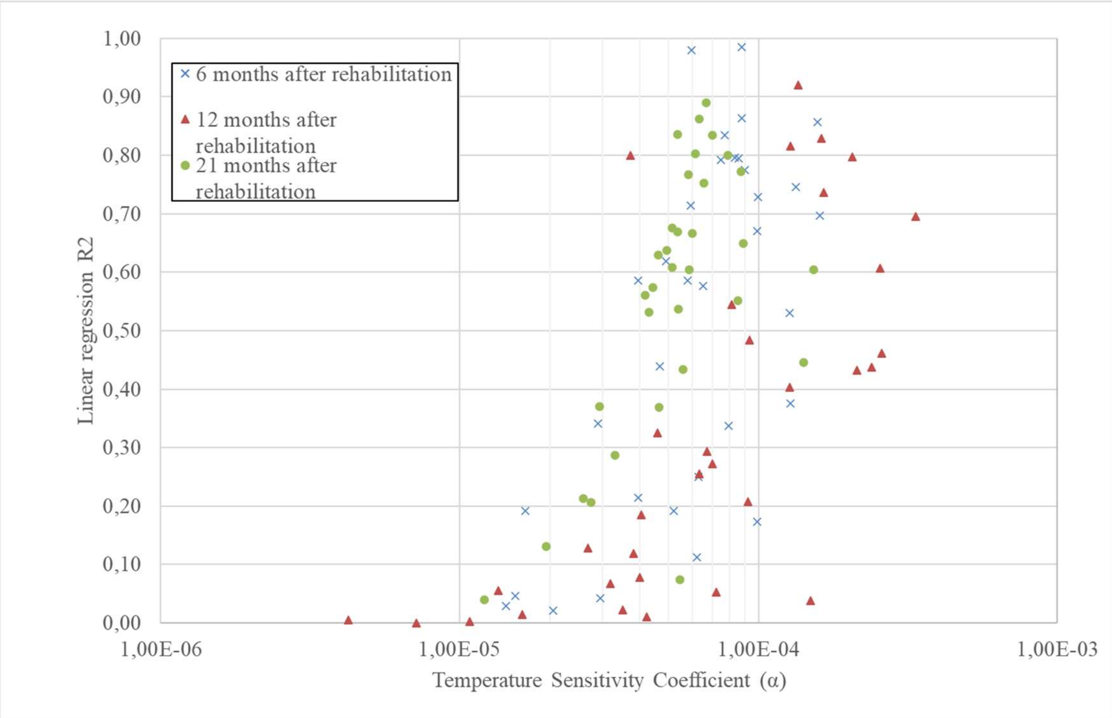


**Figure 33. Temperature sensitivity coefficients (α) and regression R², calculated along the trial section, during different surveys.**

Another important detail is that even if the FWD tests were performed in different points of the trial sections, the temperature measurements within the pavement were all made at the same point. That could be an important factor as different material conditions such as density and moisture could lead to different temperature gradients along the trial section. This could lead to different temperature gradients, and therefore introduces increased variance of the analysis.

If an average value of α is calculated with all 99 individual linear regressions, a temperature sensitivity coefficient of 0.77 x $10^{-4}$ can be achieved, with a standard deviation of 0.59 x $10^{-4}$. If the regression results calculated from the FWD surveys with 12 months of rehabilitation is discarded due to the small temperature variation during the day and discard all regressions that yielded $R^2$ lower than 0.50, the new average α for the remaining 42 values is 0.75 x $10^{-4}$, with a standard deviation of 0.24 x $10^{-4}$. That produces a better estimate for the materials temperature sensitivity coefficient, as the covariance between the average and the standard deviation is dramatically reduced from 0.71 x $10^{-4}$ to 0.32 x $10^{-4}$.

Since the material is curing on the field during the time between surveys, it is probable that the value of α is also changing, as moisture is reduced, and material densification increases. Thus, if only the last survey is considered, assuming that the curing process is already completed at this stage and discarding the unreliable regression values as previously done, the obtained temperature sensitivity coefficient will be α = 0.65 x $10^{-4}$, with a standard deviation of 0.24 x $10^{-4}$. In this scenario, from the 33 linear regressions calculated, 10 resulted in $R^2$ smaller than 0.50.

Figure 14 has a representation of the Moduli correction model from equation (4.3) using the calculated value of α = 0.65 x $10^{-}$, compared to the different Moduli and α values found in literature. To avoid overpopulating the graph, only the results obtained from mixture 5F were plotted from the study developed by Betti et al.(2017).

It is noteworthy that the correction model used by the Asphalt Institute (Harichandran et al., 2000), Betti et al. (2017) and in this study has a different mathematical structure than the ones used by Plati et al. (2010) and the one used by Fu and Harvey (2007). Although the two coefficients calculated by Fu and Harvey (2007) are from the same section in different years, it is clear how they differ from one another. It is also interesting to note how the curve has flattened in the second survey, resulting in a lower α, possibly due to the more advanced curing condition of the section.

It is important to mention how steep and sensitive to temperature change is the Asphalt Institute curve for Hot Mix Asphalt, while the calculated foamed asphalt mixture models tend to be flatter. Material composition can have a significant impact on its temperature sensitivity, from different foamed asphalt binders, aggregate sources and in particular the RAP content, as pointed out by Dal Ben (2014). Other aspects that could be relevant are material compaction (% of air voids) and moisture, as they alter the media of heat propagation and the material specific heat.

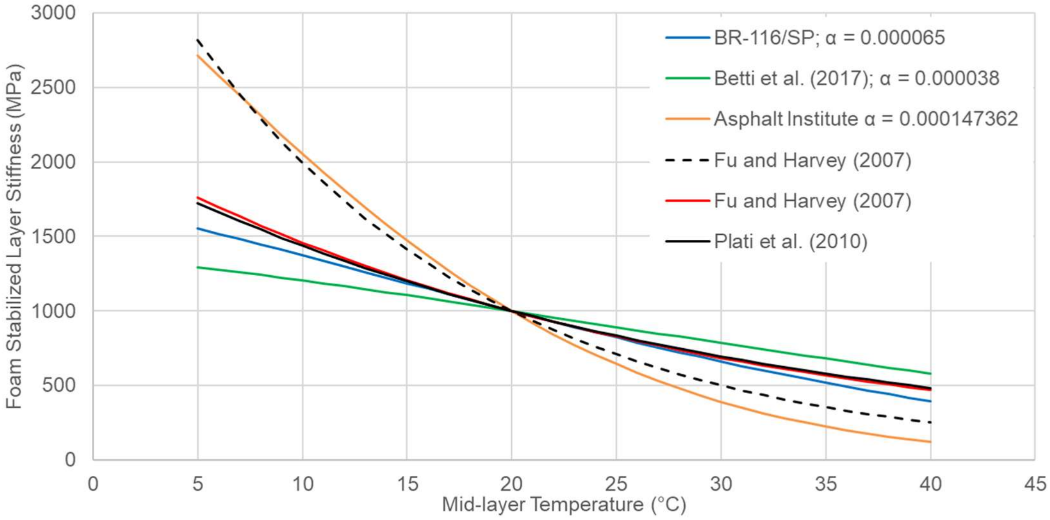


**Figure 34. Moduli correction to the reference temperature of 20 °C using different models.**

## 4.6 PARTIAL CONCLUSIONS

An assessment of foamed stabilized material’s sensitivity to temperature was made using FWD data and temperature measurements at different pavement depths. The backcalculated stiffnesses of in-service pavement structures were associated with measured temperatures, and sensitivity coefficients were calculated for each of the evaluated test stations.

It was observed a significant variation on the results of FWD surveys, the backcalculated resilient modulus and the coefficients calculated, which can be associated to the material heterogeneity, layer density in different points of the trial sections, and moisture conditions. The curing of the trial section and consolidation of the pavement proved determinant to the reduction of the deflection variability and normalization of pavement responses.

The analysis of deflection bowls showed how temperature changes significantly affected the contribution of the foamed asphalt base and asphalt wearing course for the overall deflection, especially close to the load application point. That impact of temperature variation was also verified on the backcalculation of the resilient modulus of the different layers, as the calculated values changed with the increase in temperature during the day for both the Gap graded wearing course and the foamed asphalt base.

Notwithstanding material heterogeneity, stages of curing, and mixture composition can play a decisive role on material sensitivity. Good results were obtained from the correction model used by the Asphalt Institute (Harichandran et al., 2000) for HMA, and by Betti et al. (2017) for foamed asphalt mixes (equation 4.3), with good agreement to the results obtained from literature. In this sense, the application of the calculated coefficient of $0.65 \times 10^{-4}$ may not precisely describe the temperature/moduli relation of any foamed stabilized mixture but it does present a good estimate value for analysis.

It was verified that foamed stabilized mixtures have less sensitivity to temperature variation than HMA given primarily the difference in bitumen contents, with the coefficients calculated and found on literature for foamed mixtures being two to three times smaller. The material sensitivity, however, is sufficient to provide an increase or decrease of 50% of material stiffness within a 20 °C range. This variation in pavement temperature is considered normal through the life span of pavement structures, and an increase or decrease in stiffness of 50% has a significant impact on the stress state within the foamed asphalt base layer, and consequently on its mechanical performance.

Further research is recommended so that the effect of material composition can be observed on the temperature sensitivity, as foamed stabilized layers can be composed of several different material combinations. Additionally, further research should assess the temperature sensitivity on a laboratory-controlled environment.

# 5 LABORATORY ASSESSMENT OF TEMPERATURE EFFECT ON MATERIAL PERFORMANCE

## 5.1 INTRODUCTION

Cold recycling (CR) and Full Depth Reclamation (FDR) have gained traction in the last decade as society and industry push for sustainable and cost-effective solutions for pavement maintenance. Bitumen stabilization has been largely used in these processes worldwide, either through the addition of foamed asphalt or asphalt emulsion, producing high quality base layers for road pavements. Much has been debated on the Bitumen Stabilized Material (BSM) mechanical behaviour, with many impacting factors studied such as material composition (He and Wong, 2007), mix gradation (Raschia et al., 2018), binder content (Fu et al., 2011), active filler content (Betti et al., 2017, Nivedya et al. 2018), compaction (Chomicz-Kowalska and Ramiączek, 2017), and moisture (Kuchiishi, 2019; Twagira, 2010).

The temperature effect on BSMs is an important matter as it changes the way aggregates and bitumen binder interact within the mix, resulting in changes in stiffness (Diefenderfer and Link, 2014), tensile resistance and overall performance under loading (Kavussi and Modarres, 2010). Temperature is also important during production of the cold stabilized mixes, as the temperature of both aggregates and binder agents (foam or asphalt emulsion) can have a significant impact on binder dispersion and coating (Jenkins, 2000; Ebels, 2008). The effect of temperature on the curing of BSMs has also been studied as accelerated curing in laboratory tries to replicate different curing conditions to which the material is subjected on the field (Moloto, 2010; Kuna, 2015; Twagira, 2010).

The effect of temperature on BSM performance has also been assessed, especially on how it affects material stiffness (Fu and Harvey, 2007; Plati et al., 2010). As temperature's effect on bitumen viscosity can be observed in Hot Mix Asphalt (HMA) (Ling et al., 2017; Zbiciak et al., 2019), the understanding of how relevant is this effect in cold stabilized materials is still not fully understood.

This chapter aims to investigate how temperature affects the mechanical behaviour of foamed bitumen stabilized material using laboratory tests so that material performance can be understood and considered for pavement design.

## 5.2 LITERATURE REVIEW

### 5.2.1 BSM Characterization in Laboratory

The composition of a BSM can be very variable, starting from the production process used. Cold Recycling, both in situ and in plant, favor the use of Reclaimed Asphalt Pavement (RAP) in high percentages, while FDR processes may include different materials such as crushed stone bases, reclaimed cement treated materials, and even natural gravels and soils, to some extent (Carter et al., 2013). Virgin aggregates can also be used to produce new BSM layers, although these materials are usually applied for grading correction of recycled mixtures. Even within the same method of production, the material can present great variability, depending on the RAP and aggregate sources and the equipment used for milling, recycling and processing (Zaumanis et al., 2021).

Another determining factor in material composition is the addition of hydraulic binders as active fillers, such as hydrated lime and Portland Cement. These active fillers are usually restricted to 1,0% in mass, to avoid excessive stiffening of the mixture, restricting its application to improve bitumen dispersion and to help during the curing process (Wirtgen GmbH, 2012; SABITA, 2020). The amount of foamed bitumen incorporated to the mixture will have direct effect on its mechanical resistance, especially its tensile strength, while material composition and gradation are more related to aggregate interlock and compressive resistance (He and Wong, 2008).

During the production of bitumen foam, water and air (at room temperature) are mixed with bitumen (at around 170°C) in a pressurized chamber, resulting in water turning into vapor, expanding and pressuring the bitumen film into the formation of bubbles. Once these bubbles burst in contact with the aggregates, they stick to the fine portion of mix, producing a non-continuously bound material (Jenkins, 2000). These bonds create cohesion within the mix, but they do not alter the properties of the original aggregates, reason why RAP is considered as an aggregate for gradation purposes, ignoring the primitive rock underneath the oxidized bitumen coating (Wirtgen GmbH, 2012). Since Foamed Bitumen stabilized materials have a non-continuously bound nature, their primary mode of distress is the accumulation of permanent deformation (Mondal et al., 2021).

As permanent deformation is the primary mode of failure for BSMs during its service life, the understanding of its compressive resistance is paramount, reason why the Monotonic Triaxial Test (MTT) has been adopted as the standard method to characterize the shear properties of these materials (SABITA, 2020).

Due to the variability within the material, quality control proves essential to the production of a high-quality material, with controlled characteristics. The control of mix gradation, the addition of bitumen and active fillers, material compaction and mechanical resistance are among the main parameters used for material characterization and control (Asphalt Academy, 2009).

The assessment of BSM stiffness is also important for material characterization, as it is an input for pavement design, specifically for mechanistic and mechanistic-empirical models. For that reason, different tests that allow for the assessment of BSM stiffness can be performed including Triaxial Resilient Modulus (TRM) and Indirect Tensile Resilient Modulus (ITRM) tests, which are commonly used to characterize BSM in laboratory.

The TRM tests are performed in cylindrical specimens subject to a pair of axial deviator stress and surrounding confining stress. The variation of the stress pairing results in different material stress states, yields different responses from the material and hence a stress dependent resilient modulus behaviour. Many authors have used TRM tests in the process of characterizing BSM samples in the laboratory (Dias et al., 2023; Ebels, 2008; Fu et al., 2009a, 2009b; Guatimosim, 2015; Huan et al., 2010; Kuchiishi, 2019; Twagira, 2010).

Alternatively, the ITRM tests are commonly performed in cohesive mixtures, with the cylindrical specimens being subject to a diametral stress and no confining stresses, inducing tension and a resilient response from the sample. These tests do not allow for the assessment of the stress dependency but are faster and require a simpler setup to perform than the TRM. The ITRM test is used for mix design and its results used as inputs for pavement design in both Australia (Gonzales et al., 2011; Leek, 2010) and United Kingdom (The Highways Agency et al., 2021).

### 5.2.2 Effect of Temperature on BSM Behaviour

As stress dependent materials, BSMs present an elastoplastic behaviour (Llewellyn, 2015). However, due to the presence of bitumen it also shows dependence to loading frequency and temperature variation (Jenkins, 2012).

The assessment of temperature dependence can be made through different tests. Apeagyei and Diefenderfer (2013), for instance, have performed ITRM tests according to ASTM D7369-09 (2011) on cold recycled mixtures, foam stabilized samples, at 4°C, 20°C and 38°C, resulting in decreasing resilient responses as the temperature was increased.

An efficient way of measuring temperature dependency on BSM is through Dynamic Modulus (DM) tests (Buczyński and Iwański, 2018). Bang et al. (2012) performed a series of DM tests of FDR mixtures containing RAP in proportions ranging from 25% to 75% combined with different aggregate sources, stabilized in laboratory with foamed asphalt and asphalt emulsion. In all cases, time-temperature dependence was observed, with the modulus decreasing due to the increase in temperature and due to a decrease in loading frequency. The comparison of the temperature dependence of foam and emulsion stabilized mixes has also been studied through DM tests, with emulsion stabilized BSMs resulting in steeper and more susceptible curves (Ebels, 2008; Gu et al., 2019; Kuchiishi et al., 2021; Leandri et al., 2015). This phenomenon was attributed by Kuchiishi et al. (2021) to the thin film of asphalt covering the aggregates being more dispersed and continuous than the bitumen spot welds produced during foam stabilization.

Diefenderfer et al. (2016) also performed Dynamic modulus tests (AASHTO TP79) with both foam and emulsion stabilized samples, obtained from field cores of Full Depth Reclamation (FDR), Cold In-place Recycling (CIR) and Cold Central-Plant Recycling (CCPR) projects. The results showed that all samples exhibited temperature dependence, with FDR samples presenting comparatively lower dependence, most likely due to the reduced RAP percentage in the mix. That indicates that not only the added asphalt binder plays a role on BSMs visco-elasto-plastic response but also the existing oxidized asphalt on RAP materials. Analyzing different RAP sources, Raschia et al.(2021) observed that the properties of the residual bitumen on RAP aggregates also impacted the temperature dependence of different recycled mixes.

The contribution from the asphalt in RAP materials was also observed by Dal Ben (2014), as he performed TRM tests at 10°C, 25°C and 40°C, in foamed recycled samples containing 100% RAP, 100% Crushed Stone (CS) and 50% RAP – 50% CS, resulting in different temperature dependence factors depending on the RAP content of each mix. The author also observed during sample conditioning that the presence of RAP changed the rate by which the sample increased its temperature, with higher contents of RAP reducing the time it took for specimens to go from 25°C to 40°C on a controlled oven.

### 5.2.3 Performance Tests

Due to the non-continuously bound nature of foamed mixes and its tendency to fail primarily due to permanent deformation, the evaluation of material performance has been focused on different repeated load tests.

The Uniaxial Repeated Loading (URL) tests is one possibility to assess the amount of accumulated deformation after a series of compressive stress loads, when a determined criteria is achieved (He and Wong, 2007, 2008; Mondal et al., 2021; Silva, 2019). Uniaxial Repeated Loading tests are commonly used for HMA, which present higher cohesion and less stress dependent behaviour.

He and Wong (2007, 2008) performed a series of dynamic creep tests, to investigate the effect of moisture, different contents of RAP on mix composition, and grade of asphalt binder on the resistance to permanent deformation, but no assessment of the influence of temperature was made. Silva (2019) performed URL tests with different procedures and temperatures, indicating that increased temperature reduces the viscosity of the asphalt binder in recycled mixtures, making the resistance to permanent deformation more dependent on the internal friction and aggregate interlock.

Mondal et al. (2021), on the other hand, used dynamic creep tests to determine the Primary, Secondary and Tertiary stages of cumulative permanent deformation of foam stabilized mixtures, considering three compressive stresses (100 kPa, 200kPa and 300 kPa) and three different test temperatures (30°C, 40°C and 50°C). The tests showed that Time-Temperature Superposition (TTS) principle can be applied to BSMs, allowing for the determination of cumulative permanent deformation master curves.

Triaxial Repeated Load (TRL) tests have also been used to evaluate the performance of BSM mixtures, as it allows for the control of both deviatoric and confining stresses to assess its impacts. Bang et al. (2012) tested foam and emulsion BSMs from different material sources, subject to a confining stress of 35 kPa and a deviatoric stress of 226 kPa, to achieve 5% permanent strain after 30.000 load cycles. The BSM samples were resistant to permanent deformation and the deviatoric stress was increased in 69kPa increments per test, until each sample achieved the desired 5% accumulated strain in 30.000 load cycles. Although the publication indicates tests were conducted at 30°C, 40°C and 50°C, only the results at 30°C are presented, with no significant finding reported regarding the effect of temperature during the tests.

Dal Ben (2014) performed a series of TRL tests evaluating the amount of RAP and virgin aggregates on foamed bitumen stabilized mixtures, and different test temperatures to determine its effect on material performance. The results showed that different mix compositions required different stress combinations to achieve failure, higher RAP content reduced the deviator stress necessary to achieve failure. Material characteristics and test temperature played a significant role on the outcome of each test, with the increase in temperature from 25°C to 40°C and 50°C having a clear impact on the increased accumulated permanent axial strain.

The great variability of the material, caused by its recycled nature, and the variables impacting its behaviour, makes the development of a performance model a challenge. Through a comprehensive analysis and association of TRL permanent deformation tests, historical monitoring data and characterization through MTT, Bierman (2018) presented a design function for BSMs that considers material shear properties, compaction and mechanical resistance to predict permanent deformation over time under loading. The transfer function allows for pavement design and performance prediction.

## 5.3 LABORATORY TESTS

To further assess the effect of temperature on foam bitumen stabilized mixtures a series of laboratory tests were performed to determine the materials resistance to permanent deformation, and how temperature affects its properties and performance under loading. The BSM samples used in this study are from a trial section on highway BR-116, where a foam bitumen recycled base was constructed during pavement rehabilitation in 2018. This section is described in more details in Chapter 3 (Gutierrez et al.2018). A flowchart with the laboratory tests used in this study to characterize and evaluate the BSM is presented in Figure 35.

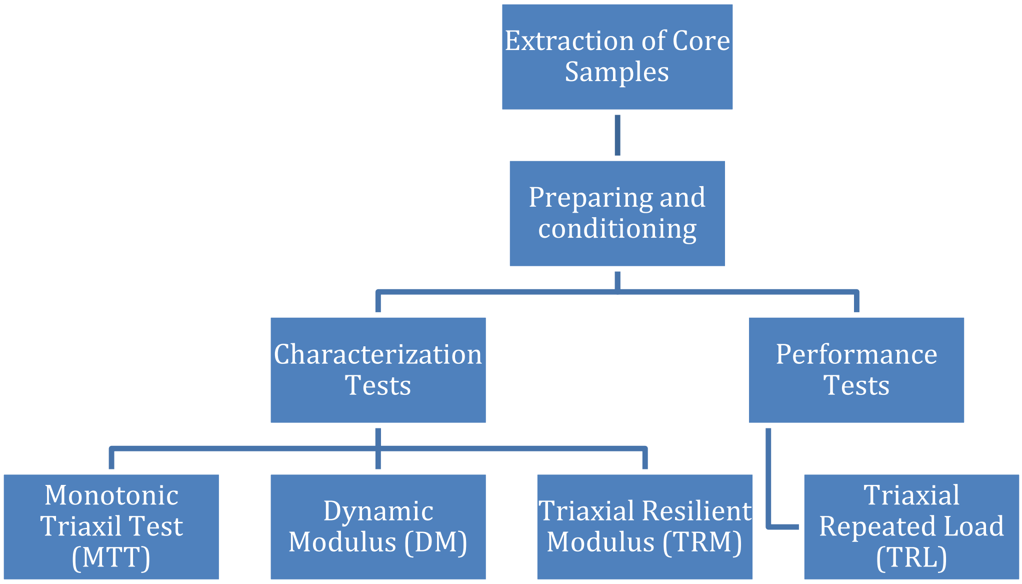


**Figure 35. Laboratory tests and procedures flow chart**

### 5.3.1 Mechanical Characterization

The mixture of the BSM layer of the trial section from where the laboratory samples were extracted is composed of 85% RAP and 15% Crushed Stone Dust (CSD), with an additional 1% of hydrated lime added as active filler and 2,3% of bitumen with a 50-70 penetration classification. The mix was designed for the rehabilitation of the trial section and Quality Control Tests were performed during the construction phase. After the rehabilitation of the section, pavement monitoring was performed to access material curing on the field, as discussed in Chapter 3, and after 21 months from the section rehabilitation, core samples of 100 mm and 150mm in diameter were extracted from the pavement to be further tested in the laboratory.

In the laboratory, all core samples extracted were placed over a counter and left for at least 30 days to achieve equilibrium moisture, which was observed to range between 0.5% and 0.7%. Although the design thickness for the BSM layer on the field was 310 mm, the extracted cores presented 30 mm surface Gap-graded layer, and a variation in BSM height from 200 mm to 350 mm, and therefore had to be sawed, reducing this variation according to each test to be performed. Some of the variation in specimen height can be attributed to the roughness of the BSM's support layer, however, most of the smaller specimens were result of the material breaking on its bottom portion during extraction. For this reason, all specimens were carefully inspected to determine if they had been damaged. The sample was discarded if any distress was identified.

#### 5.3.1.1 Monotonic Triaxial

Monotonic triaxial tests were performed in the extracted cores to characterize the shear properties of the cured BSM layer. The 150 mm diameter cores were sawed with 300 mm height, then subjected to a compressive monotonic load with different confining pressures. Although the TG2 (SABITA, 2020) indicates tests at 4 different confining pressures, tests were performed at 0 kPa (no confinement), 100 kPa and 200 kPa. The tests at 50 kPa of confining pressure were skipped to reduce the number of specimens used, as the test is destructive, and a limited number of samples was available. During the test, a constant displacement of 3 mm per minute is applied, compressing the samples while the total displacement is measured, and the reaction load is registered by the load cell. The test is stopped when either the compressive resistance starts to decrease, or 6% deformation (18 mm) is achieved. Figure 36 shows the Hydraulic pressed that was used to run the Monotonic Triaxial Tests, as well the confinement chamber produced by Wirtgen GmbH., composed by a metal base, a hard metal casket, an inflatable double-wall rubber chamber and a metal top cap.

From the results obtained from the tests with different confining stresses it is possible to plot the Mohr-Coulomb graph, and with that, determine the rupture envelope, of which the intercept is the Cohesion (C) of the mix, and the slope is the angle of internal friction (ϕ) of the mix (Theyse et al., 1996).

(a) (b)

**Figure 36. (a) Hydraulic press used for the MTT and (b) the disassembled confinement chamber produced by Wirtgen GmbH.**

These parameters are directly influenced by mixture composition, with the aggregate nature and gradation directly influencing aggregate interlock and thus, influencing the angle of friction, while asphalt binder contents affect material cohesion. In this sense, mixtures with higher crushed aggregate contents and tend to produce higher interlock and shear strength, with increased angle of internal friction. Meanwhile, higher RAP contents tend to produce mixtures of lower angle of friction (Dal Ben, 2014). The increase in foamed asphalt and active filler contents tend to increase material cohesion, as it diminishes material stress dependency, and therefore reduce the angle of friction (Ebels, 2008).

The TG2 (SABITA, 2020) indicates as reference for BSM 1 a cohesion of 265 kPa and 250 kPa for mixtures composed of more or less than 50% of RAP respectively. That indicates the expected increase in cohesion for high RAP content mixtures. However, it indicates a reference value of 38° ϕ for BSM 1 mixtures containing more than 50% of RAP, as opposed to 40° ϕ for mixtures with less than 50% RAP.

#### 5.3.1.2 Triaxial Resilient Modulus

As the TRM tests allow for the evaluation of material stiffness while assessing its stress dependency, the samples were tested to determine the materials resilient response under load after curing on the field. The test was conducted according to the Brazilian specification DNIT ME 134/2018 which is similar to AASHTO T-307 (2011), although with a wider combination of loads. The sample is tested in a servo-pneumatic machine, with deviatoric stress run by the press, while confining stress is maintained inside the pressure chamber. Table 13 details the stress states during the test, that was performed in 200 x 100 mm cylindrical specimen (properly sawed to provide parallel faces and to provide the required geometry).

**Table 13. Combination of deviatoric and confining stresses for TRM test according to DNIT ME 134/2018**

| $\sigma_3$ (kPa) | $\sigma_d$ (kPa) | $\sigma_1/\sigma_3$ |
|---|---|---|
| 20.7 | 20.7 | 2 |
| | 41.4 | 3 |
| | 62.1 | 4 |
| 34.5 | 34.5 | 2 |
| | 68.9 | 3 |
| | 102.9 | 4 |
| 50.4 | 50.4 | 2 |
| | 102.9 | 3 |
| | 155.2 | 4 |
| 68.9 | 68.9 | 2 |
| | 137.9 | 3 |
| | 206.8 | 4 |
| 102.9 | 102.9 | 2 |
| | 206.8 | 3 |
| | 309 | 4 |
| 137.9 | 137.9 | 2 |
| | 274.7 | 3 |
| | 412 | 4 |

#### 5.3.1.3 Dynamic Modulus

As indicated by the literature, it is possible to assess the temperature dependency of BSMs through the Dynamic Modulus tests. Although the temperature dependency and sensitivity were evaluated in Chapter 4, the great variability obtained from FWD results demanded the laboratory verification, considering an environment in which temperature measurements and moisture conditions could be controlled. In this sense, DM tests were performed to the 100 mm diameter samples, according to AASHTO T 342/11, at temperatures 4.4°C, 21.1°C and 37.8°C. The tests could not be conducted at 54°C, as indicated by the AASHTO specification, due to the significant reduction in material stiffness. All tests were conducted at frequencies of 0.1 Hz, 0.5 Hz, 1 Hz, 5 Hz, 10 Hz and 25 Hz.

### 5.3.2 Performance

In terms of material performance under loading, literature indicates that repeated load tests to determine permanent deformation accumulation are regarded as the most practical laboratory test. Therefore, TRL tests were selected to evaluate the resistance to permanent deformation while also assessing how temperature and different stress conditions affected material behaviour.

#### 5.3.2.1 Triaxial Repeated Load - Permanent Deformation

As foamed bitumen stabilized materials are stress dependent and exhibit higher resistances when subjected to confining stresses, the TRL test was used instead of URL to allow longer tests, resulting in more comprehensive results. It was previously attempted to test extracted samples using the URL Flow Number test, according to AASHTO T342/11, but the number of load cycles until failure was small, and difference between different test conditions too small to allow proper evaluation.

All repeated load tests, including DM, TRM and TRL tests were performed using an IPC Global's UTM-25 Servo Hydraulic Universal Testing Machine, with a maximum load of 25 kN, confining and temperature controlled environmental chamber, as illustrated in Figure 37. The tests were performed with a confining pressure of 100 kPa, a haversine loading function with 0,1 seconds of load and 0,1 seconds of rest period, in a frequency of 5 Hz. The seating stress was set at 5 kPa, and static pre-loading of 50 kPa of axial stress was applied for 10 minutes before the test started. The end of the test was defined as the moment when 500,000 cycles were achieved or 4% of total deformation was accumulated. Due to the size of the specimens, and the high amplitude of strains, no LVDT was used, with the total strain measured by the actuator.

According to the literature review on TRL tests, a good parameter to determine the deviatoric stress for permanent deformation tests is the Deviator Stress Ratio (DSR) (Bierman, 2018; Dal Ben, 2014; Mulusa, 2009; Twagira, 2010). This parameter is the ratio between the acting deviator stress and the deviator stress at rupture, as determined by the Mohr-Coulomb envelope in MTT.


*(a)* *(b)*

**Figure 37. (a) IPC Global's UTM-25 Servo Hydraulic Universal Testing Machine and (b) a picture of the interior of the climate conditioned chamber, showing the confining chamber with the specimen inside ready for a TRL test.**

According to Ebels (2008) the increase in DSR results in significant decrease in material permanent deformation performance, with Bierman (2018) stating that DSR should be kept as low as possible for BSM structural design. Figure 38 shows the plastic strain accumulation from repeated load tests for different DSR values, calculated by the reason between the acting deviator stress (σd) and deviator stress that leads to material failure (σd,f), as presented by Bierman (2018).

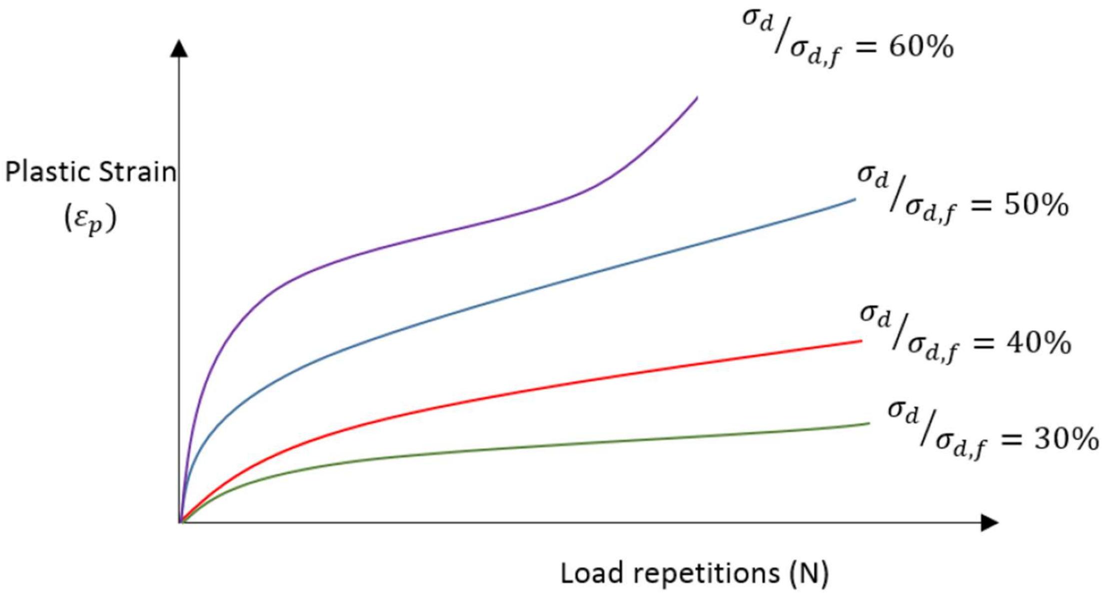


**Figure 38. Plastic Strain accumulation for different DSR values (Bierman, 2018).**

Since the samples used in this laboratory study were extracted from the field, and conditioned until constant mass was achieved, the moisture on the specimens greatly differs from the equilibrium moisture of 60% of OMC that is used for MTT during the mixture and pavement design phase. Consequently, with the reduced moisture, the values obtained from MTT for Cohesion and angle of friction were higher than they would've been at equilibrium moisture, resulting in high σd,f. As a result, the calculated values of σd were higher than expected, and the first specimens tested at such high stresses did not resist, failing before load stabilization.

After some trial and error, the Deviatoric stresses for the tests were determined as being 200 kPa, 250 kPa and 300 kPa. For each stress condition defined, three different temperatures were used for testing, producing the test matrix presented in Table 14.

**Table 14. Triaxial Repeated Load tests matrix**

| Test Condition | Confining stress | Deviatoric Stress | Test Temperature |
|---|---|---|---|
| 1 | 100 kPa | 300 kPa | 15°C |
| 2 | | | 25°C |
| 3 | | | 40°C |
| 4 | | 250 kPa | 15°C |
| 5 | | | 20°C |
| 6 | | | 25°C |
| 7 | | 200 kPa | 25°C |
| 8 | | | 30°C |
| 9 | | | 35°C |

Different researchers have used the modeling of three-stage permanent behaviour for BSMs (Dal Ben, 2014; Mondal et al., 2021; Silva, 2019) determining three different phases during the tests when the strains: (i) accumulate rapidly in decreasing rate (primary stage), (ii) accumulate slowly at a constant rate (secondary stage), and lastly (iii) the rate of strain accumulation increases rapidly until failure is achieved (tertiary stage). Figure 39 shows an example of permanent deformation test with the three stages well defined, and the regression models used to describe each stage, as described by Mondal et al. (2021).

During the primary stage, the sample suffers elastic and plastic deformation, with the unrecoverable deformation being caused mainly due to material densification. After the densification process stops, the specimen continues to accumulate plastic deformation at a constant rate, during secondary stage. The material reaches the tertiary stage when the plastic deformation at each consecutive cycle increases exponentially, rapidly leading to material failure.

The results of each tested specimen were evaluated so that the borders between the three stages were identified, and that each phase could be described in terms of the mathematical models shown in Figure 39. The values of a, b, c, d, f and g are regression constants used to model the test results, while ε is the accumulated strain and N the number of applied load cycles.

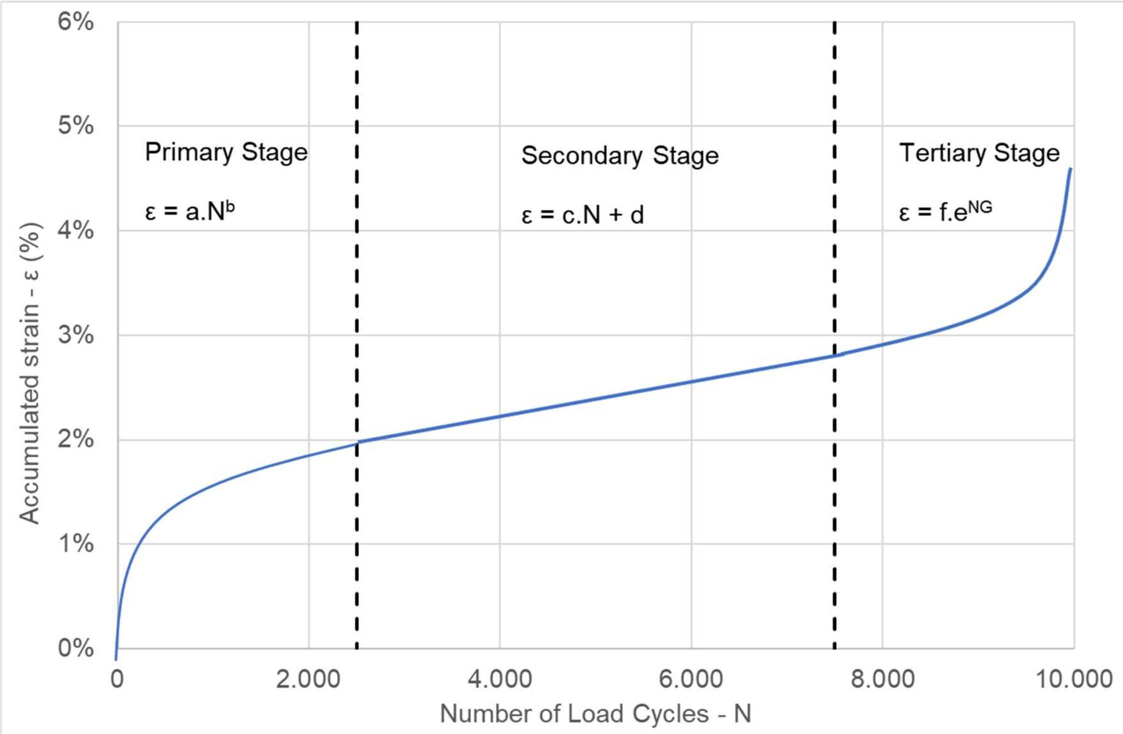


**Figure 39. Three-stage model of permanent deformation (adapted from Mondal et al., 2021)**

## 5.4 RESULTS AND DISCUSSION

### 5.4.1 Monotonic Triaxial Test

The cored samples from the trial section were prepared for the tests through the sawing of its height, resulting in 300 mm height by 150 mm diameter specimens. Afterwards, the specimens were conditioned at 25°C for 24 hours before being tested. The results from the tests, conducted at 0 kPa, 100 kPa and 200 kPa deviatoric stresses are presented in Figure 40.

Since the tested specimens were cured on the field, while under traffic loading, and were air dried in the laboratory until constant mass, the results obtained for the cohesion and internal friction angle of the foamed mix are higher than those expected from literature review. For a mixture composed of 85% RAP, the TG2 (SABITA, 2020) indicates reference values for mix design tests of 265 kPa for cohesion and 38° for the friction angle. Meanwhile Mulusa (2009) achieved results much lower for BSM emulsion mixes of RAP, with cohesion ranging from 158 kPa to 169 kPa, while the angle of friction was higher, between 42.3° and

47.1°. On the other hand, much higher results were obtained by Dal Ben (2014) with cohesion values ranging from 374 kPa to 516 kPa and angle of friction values that varied from 36° to 45.5° and even 8°, which indicates a highly cohesive behaviour from that one specific mix.

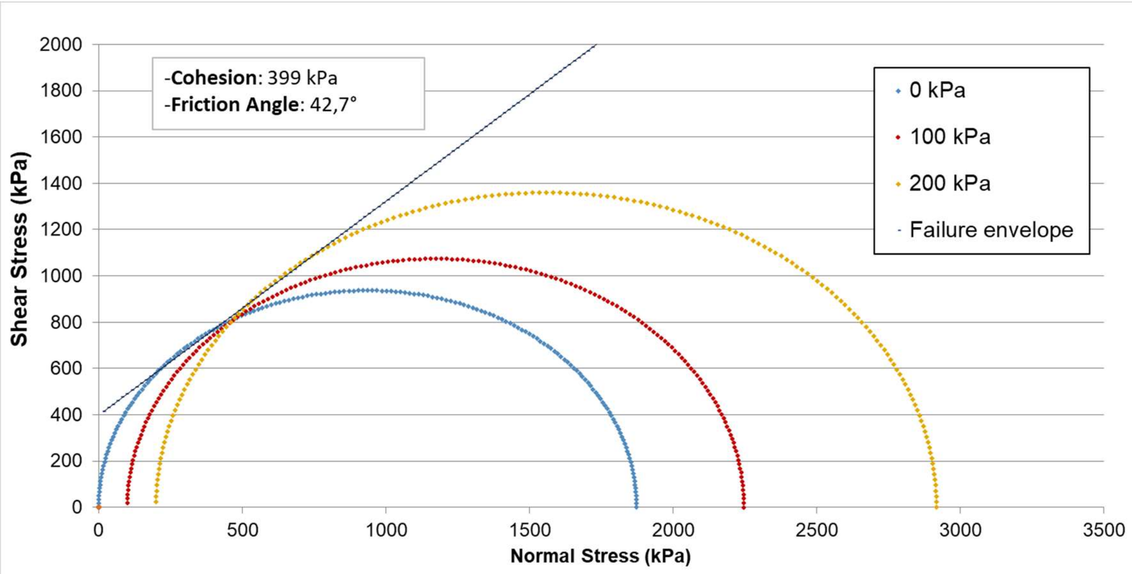


**Figure 40. Monotonic Triaxial Results for trial section extracted core samples, tested in the laboratory.**

The results obtained during these tests were considered adequate, especially considering the low moisture content of the specimens and the fact that it was extracted from the field 21 months after rehabilitation. This long period possibly contributed for the material densification under traffic, achieving higher compaction than its initial design density, and also long-term curing instead of the accelerated laboratory curing method.

### 5.4.2 Triaxial Resilient Modulus

Due to a limitation on the amount of core samples available, only one specimen was used for TRM. This specimen was prepared from a 100 mm diameter core sample and was cut with 200 mm height, corresponding to the top portion of the base layer, to achieve the desired geometry and was conditioned at 25°C for 24 hours before being tested. The 3D graph shown in Figure 41 shows the results of the test, and how the increase in confining and deviatoric stress result in higher Resilient Modulus values for the tested mix.

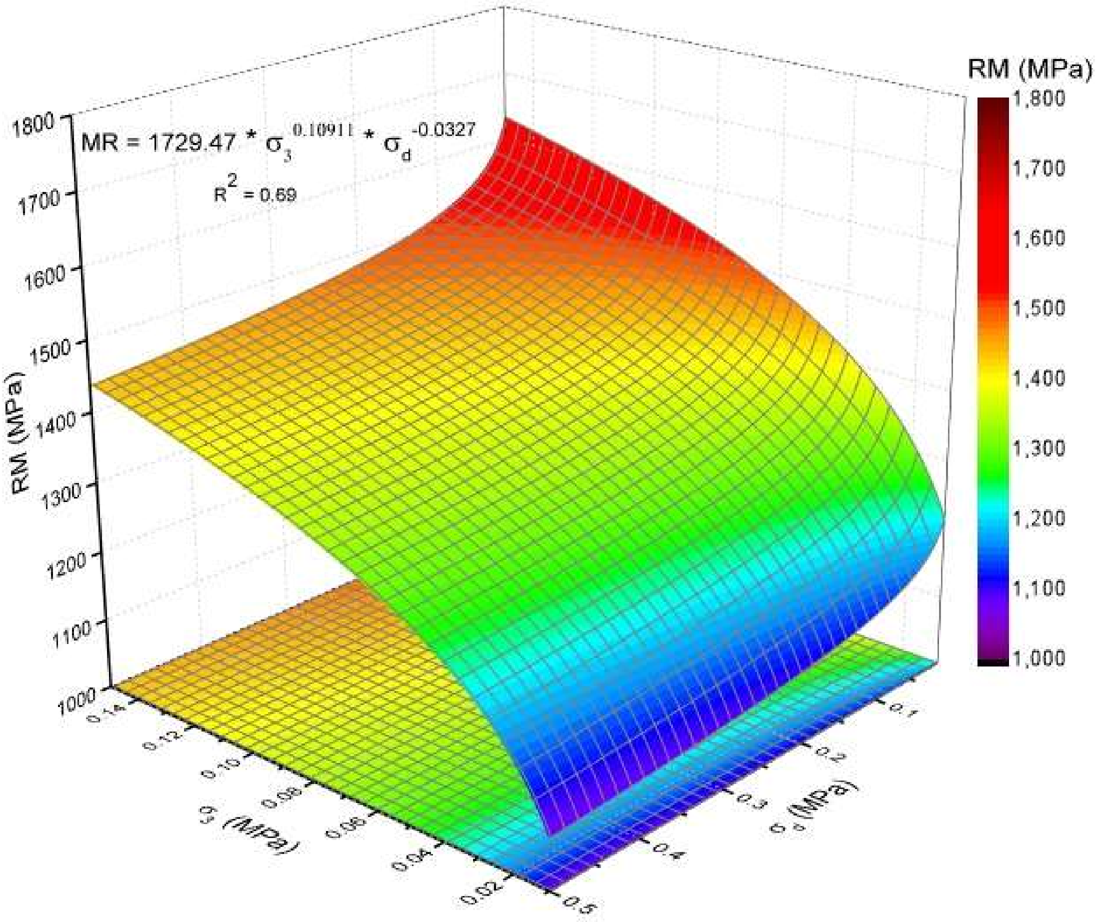


**Figure 41. 3D graph produced with Origin showing the influence of both the confining and deviatoric stress on the Resilient Modulus of the studied Foamed Asphalt BSM.**

These results corroborated with the MTT results, in the sense that both indicated that the foamed asphalt mix present a stress dependent behaviour. The Resilient Modulus values varied from 1070 MPa to 1636 MPa (52.9% variation), depending on the stress combination, showing that although the material presented higher cohesion value from the MTT test, 399 kPa compared to the TG2 reference 265 kPa, it still exhibits a high sensitivity to the stress state.

In terms of magnitude, the values are in line with those observed by other researchers (Dal ben, 2014; Ebels, 2008; Kuchiishi, 2019; Silva, 2019) and the values obtained for foamed asphalt mixes of other trial sections, as discussed in Chapter 3.

### 5.4.3 Dynamic Modulus

The Dynamic Modulus test was performed at different temperatures, with different load frequencies applied to the specimens. The different tests performed at various temperatures and frequencies can be shifted using the time-temperature superposition principle to produce the dynamic modulus master curve.

This procedure is usually performed shifting the different frequencies tested, to produce a curve of the modulus in terms of the reduced frequency. As the main objective of this study is to evaluate the effect of temperature on the behaviour of BSMs, it was decided to produce the isochronous master curve with reduced temperatures, as to evidence its impact on the material dynamic modulus. The isochronous master curve of the foamed asphalt mix tested in this study is presented in Figure 42 with test conditions shifted to a reference temperature of 21.1°C. The master curve is presented with two other curves, one for a RAP stabilized mixture with 2.2% foamed asphalt and 1.0% hydrated lime and a Hot Mix Asphalt (HMA) tested by Kuchiishi (2019).

Alternatively, the isochronous master curve of the mixture tested in this study is also presented in Figure 43, with the dynamic modulus calculated in terms of the reduced temperature, at the reference frequency of 5 Hz. The master curve is also presented with the HMA mixture master curve obtained by Kuchiishi (2019), allowing the observation that the BSM material is less sensitive to temperature changes than HMA, but still temperature dependent.

Although the graph is plotted in terms of the Log values of the dynamic modulus and the temperature, it is possible to see how the stiffness is susceptible to the effect of temperature, with significant changes from 4,367 MPa at 4.4°C and 25 Hz, to 244 MPa at 37.8 °C and 0.1 Hz.

The results obtained in this test are in line with some of the results verified in the literature, in terms of magnitude of the measured modulus for similar materials. Kuchiishi et al. (2021) observed values ranging from around 200 MPa to 2,000 MPa, while Diefenderfer et al. (2016) found an even greater amplitude of the modulus, with minimum values close to 100 MPa and maximum values obtained of almost 8,000 MPa for foamed asphalt stabilized samples tested for similar frequencies and temperature conditions.

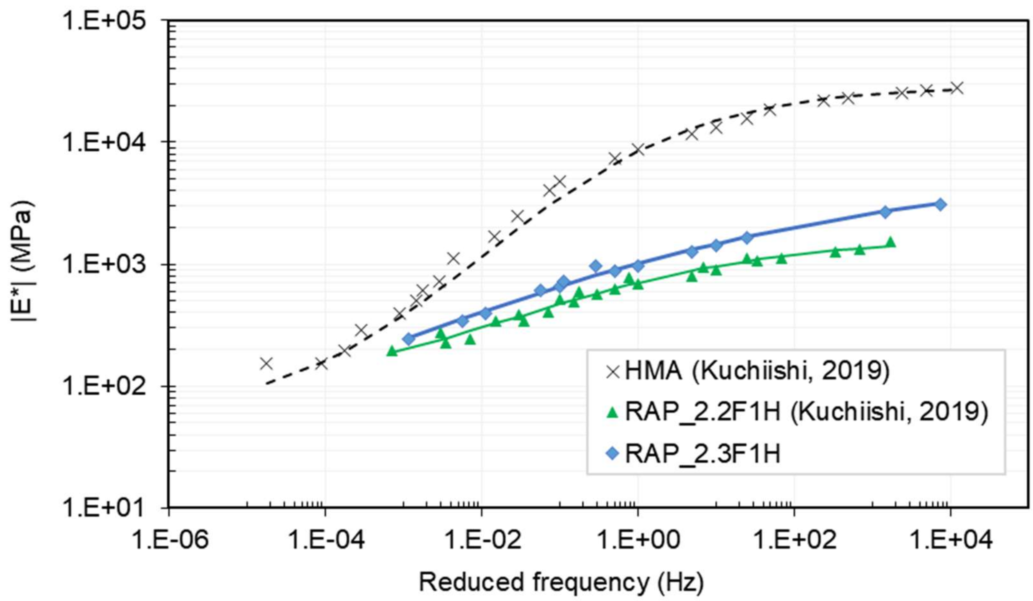


**Figure 42. Isochronous Master Curve for Reference temperature of 21.1°C**

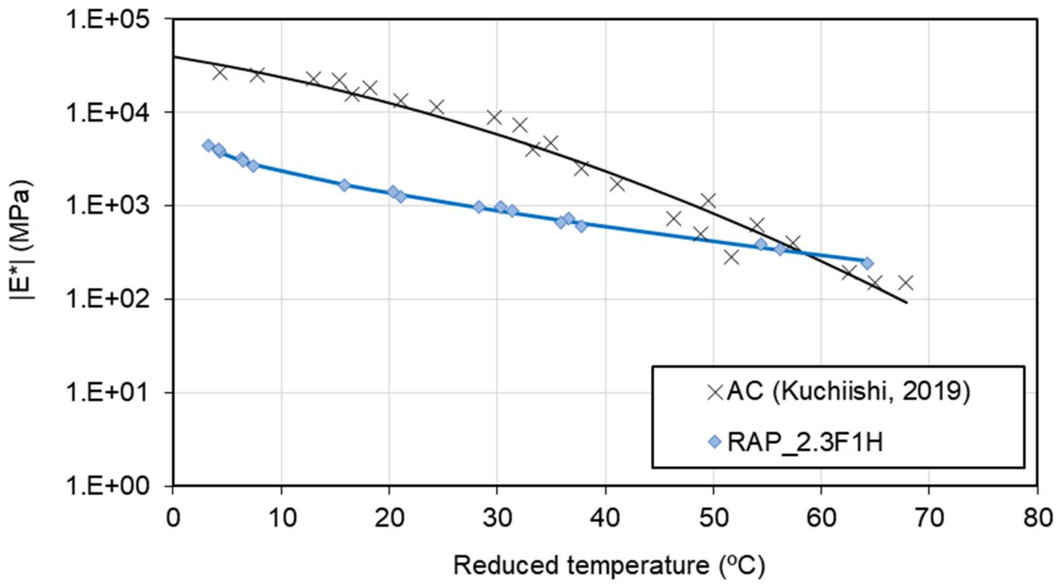


**Figure 43. Isochronous Master Curve for Reference frequency of 5 Hz**

### 5.4.4 Triaxial Repeated Load – Permanent Deformation

As discussed, a good parameter to define the stress state to which a BSM sample is subjected during TRL test to assess permanent deformation, is the DSR. This parameter can be calculated based on the failure envelope presented in Figure 40, given a confining stress, producing a relation between the deviatoric stress applied and the deviatoric stress that produces failure (SABITA, 2020).

From the shear parameters cohesion and angle of friction from the MTT, and considering 100 kPa of confining stress, the deviatoric stress necessary to produce DSR values of 25% and 40%, which were the initial test values, were 661 kPa and 998 kPa respectively. These values are close to the load limit of the equipment used and therefore some tests were conducted at 600 kPa to evaluate its feasibility. The results, however, showed that this level of stress was too high, resulting in failure within few load cycles, reaching tertiary stage. Since the results obtained in MTT were higher than some of the reference values encountered in literature, most likely due to its field curing during a prolonged time and reduced moisture content, the DSR was deemed not adequate as a parameter for this specific situation.

As result, new TRL tests were performed considering 100 kPa of confining stress and 300 kPa of deviatoric stress. This value equaled half of the previous deviatoric stress, but still represented a significant higher value than the confining stress, producing good results. From there, new tests were later conduced with lower deviatoric stresses of 250 kPa and 200 kPa, to produce longer tests than the initial ones, that allowed for better comparisons between different test temperatures.

The initial tests were performed at 40°C, as a maximum test temperature that represented realistic temperatures that could occur for BSM base layers in Brazil, specifically for the state of São Paulo, where the trial section (Section 5 from chapter 3) was constructed. It is common to measure surface temperatures of asphalt pavements between 40°C and 50°C in this region, especially during the summer, when the air temperature can go beyond 30°C, and the pavement heats significantly due to direct sun exposure.

Temperature measurements on different pavement depths were made all year long in BR-381, where sections 2, 3 and 4 presented in chapter 3 are located, approximately 60 km from trial section 5, where the specimens investigated in this chapter were extracted. These measurements indicated that the temperatures reached maximum values of 55°C, 49°C and 30°C at pavement depths of 30 mm, 90 mm, and 130 mm, respectively (Kuchiishi, 2019).

Although thermal conductivity differs between materials, Dal Ben (2014) investigated the conductivity of different BSM mixtures, indicating that the increase in RAP material, and therefore the amount of existing bitumen within the mixture increases thermal conductivity. In that sense, a BSM will transfer heat more slowly than a HMA layer, and although the foamed asphalt layer is placed on the base, the proximity to the surface due to the thin wearing courses may result in the top portion of the layer being subject to temperatures up to 40°C, hence the selection of this temperature as a possible critical condition.

Since the focus was on the different temperatures during the tests, Figure 44 shows a comparison between tests performed with 300 kPa deviatoric stress and temperatures of 15°C, 25°C and 40°C. As the 40°C test results showed, the combination of applied deviatoric stress and high temperature was very challenging, resulting in material failure after 50 to 200 cycles, depending on the specimen. For that reason, the temperature for the next set of tests was reduced to 25°C, to simulate an equilibrium average temperature for the material all year round, and 15°C to simulate colder condition to which the pavement would be subject to during winter.

The results showed how the decrease in temperature from 40°C to 25°C and subsequently to 15°C increased the number of cycles needed to achieve 4% accumulated strain, from around 200 to around 5.000 and then to 80.000, respectively. The effect of temperature in these tests was significant and resulted in an increase of 10 to 20 times for each temperature reduction.

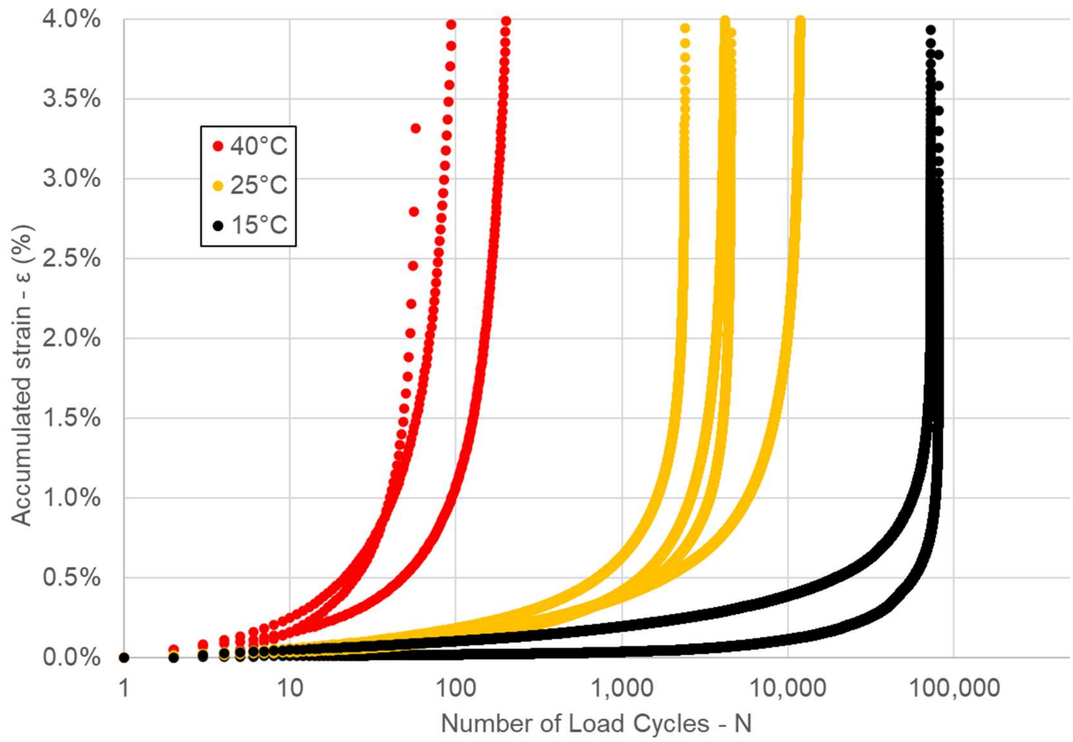


**Figure 44. Test results for 100 kPa confining stress, 300 kPa deviatoric stress and different temperatures**

As all tests performed using 300 kPa as deviatoric stress reached terminal state, it was decided to reduce the magnitude of the applied stress, and try to achieve longer tests, that could provide clearer trends for material strain accumulation under loading.

Figure 45 shows the results performed at 250 kPa, considering lower array of temperatures, that resulted in the increase in the number of accumulated cycles to failure. The effect of temperature was clear throughout the tests, with reduced rate of strain accumulation as the temperature decreased. At both 25°C and 15°C, the reduction of deviatoric stress from 300 kPa to 250 kPa was enough to dramatically increase the number of cycles to failure. The tests conducted at 15°C were stopped before the end criterion was achieved due to a power shortage that interrupted the test, but the rate of strain accumulation was lower than any other test and they might have reached 500.000 cycles without achieving the maximum allowed accumulated strain. One of the tests performed at 25°C was also interrupted due to power shortages, but in this case, the graph shows that the material was already I the tertiary stage, with an increasing rate of accumulation of plastic strain.

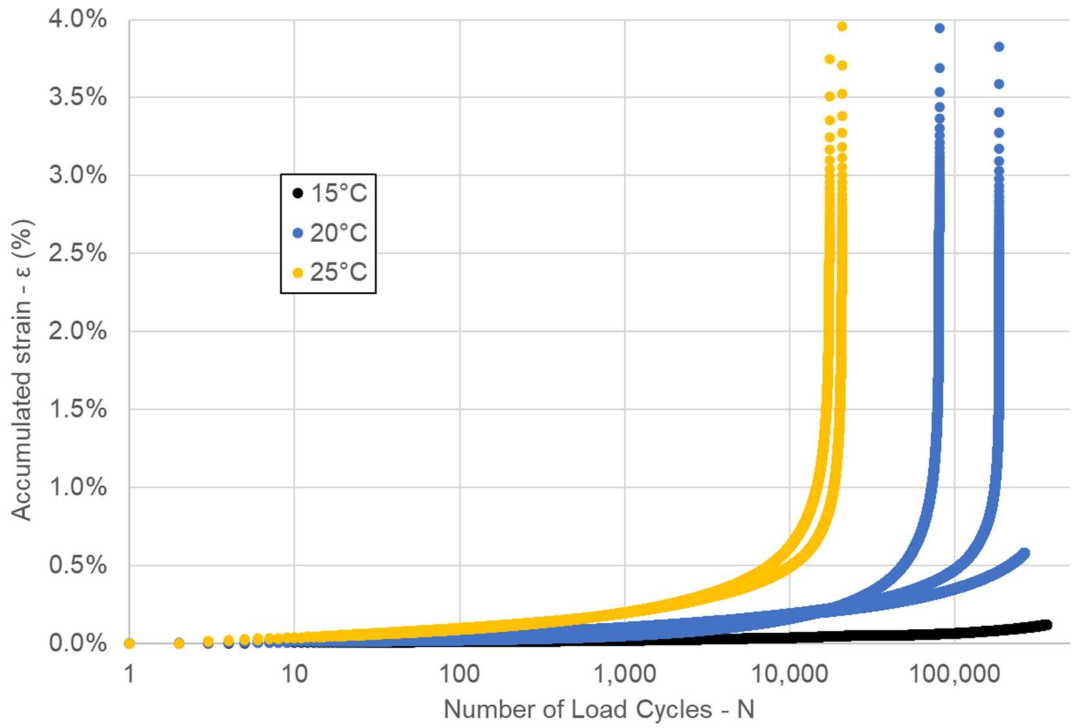


**Figure 45. Test results for 100 kPa confining stress, 250 kPa deviatoric stress and different temperatures.**

For the third set of tests, Figure 46 presents the results of the tests conducted using 200 kPa of deviatoric stress. Since the 25°C tests had already resulted in low values of permanent deformation accumulation, the other temperatures tested were defined as 30°C and 35°C. One of the tests performed at 25°C reached 500,000 cycles and was stopped before failure, but its curve shows that the material was entering the tertiary stage.

The results obtained for this set of tests still showed the impact of temperature and its reduction of material performance under loading. Differently from previous tests (with higher deviatoric stresses), where the temperature increments resulted in a clear decrease in performance, the reduction verified when the temperature surged from 30°C to 35°C was less noticeable graphically. However, the decrease in performance was still considerable, reaching 30% to 60% depending on the tested specimen.

As this observation was only possible for this set of tests, with lower deviatoric stress, it may indicate that higher stress may highlight the effect of temperature, especially for high temperatures, as they reduce the contribution of the bitumen binder for material stability and rely heavily on the internal friction of its aggregate particles.

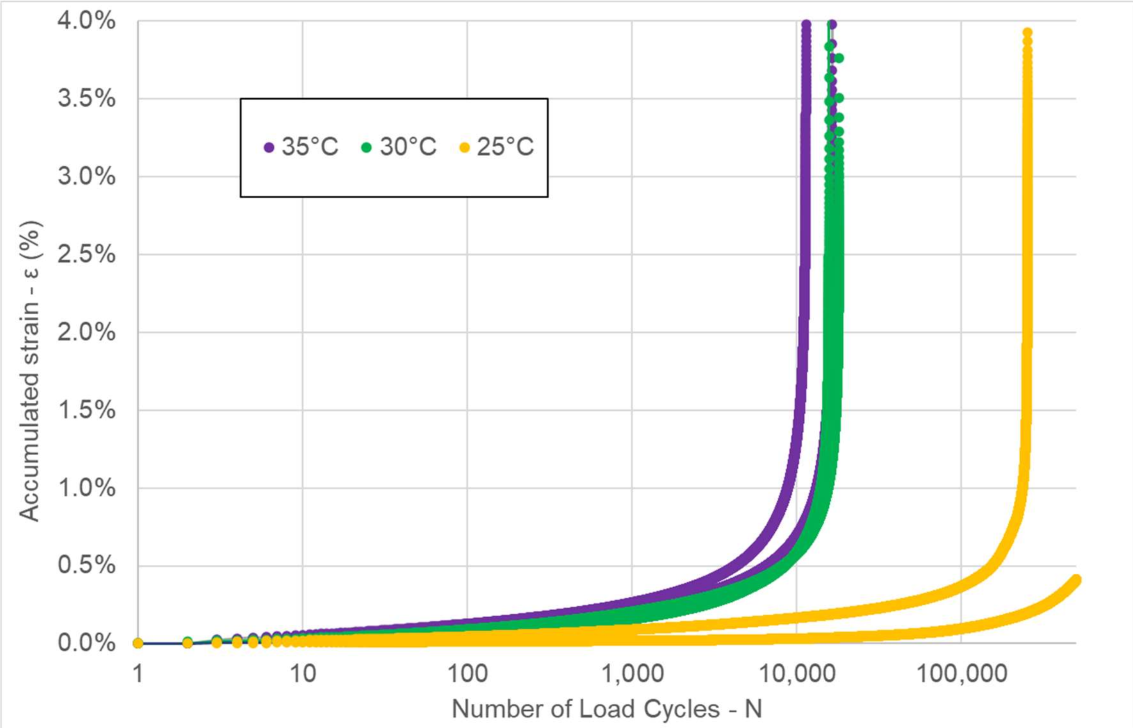


**Figure 46. Test results for 100 kPa confining stress, 200 kPa deviatoric stress and different temperatures.**

Figure 47 presents a comparison between tests performed at the same temperature of 25°C, but at different deviatoric stresses. The graph clearly shows how the reduction of the applied deviatoric stress results in an improvement in material performance, with increments of 25% and 50% resulting in an exponential reduction of 12 to 55 times, respectively.

For all TRL tests performed it can be observed how the results of tested specimens for the same for the same condition can be variable. That variability can be associated with material heterogeneity, especially for samples extracted from the field, that can have small gradation and composition variations that would not occur in the laboratory.

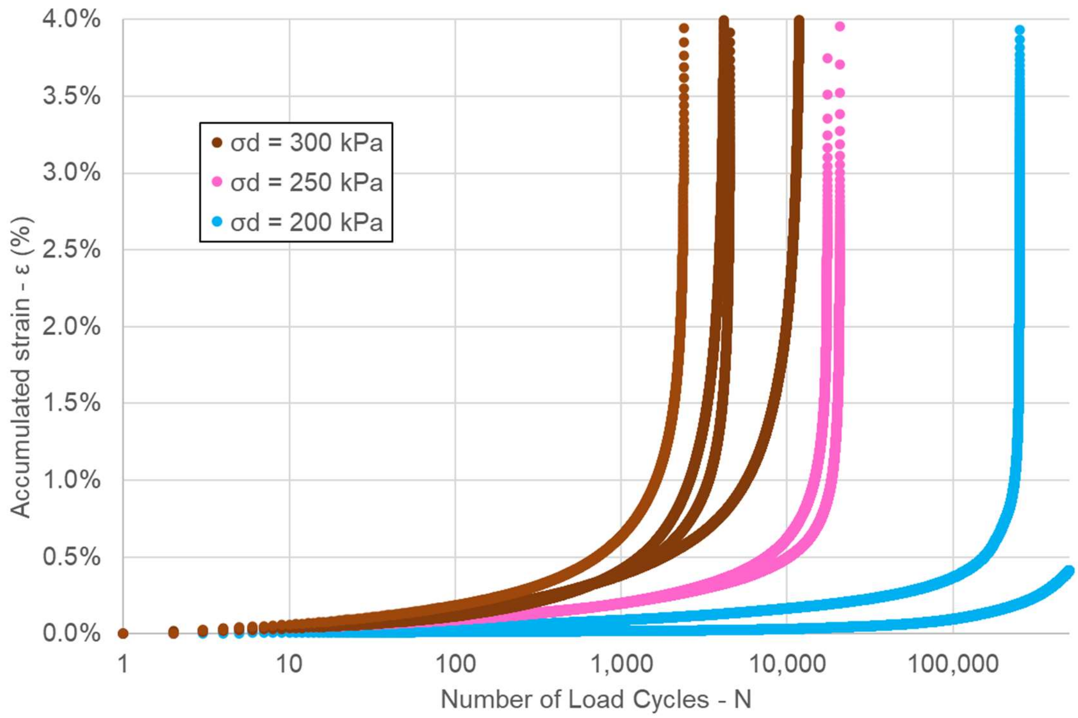


**Figure 47. Test results for 100 kPa confining stress, 25°C and different deviatoric stresses.**

Table 15 presents all the results obtained from the TRL tests with the parameters used for each test and the regression coefficients for the Primary, Secondary and Tertiary stages as described in in Figure 39. The tests performed with samples 58 and 48 were stopped due to power shortages and were not restarted afterwards to avoid alteration of the test results, and therefore have no tertiary stage coefficients.

**Table 15. TRL test results and regression coefficients for Primary, Secondary and Tertiary stages.**

| Sample Nº | σd (kPa) | Temp. (°C) | Max number of Cycles | Accum. strain. | Primary Stage | | | Secondary Stage | | | Tertiary Stage | | |
|---|---|---|---|---|---|---|---|---|---|---|---|---|---|
| | | | | | a | b | $R^2$ | c | d | $R^2$ | f | g | $R^2$ |
| 38 | 300 | 40 | 95 | 4,11% | 2,71E-04 | 9,84E-01 | 0,994 | -1,98E-04 | 2,47E-04 | 0,998 | 3,28E-03 | 2,62E-02 | 0,997 |
| 40 | | | 201 | 4,06% | 3,34E-04 | 6,83E-01 | 0,998 | 4,43E-04 | 9,87E-05 | 0,997 | 2,90E-03 | 1,30E-02 | 0,999 |
| 1 | | | 56 | 4,16% | 2,23E-05 | 1,91E+00 | 0,974 | -8,95E-04 | 2,40E-04 | 0,998 | 8,61E-04 | 6,20E-02 | 0,927 |
| 39 | | 25 | 11.839 | 4,00% | 1,98E-04 | 4,30E-01 | 0,999 | 2,66E-03 | 1,27E-06 | 0,999 | 2,93E-03 | 2,00E-04 | 0,971 |
| 30 | | | 4.544 | 4,00% | 1,79E-04 | 4,45E-01 | 0,998 | 1,68E-03 | 2,20E-06 | 0,994 | 9,13E-04 | 7,08E-04 | 0,909 |
| 37 | | | 4.164 | 4,01% | 1,02E-04 | 5,27E-01 | 0,999 | 9,60E-04 | 3,26E-06 | 0,995 | 1,36E-03 | 7,42E-04 | 0,962 |
| 31 | | | 2.397 | 4,05% | 1,94E-04 | 4,94E-01 | 0,997 | 1,53E-03 | 4,93E-06 | 0,999 | 1,47E-03 | 1,15E-03 | 0,914 |
| 32 | | 15 | 72.849 | 4,03% | 2,69E-04 | 2,91E-01 | 0,991 | 2,34E-03 | 1,32E-07 | 0,991 | 5,91E-04 | 4,74E-05 | 0,857 |
| 34 | | | 81.031 | 4,01% | 6,53E-05 | 2,45E-01 | 0,994 | 2,26E-04 | 8,02E-08 | 0,990 | 9,12E-04 | 2,94E-05 | 0,996 |
| 46 | 250 | 25 | 20.769 | 4,30% | 2,34E-04 | 3,10E-01 | 0,990 | 1,66E-03 | 3,51E-07 | 0,981 | 9,28E-05 | 2,53E-04 | 0,882 |
| 49 | | | 17.451 | 4,14% | 1,73E-04 | 3,55E-01 | 0,995 | 1,12E-03 | 5,57E-07 | 0,968 | 5,57E-05 | 3,38E-04 | 0,873 |
| 42 | | 20 | 80.795 | 4,41% | 4,31E-05 | 3,53E-01 | 0,994 | 4,37E-04 | 9,81E-08 | 0,985 | 1,98E-04 | 5,47E-05 | 0,900 |
| 58 | | | 265.141 | 0,58% | 1,27E-04 | 2,88E-01 | 0,996 | 1,98E-03 | 1,44E-08 | 0,991 | - | - | - |
| 54 | | | 186.840 | 4,15% | 1,36E-04 | 2,96E-01 | 0,990 | 1,42E-03 | 3,61E-08 | 0,978 | 5,67E-05 | 2,97E-05 | 0,850 |
| 48 | | 15 | 364.963 | 0,12% | 3,45E-05 | 2,65E-01 | 0,988 | 4,58E-04 | 2,12E-09 | 0,999 | - | - | - |
| 43 | 200 | 35 | 11.381 | 4,02% | 2,77E-04 | 3,26E-01 | 0,995 | 1,68E-03 | 8,15E-07 | 0,992 | 6,77E-04 | 3,05E-04 | 0,904 |
| 44 | | | 11.637 | 4,14% | 2,67E-04 | 3,12E-01 | 0,996 | 1,68E-03 | 5,30E-07 | 0,992 | 5,50E-04 | 2,20E-04 | 0,908 |
| 51 | | 30 | 18.102 | 4,42% | 1,64E-04 | 3,67E-01 | 0,997 | 1,60E-03 | 4,37E-07 | 0,989 | 3,51E-04 | 2,19E-04 | 0,894 |
| 52 | | | 15.696 | 4,12% | 1,24E-04 | 3,67E-01 | 0,998 | 1,21E-03 | 4,56E-07 | 0,999 | 9,01E-04 | 1,77E-04 | 0,898 |
| 45 | | 25 | 500.000 | 0,41% | 5,31E-05 | 1,79E-01 | 0,967 | 1,84E-04 | 7,42E-09 | 0,995 | - | - | - |
| 55 | | | 251.989 | 4,01% | 1,11E-04 | 3,05E-01 | 0,997 | 1,48E-03 | 2,25E-08 | 0,993 | 8,66E-04 | 1,07E-05 | 0,879 |

The secondary stage regression coefficients described in Table 15 as c and d represent respectively the intercept and slope of the curve. The slope is commonly referred to in the international literature as Creep Strain Slope (CSS) and represents the rate of strain accumulation. It can be observed in Table 15 that the magnitude of d increases and decreases according to the shift in temperature, as previously pointed out. Figure 48 shows the influence of temperature on the magnitude of CSS, with a decreasing exponent as temperature drops, resulting in lower strain accumulation rates.

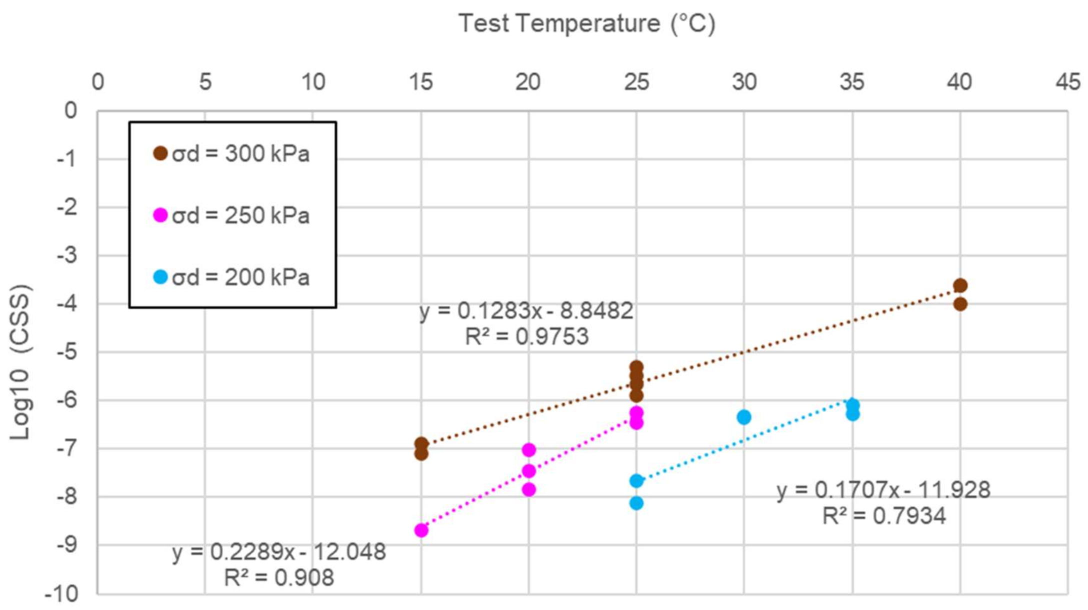


**Figure 48. Influence of temperature on the CSS, for each set of tests separated by the applied deviatoric stresses.**

Although the results in Table 15 showed some dispersion between results within the same test conditions, the values of CSS for the tested specimens for each condition resulted in a good relation in terms of the temperature variation, as shown in Figure 48.

A similar relation can be drawn between the effect of the deviatoric stress on the magnitude of CSS, as shown in Figure 49, with the values of tests performed at 25°C at each deviatoric stress condition creating a clear trend.

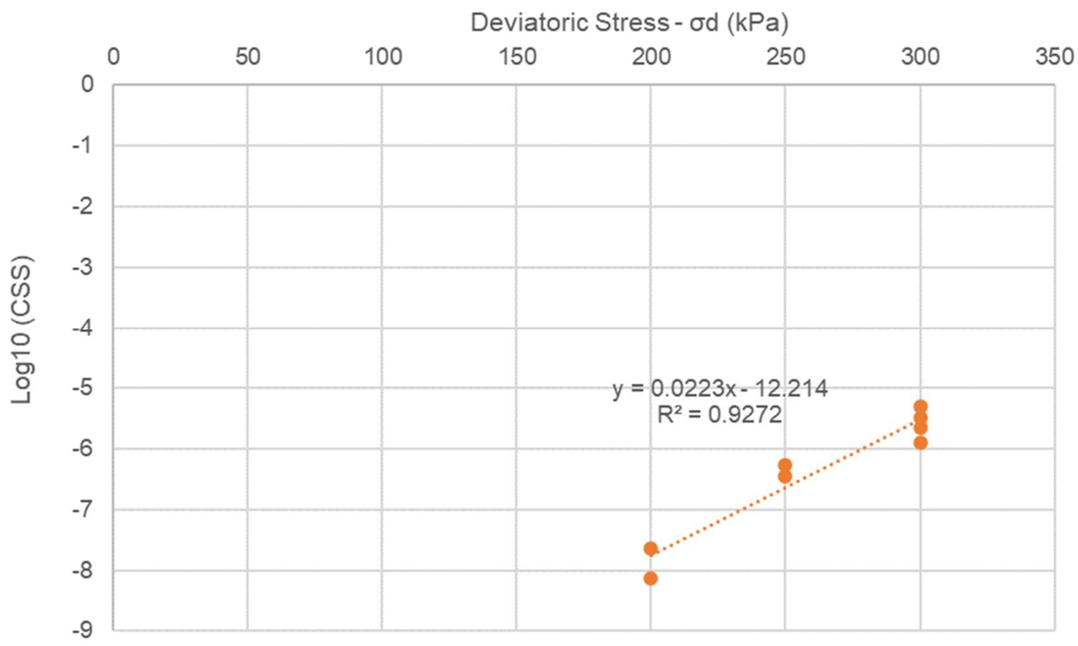


**Figure 49. Influence of the deviatoric stress on the magnitude of CSS, for tests performed at 25°C.**

It is important to observe that the magnitude of CSS changes for increments in deviatoric stress, just as much as it changes for increments in temperature. The rate of strain accumulation is as sensible to temperature changes as it is to changes to the applied stress for the material evaluated in this chapter (low asphalt binder and low hydrated lime content).

Although much thought is given to controlling the stresses that occur within a pavement structure under loading, not many considerations are made regarding the temperature to which BSMs are subject to. As most laboratory tests are performed on controlled environments, and usually at temperatures around 20°C to 25°C, the performance obtained in these tests will usually be conservative for colder conditions. For temperate and tropical areas, where temperature amplitude is high, and pavement temperature can easily go above 35°C, the assessment of the effect of temperature becomes extremely important, as it may reduce material performance significantly.

## 5.5 PARTIAL CONCLUSIONS

This chapter investigated the effect of temperature on the mechanical behaviour of foamed bitumen stabilized material using different laboratory tests. The tests performed were able to properly characterize the material and provided evidence on how temperature significantly affected the material performance, and should, therefore, be considered for pavement design.

The literature review provided insights and comparative bases for some of the tests performed. For the TRM and DM tests, the results were comparable to those identified in international literature for foamed asphalt stabilized materials with high percentage of RAP.

The results of MTT were also compared to values found on literature, with higher cohesion and friction angle than expected. This effect could have been a result of the low moisture contents of the specimens during test and higher consolidation due to its curing under loading on the trial section, when compared to laboratory manufactured design samples.

The TRM tests showed how dependent on the stress state the foamed asphalt material is, with considerable dependency of both the confining and deviatoric stresses. The results showed an increase of 50% on material stiffness depending on the stress state it was subject to, which is significant and should be accounted for during pavement design phase.

The results of the DM tests showed a clear correlation between stiffness and test temperature/frequency, with decreasing values as temperatures rose. The test results showed how dependent on the aggregate structure the material stiffness become as temperature rises, and how the contribution of the asphalt binder increases as it gets colder.

As anticipated by the characterization tests results, the permanent deformation tests showed great influence of both the stress state and the temperature. Although different mixtures may suffer differently with the effect of temperature, it was significant to observe how small variations in temperature produced exponential impact on the rate of strain accumulation. For the studied mixture, composed of 85% RAP, an increase in 5°C was sufficient to reduce by 10 times the number of load cycles to failure. That trend was confirmed for different test conditions, with varying temperatures and stresses conditions.

The effect of the stress state on the rate of strain accumulation was also significant. However, it is important to observe that the magnitude of its impact was comparable of that from the variation of temperature, which further suggests the importance of temperature consideration during pavement design phase.

Lower deviatoric stresses may reduce the effect of temperature on CSS, as the low stresses become more easily supported by the internal friction of the aggregates composing the mix, as the binder contribution diminishes. These results indicate that to mitigate for the impact of temperature when designing pavements, it is desirable lower acting stresses on the BSM layer, as well as providing sufficient cover to control temperature amplitude.

# 6 THE EFFECT OF TEMPERATURE IN THE MECHANISTICAL ANALYSIS OF FOAMED ASPHALT STABILIZED PAVEMENT STRUCTURES

## 6.1 INTRODUCTION

The design of pavement structures composed by foamed asphalt layers is a challenge faced by many engineers, while the growth and popularity of the technique demands a greater understanding of the material behaviour.

Different Road Transportation Agencies around the world adopt distinct approaches when designing these layers, as mentioned in Chapter 2, while the question over which procedure better describes the material, and which one is more suitable for each project remains among many researchers. Additionally, reported resilient moduli for different foamed asphalt stabilized mixtures can range from 700 MPa to 5,500 MPa (Khosravifar et al., 2015), values that were obtained both in the field and in the laboratory for the mixtures studied in Chapters 3 and 5, bringing extra challenge to define how material stiffness and mechanical behaviour should be approached.

Bitumen Stabilized Materials (BSM), which can be foamed asphalt stabilized mixtures, can be produced using reclaimed aggregates from existing pavements or new materials, with addition of asphalt binder and an active filler such as cement, lime or fly ash (Kuna, 2015). Depending on the aggregate sources and the nature and proportion of the binders used, the mechanical properties of the resulting mixture may differ greatly, resulting in different structural behaviour (Graziani et al. 2018a; Kuchiishi et al. 2019).

Triaxial resilient modulus tests in Chapter 3 and 5, showed that foamed asphalt stabilized materials can present stress dependent behaviour under loading. As a result, traditional mechanistic design procedures using linear elastic layer systems can lead to deviations from the field conditions.

The mechanical behaviour of foamed asphalt stabilized materials is also affected by temperature, as shown in Chapter 5, with material stiffness and resistance to rutting decreasing as temperature increased. The variation of stiffness with temperature can be clearly identified during Dynamic Modulus test and could be used as input parameter during structural analysis. The mechanical responses under loading of pavements containing foamed asphalt stabilized layers were assessed using three different approaches.

The analysis was conducted using: (i) a linear elastic model, considered as the control; (i) a nonlinear elastic model, to evaluate the effect of stress dependency; (iii) and a viscoelastic model, to evaluate the effect of temperature and frequency loading.

The objective of this study is to evaluate the effect of temperature changes and stress state conditions on material responses under loading, assessing if the performance predicted through mechanistic-empirical analysis corresponds to field and laboratory observations.

## 6.2 MECHANISTIC-EMPIRICAL APPROACH

Considering the pavement structure composed by different layers, the stresses and strains in particular points are important for the mechanistic-empirical approach for pavement design.

The structure evaluated in this study was based on the pavement Section 5, BR-116/SP, presented in Chapters 3 and 4. The structure evaluation varied according to the limitations and capabilities of the softwares used in each analysis, and are discussed in detail in the following items. The software choice for the analysis was based on availability and common use, prioritizing free and broadly used software.

The pavement structure from trial section 5 is composed by a 30 mm Gap Graded wearing course (GGWC), laid on top of a BSM base of 300mm. During rehabilitation, this BSM layer was placed on top of an existing granular subbase of unknown thickness, and for that reason, the existing underlying layers were considered as Remaining Infrastructure (RI) semi-infinite layer. The BSM base layer, was generally divided in three 100 mm sublayers during the structural analysis, to allow for different considerations of temperature and material modulus.

In the analysis, pavement structure was subjected to two loads of 20 kN each, placed 300 mm away from each other, with a contact pressure of 560 kPa, simulating half of a standard single axle loading.

As described by Huang (2003), conventional flexible pavements are usually evaluated in mechanistic-empirical methods for the tensile strains at the bottom of the asphalt layer and the compressive strains on top of the subgrade. As traffic loading is commonly described in terms of equivalent single axle loads (ESALs), the points of interest where stresses and strains are critical are usually located either under the centre of the loading area, or between loads. Another parameter of particular interest is the surface displacement, usually related to the deflection measured by the Falling Weight Deflectometer. In this analysis, however, the evaluation focused on the mechanical responses of the BSM material, assessing how it responds to different temperature and loading conditions, even though the behaviour of the base layer influences the overall performance of the entire pavement structure.

During the mechanistical analysis of pavement structures, the material stresses and strains at different points of the structure are typically evaluated. For the performance prediction and analysis of the BSM layer, the permanent deformation model presented by Bierman (2018) and detailed on equation (6.1) was used:

$$logN = A - 57.286(DSR)^3 + 0.0009159(P_{mod}.RetC) + 0.086753(PS) \quad (6.1)$$

where: N = the allowable number of load repetitions;

$P_{mod}$ = material density in terms of its Modified AASHTO density (%);

RetC = Retained Cohesion obtained from Monotonic Triaxial Tests (%);

*PS* = allowed plastic strain (%);

DSR = deviator stress ratio (Theyse et al, 2000);

A = Reliability adjustment term, as described in Chapter 2.

While $P_{mod}$, PS and RetC have a direct effect on the allowable number of load repetitions, the DSR has an inverse effect, reducing N. This model uses the Deviator Stress Ratio, as proposed by Theyse et al (2000), which, as discussed by Bierman (2018), has significant effect in material performance. This is highlighted by the power of 3 to which the DSR parameter is subjected in the transfer function, increasing the parameter relevance during structural design.

As mentioned in Chapter 2, the DSR represents the stress relation between the acting deviator stress in the material, and the maximum deviator stress that leads to failure, defined by the Mohr-Coulomb failure envelope. The DSR can be calculated for BSM layers using equation (6.2):

$$DSR = \frac{(\sigma_1 - \sigma_3)}{\sigma_3\left[K\left(\tan^2\left(45+\frac{\phi}{2}\right)-1\right)\right]+2C\tan\left(45+\frac{\phi}{2}\right)} \tag{6.2}$$

where: DSR = Deviator Stress Ratio;

$\sigma_1$ and $\sigma_3$ = Applied major and minor principal stresses;

C = Cohesion (399 kPa for the trial section material, as tested in Chapter 5);

ϕ = Internal Friction Angle (42.7° for the trial section material, as tested in Chapter 5);

As a combination of major principal stresses and shear parameters (cohesion and friction angle), it is not trivial to predict how these single variables affect the mixture performance. The TG2 (SABITA, 2020) recommends that the DSR should be calculated for the critical point located at a depth of 25% of the layer thickness.

To evaluate the BSM layer, the assessment of material behaviour in this analysis was performed using pavement structures analyzed on the critical points presented in Figure 50. Positions evaluated for stresses and strains during mechanistic analysis. Figure 50 and described as follows:

- Major principal stresses (σ1 and σ3) to calculate DSR on the BSM at 25%, 50% and 75% of each base sublayer depth;
- Vertical and horizontal strains on the BSM at 25%, 50% and 75% of each base sublayer depth.

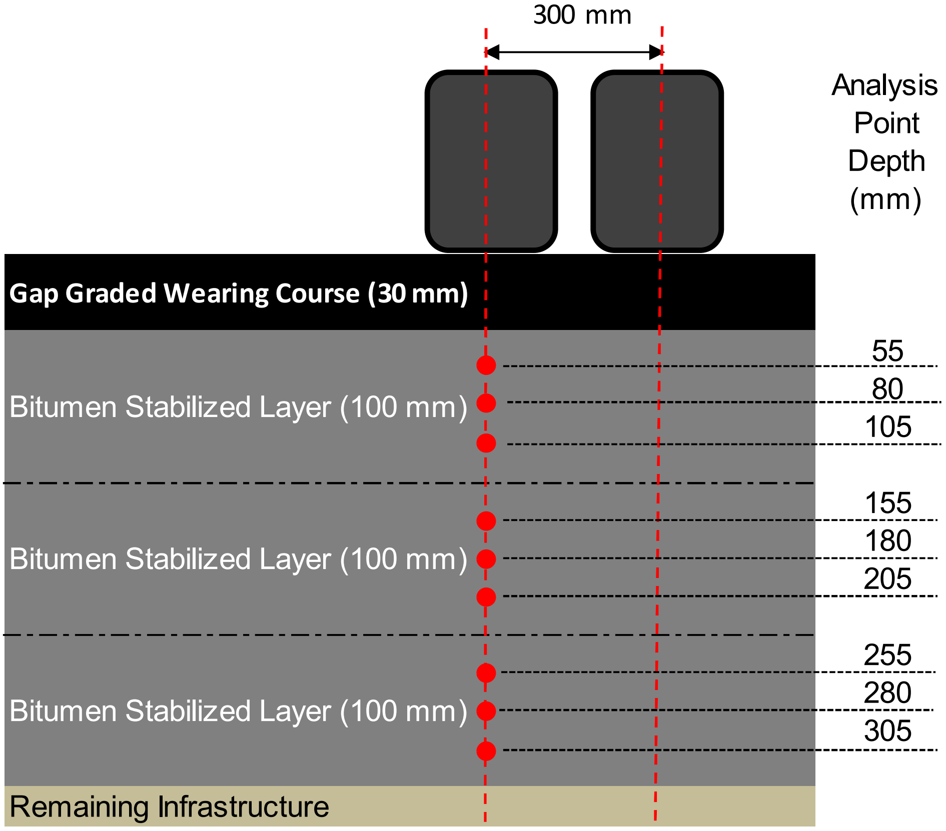


**Figure 50. Positions evaluated for stresses and strains during mechanistic analysis.**

### 6.2.1 Linear Elastic Analysis

The linear elastic (LE) analysis was conducted using ELSYM 5 software, which was developed in the University of California at Berkeley in the 1980's and has since been widely used globally (Evangelista et al., 2005). The software allows for a structure of up to 5 layers, with layers being characterized in terms of their thickness (h), Elastic Modulus (E) and Poissons' Ratio, while also considering all layers to be fully bonded.

Two different structure conditions were evaluated with LE analysis. One of the conditions considered the 300 mm BSM layer stratified in three 100 mm layers with different material moduli considerations, as shown in Figure 50. The other condition, however, considered the BSM as one single 300 mm layer, which represents the most common approach for the design of these structures.

### 6.2.2 Non-linear Elastic Analysis

The non-linear elastic (NLE) analysis was conducted using the KENPAVE software (Huang, 2003). The software is divided in two different sections called KENSLAB, used for rigid pavement structural design, and KENLAYER, used for the design of flexible pavement structures. The software allows for the characterization of granular layers as non-linear elastic materials, using the K-θ model presented in Equation 6.3 to describe the material modular response to its stress state:

$$Mr = K_1 \times \theta^{K2} \tag{6.3}$$

Where: Mr is the Resilient modulus;

$\theta$ is the sum of the major principal stresses $\sigma_1$, $\sigma_2$, $\sigma_3$;

$K_1$ and $K_2$ are regression coefficients.

The KENLAYER software has three different calculation methods to determine the resilient modulus of granular layers, considering the non-linearity of the material. Method 1 is recommended when base layers are subdivided in different layers, with the stresses being calculated at mid-depth of each sublayer and associated with its respective material modulus, through an iterative process. Methods 2 and 3 use similar iterative processes for moduli calculation, however, they assume the granular base layer as a single layer, calculating the stresses at either the top portion or the middle of the layer, considering the modulus for the entire layer. For this analysis, method 1 was the one chosen, due to the subdivision of the base layer, as well as for being the method recommended for granular layers under thin layers (less than 127mm) of hot mix asphalt (Huang, 2003; Kuchiishi et al. 2021).

Although the KENLAYER software allows for the evaluation of pavement structures considering different layers to be either adhered or non-adhered, as the other software considered adhered layers, that consideration was preserved in the NLE analysis. Considering completely non-adhered layers could result in significant changes in horizontal stresses and strains, especially close to material interfaces (Kuchiishi, 2019). The adherence consideration, however, is adequate to this study, since the BSM sublayers are an artifice for structural analysis and do not have actual interfaces, effectively working as adhered layers, while the GGWC has some adherence to the base layer due to existing the tack coat.

In this analysis, both the GGWC and the RI layers were considered as linear elastic, using the same values for elastic modulus considered for the LE analysis presented. Meanwhile, the BSM layer was defined as nonlinear, using the K-θ model described in Equation (6.3), and obtained from the Triaxial Resilient Modulus (TRM) tests presented in Chapter 5. For the NLE analysis, as illustrated in Figure 50. Positions evaluated for stresses and strains during mechanistic analysis. Figure 50, the BSM layer was subdivided in three 100 mm layers, that had the same modulus characteristics, but depending on the active stress conditions, produced different modular responses.

### 6.2.3 Viscoelastic Analysis

The viscoelastic (VE) analysis of the pavement structure was performed using the software 3D-Move Analysis 2.1. The software, developed by the University of Nevada allows for three-dimensional analysis of pavement structures using continuum-based Finite Layer Method to assess the impact of moving loads and different temperature conditions on material responses (Vijayaruban, 2011; Liu et al. 2017).

Although the pavement structure is the same as the previous methodologies in terms of thicknesses and positions analysed, material characterization is different. As the software allows for a viscoelastic analysis of the pavement structure, the top GGWC and BSM layers were considered in terms of their linear viscoelastic properties.

To properly assess the responses of the pavement structure under different loading frequencies and temperature conditions, the mechanical analysis was performed using 5 different scenarios. The different scenarios are presented in Table 16. and represent real temperature measurements from the trial section, as presented in Chapter 4. These temperature measurements were performed in three separated days and were chosen for the analysis as they represent common conditions for pavements in the southeast of Brazil. The last two scenarios were evaluated with the same temperature gradient as Scenario 3, but with different vehicle speeds, impacting the pavement loading frequency and, consequently, its response.

**Table 16. Description of the evaluation scenarios in terms pavement temperatures and vehicle speed**

| Scenario | 1 | 2 | 3 | 4 | 5 |
|---|---|---|---|---|---|
| Measurement Date | 13/03/2019 | 25/09/2019 | 16/06/2020 | | |
| Time of day | 11:15 | 11:13 | 15:00 | 15:00 | 15:00 |
| Surface | 45°C | 21°C | 34°C | 34°C | 34°C |
| 20 mm depth | 42°C | 21°C | 35°C | 35°C | 35°C |
| 40 mm depth | 37°C | 19°C | 32°C | 32°C | 32°C |
| 160 mm depth | 31°C | 21°C | 25°C | 25°C | 25°C |
| 300 mm depth | 30°C | 23°C | 23°C | 23°C | 23°C |
| Vehicle Speed | 80 km/h | 80 km/h | 80 km/h | 40km/h | 120 km/h |

The BSM layer was characterized using de dynamic modulus test results presented in Chapter 5, while the asphalt binder used for the foamed stabilization was characterized as a default “Conventional Penetration Grade Pen 60 – 70”, which was the closest to the actual Pen 50-70 used in the trial section. The characterization for the GGWC was made using data from Kuchiishi (2019), who tested both the mixture and the binder (see Table 17) for a GGWC of similar material sources.

Table 18 shows the dynamic modulus results used for the characterization of the GGWC and the BSM. Similar to previous analysis, the remaining infrastructure layer was considered as a semi-infinite layer with linear elastic behaviour.

**Table 17. Material characterization for the GGWC binder based on Dynamic Shear Rheometer (DSR) test (Kuchiishi, 2019).**

| DSR | Sample 01 | |
|---|---|---|
| Temp (ºC) | G* (kPa) | δ (°) |
| 40 | 45.30 | 73.4 |
| 50 | 11.42 | 71.2 |
| 60 | 3.65 | 69.7 |
| 70 | 1.35 | 70.2 |
| 80 | 0.53 | 72.4 |

**Table 18. Material characterization for the BSM and the GGWC based on Dynamic Modulus Test results (GGWC characterization from Kuchiishi, 2019).**

| Specimen | Temp. | Dynamic modulus (kPa) | | | | | | Phase angle (kPa) | | | | | |
|---|---|---|---|---|---|---|---|---|---|---|---|---|---|
| | ºC | 0.1 Hz | 0.5 Hz | 1 Hz | 5 Hz | 10 Hz | 25 Hz | 0.1 Hz | 0.5 Hz | 1 Hz | 5 Hz | 10 Hz | 25 Hz |
| BSM | 4.4 | 2658333 | 3074667 | 3244000 | 3730333 | 3998667 | 4366667 | 12.28 | 10.42 | 9.94 | 8.66 | 7.89 | 6.81 |
| | 21.1 | 660167 | 878100 | 961933 | 1269133 | 1408700 | 1655600 | 20.65 | 19.13 | 18.66 | 16.08 | 15.15 | 13.82 |
| | 37.8 | 243900 | 343567 | 391033 | 610800 | 721100 | 963967 | 24.47 | 24.76 | 25.32 | 22.45 | 21.45 | 19.68 |
| | 54 | - | - | - | - | - | - | - | - | - | - | - | - |
| GGWC | 4.4 | 11661000 | 15540000 | 17044000 | 20510000 | 22066000 | 26301000 | 19.53 | 15.05 | 11.72 | 9.69 | 8.95 | 10.65 |
| | 21.1 | 2214000 | 4132000 | 5282000 | 8354000 | 9855000 | 12029000 | 34.54 | 31.83 | 26.64 | 21.63 | 20.12 | 18.75 |
| | 37.8 | 318000 | 568000 | 774000 | 1784000 | 2404000 | 3492000 | 27.96 | 33.42 | 34.31 | 34.69 | 34.19 | 33.09 |
| | 54 | 155000 | 203000 | 242000 | 462000 | 609000 | 901000 | 16.50 | 21.68 | 24.39 | 28.26 | 30.41 | 33.80 |

### 6.2.4 Pavement Structures Analyzed

To allow the comparison of pavement structural responses between different pavement temperature conditions, loading frequencies due to the vehicle speed and different material behaviour considerations, 8 scenarios were evaluated. The difference between the scenarios is presented in Table 19, where scenarios 1 to 5 considered the VE behaviour of the BSM in the analysis, scenario 6 considered the NLE behaviour and scenarios 7 and 8 considered LE analysis. Apart from the software used, the main difference among the scenarios lies in the modulus adopted for the BSM and GGWC layers, and in the case of the VE analysis, the loading frequency due to the different vehicle speed.

The dynamic modulus ($|E^*|$) of the BSM and GGWC were used for the VE analysis, with the respective temperature considered for each layer defined according to the real measurements made on the trial section and indicated in Table 16. For the NLE analysis, the modulus for each layer was defined via software interaction based on the Triaxial Resilient Modulus (TRM) test and the stress state calculated.

The LE analysis of scenarios 7 and 8 considered two different conditions for the BSM layer characterization. In scenario 7 the BSM layer is subdivided in three 100 mm layers, as was the case in the previous six analysis, and the modulus was defined based on the results of the Dynamic Modulus tests, considering the same temperature conditions as scenario 3. In scenario 8, the BSM layer is considered as a single 300 mm layer, which is the most common approach for the design of such structures, with an elastic modulus corresponding to the average value of the TRM test results.

For the LE and NLE analysis, the elastic modulus of the GGWC was defined based on the Dynamic Modulus for the material at 35°C, same temperature as scenario 3, so the different calculation approaches could be compared.

**Table 19. Summary of the different conditions and pavement structures analyzed.**

| **Calculation method** | **VE** | | | | | **NLE** | **LE** | |
|---|---|---|---|---|---|---|---|---|
| **Pavement Structure** | **1** | **2** | **3** | **4** | **5** | **6** | **7** | **8** |
| GGCW (30 mm) | \|E*\|; @42°C | \|E*\|; @21°C | \|E*\|; @35°C | \|E*\|; @35°C | \|E*\|; @35°C | E = 1,000 MPa @35°C | | |
| BSM (3 layers of 100 mm each) | \|E*\|; @37°C | \|E*\|; @19°C | \|E*\|; @32°C | \|E*\|; @32°C | \|E*\|; @32°C | TRM | E=829 MPa; @32°C | E=1.359 MPa |
| | \|E*\|; @31°C | \|E*\|; @21°C | \|E*\|; @25°C | \|E*\|; @25°C | \|E*\|; @25°C | TRM | E=1,115 MPa @25°C | |
| | \|E*\|; @30°C | \|E*\|; @23°C | \|E*\|; @23°C | \|E*\|; @23°C | \|E*\|; @23°C | TRM | E=1,219 MPa @23°C | |
| RI | E = 150 MPa | | | | | | | |
| Vehicle speed (km/h) | 80 | 80 | 80 | 40 | 120 | - | - | - |

Although different methods and specific conditions were used to calculate pavement responses, the loading characteristics, pavement thickness and poisson ratio were kept the same in all scenarios.

The Poisson ratio used for the GGWC was 0.30, for the BSM 0.35 and for the RI 0.45 in all analysis. The value of Poisson ratio for the GGWC layer was defined on recommendations for pavement structural analysis from the South African Pavement Engineering Manual (SANRAL, 2014), and Brazilian specification IP-DE-P00/001 (DER-SP, 2006). The Poisson Ratio for the BSM was defined assuming that the material would behave as a stress dependent granular material (Kuchiishi, 2019; Loizos et al. 2012) while the remaining infrastructure Poisson ratio was defined as 0.45. The elastic modulus of the Remaining Infrastructure for all scenarios was defined based on backcalculated modulus from FWD surveys presented on Chapter 3.

## 6.3 RESULTS AND DISCUSSION

When evaluating the mechanical behaviour of pavement structures, it is important to assess the points within the structure where each parameter produces critical responses.

Considering scenario 3 as an example, Figure 51Figure 51 present the Normal Strain in the longitudinal and transversal direction during the passage of the dynamic load, measured at the bottom portion (75% depth) of each 100 mm BSM layer. All graphs are presented considering positive values as compression and negative values represent tension. The bottom portion of each layer was considered for the higher tensile strains that it exhibits, being critical for BSMs due to its high compressive strength but low tensile resistance. As it can be noted in Figure 51, the lower BSM layer, represented by the 305 mm depth point of analysis, is the one demanded the most, with tensile strains reaching 80μ.

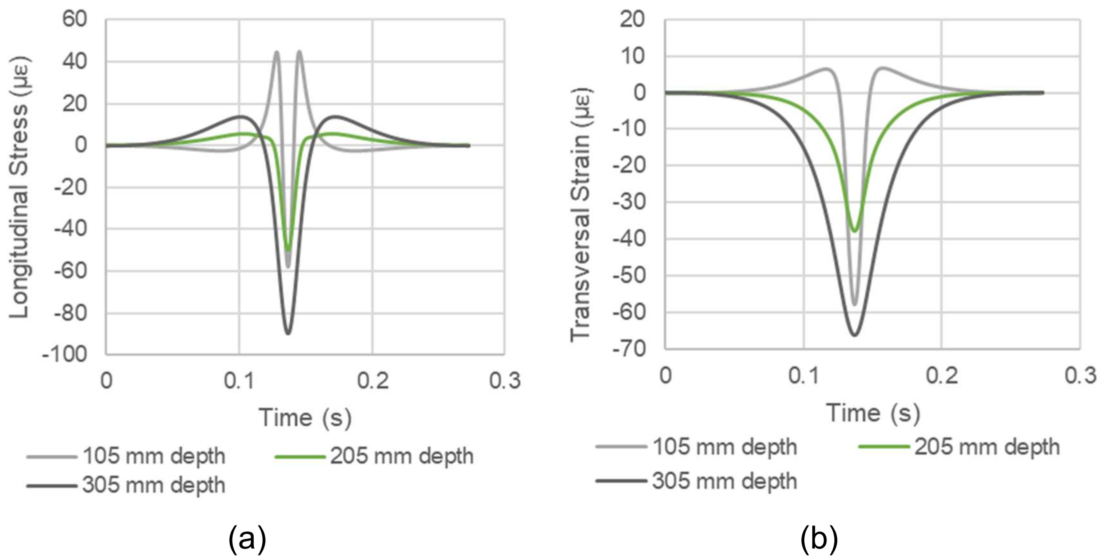


**Figure 51. (a) Normal Longitudinal Strains and (b) Normal Transversal Strains at different depths of the BSM layer, calculated using VE analysis (scenario 3).**

Considering the load dissipation within the structure, it is also possible to infer that compressive stresses and therefore the vertical strains would be larger closer to load application point, in the top portion of each BSM layer. Evaluating the vertical strains and vertical stresses on the top portion of the BSM layers (25% depth), Figure 52 shows how both compressive strains and stresses decrease with pavement depth. As observed, the compressive strain on the first 100 mm layer is more than three times higher than that on the bottom BSM layer, while the compressive stresses decrease as much as five times.

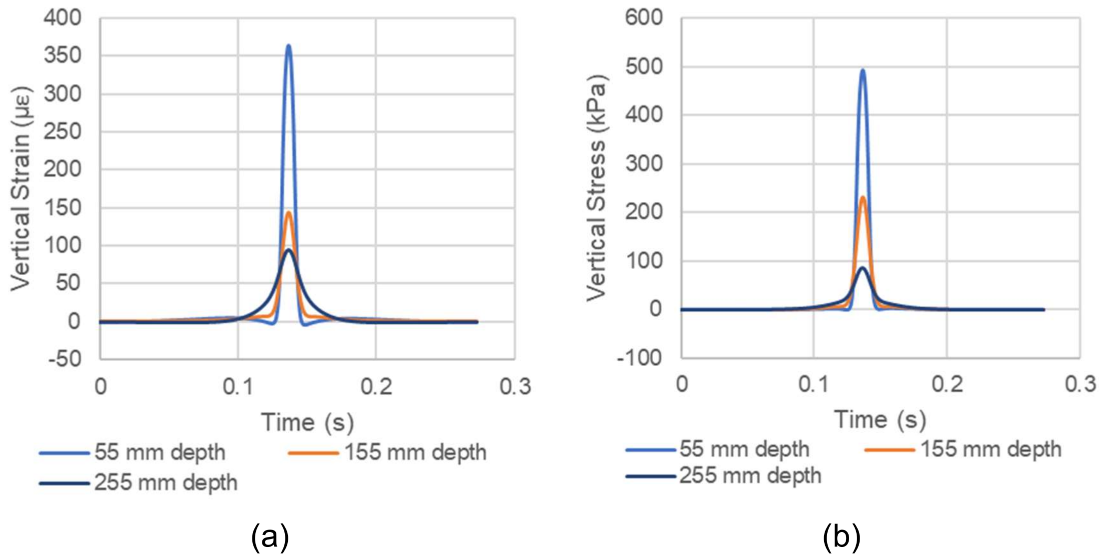


**Figure 52. (a) Vertical strains and (b) Vertical Stresses calculated at different depths of the BSM layer, calculated using VE analysis (scenario 3).**

The strains and stresses calculated at mid-depth of the BSM base resulted in neither the highest values for compression nor tension. This verification was confirmed for all 8 scenarios analysed. In that sense, when evaluating horizontal tensile strains, the bottom portion of the BSM layer is critical for analysis, while the top portion is critical for the evaluation of compressive strains and stresses.

### 6.3.1 Effect of Load Frequency

The analysis performed on ELSYM5 and KENLAYER for the Linear Elastic (LE) and Non-linear Elastic (NLE), considered the application of static loads on the pavement surface, and material responses on pre-defined positions of the structure. In contrast, the viscoelastic (VE) analysis considers the passage of a moving load, and pavement responses in the pre-defined positions with time, considering the approach, passage, and distancing of the load.

Figure 53 shows the results of longitudinal and transversal strains at 305 mm depth for the analysis of Scenarios 3 to 5, where the temperature gradient is the same, but the speed of the vehicle, and hence, the loading frequency is different. The reduction of the loading frequency due to the decrease in vehicle speed, from 120 km/h to 40 km/h, resulted in increase of the tensile strains of approximately 13% (from 85.8μ to 96.9μ) considering the longitudinal strains, and 12% (63.6μ to 71.1μ) for transversal strains.

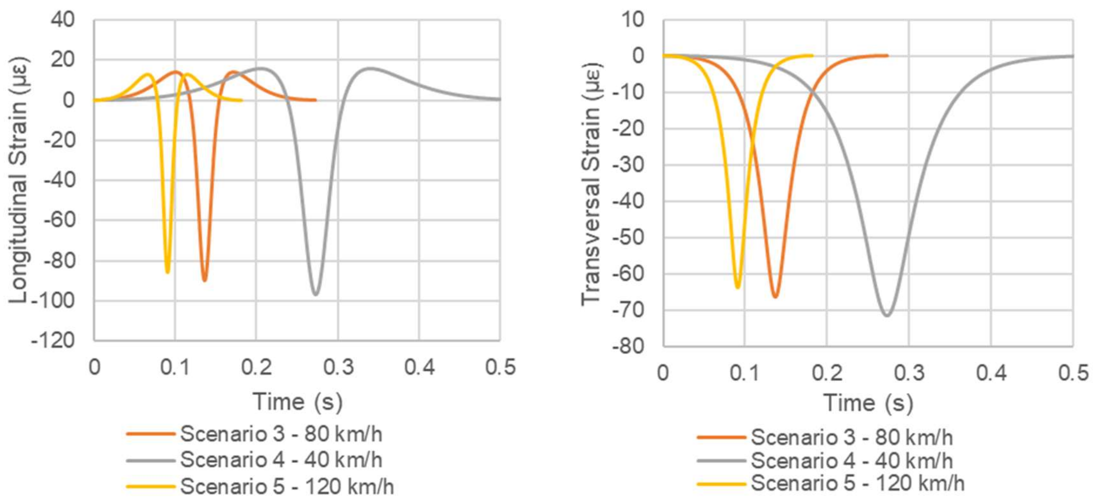


(a) (b)

**Figure 53. (a) Normal Longitudinal Strains and (b) Normal Transversal Strains at 305 mm depth for different vehicle speeds, calculated using VE analysis.**

The effect of different vehicle speeds on the vertical strains calculated for Scenarios 3, 4 and 5 at the top portion (55 mm of depth) of BSM structure is presented in Figure 54. The compressive strain on the top portion of the BSM layer also was sensitive to the reduction of vehicle speed from 120 km/h to 40km/h, increasing the vertical strain by 24.5%.

While observing the effect of the vehicle speed on the responses of the BSM layer in terms of strains, it is also important to understand the effect caused on the material stress state through the major and minor principal stresses ($\sigma_1$ and $\sigma_3$), allowing the calculation of the DSR (Equation 6.2), which is used for the performance prediction model of the material, using the TG2 transfer function in Equation 6.1.

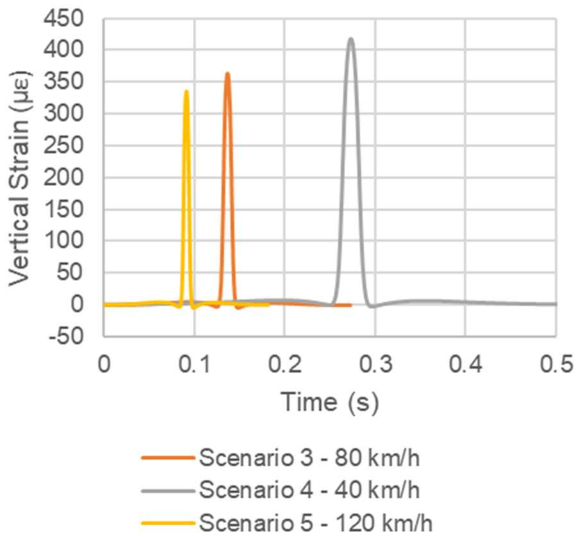


**Figure 54. Vertical strains at 55 mm depth for different vehicle speeds, calculated using VE analysis.**

The $\sigma_1$ and $\sigma_3$ are presented in Figure 55, where it can be observed that the effect of the loading frequency on the magnitude of the calculated stresses was small.

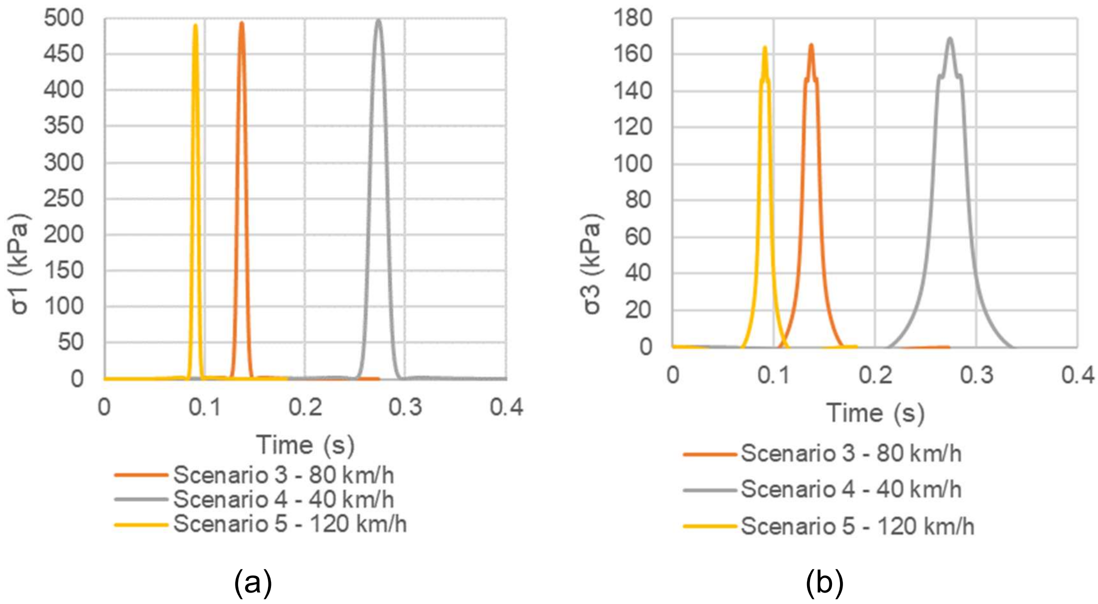


**Figure 55. (a) Major Principal Stress (σ1) and (b) Minor Principal Stress (σ3) Strains at 55 mm depth for different vehicle speeds, calculated using VE analysis.**

The increase in stresses verified was approximately 1.5% for $\sigma1$ and 3% for $\sigma3$, indicating that the calculated strains were more sensitive to the change in vehicle speed than the calculated stresses. Using equation 6.2, considering the values of cohesion and friction angle from the Monotonic Triaxial Tests presented in

Chapter 5, the DSR was calculated for the different scenarios evaluated, as presented in Figure 56. The value of DSR was also calculated as a function of time, to verify the moment of higher DSR.

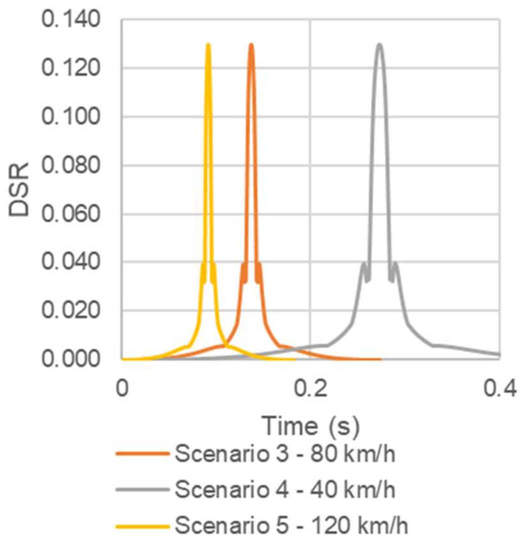


**Figure 56. Calculated values of DSR for three different conditions of loading frequency.**

Although the values of DSR presented in Figure 56 were calculated for the top portion (25% of layer thickness, at 55 mm) of the upper BSM layer, the calculated values of DSR were critical between 25% and 50% of the layer depth, depending on the combination of $\sigma 1$ and $\sigma 3$. These consideration of 25% of layer thickness is in line with the recommendations from the TG2, and observations made by Bierman (2018).

The calculated DSR is highest when the applied load is directly above the analysis point, and the calculated value for the three scenarios was 0.130. As observed in Figure 56, the difference in the principal stresses among the different scenarios did not result in significant change in DSR.

### 6.3.2 Effect of Temperature Variation

After assessing the effect of temperature on the BSM base on the field and on the laboratory in chapters 4 and 5, respectively, the evaluation of theoretical materials response due to changes in pavement temperature was considered. As described in Table 19, three different scenarios of temperature gradients in the pavement structure were analysed, to evaluate the influence of temperature variation on the BSM base behaviour.

The longitudinal and transversal horizontal strains on the bottom portion of the BSM base (305 mm) are presented in Figure 57, with Scenarios 1, 2 and 3. As expected, higher temperatures resulted in lower modulus for the asphalt surfacing and the BSM base, hence increasing material deformation, which is shown by the higher tensile strains. The difference between scenarios 1 and 2 in terms of longitudinal and transversal strains, was of 44% and 38%, respectively.

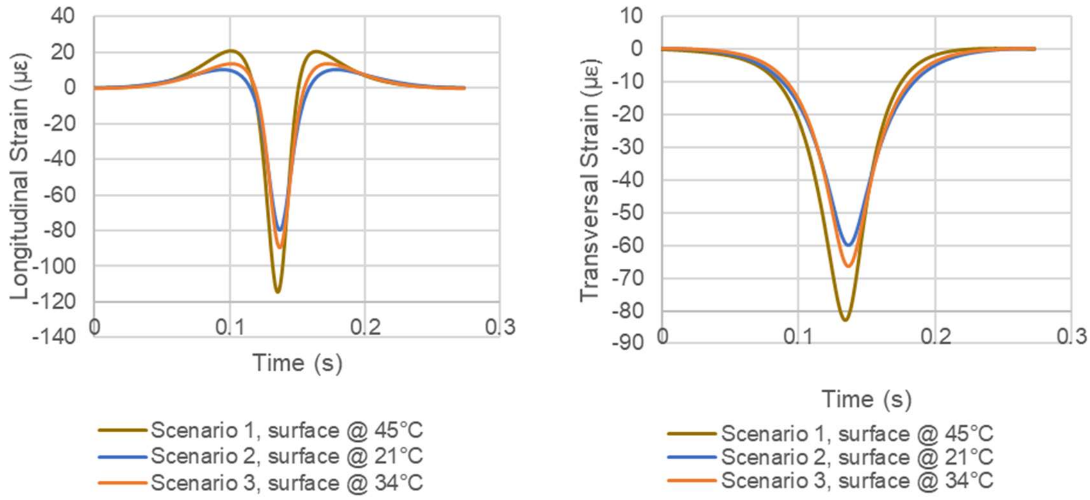


(a) (b)

**Figure 57. (a) Normal Longitudinal Strains and (b) Normal Transversal Strains at 305 mm depth for different pavement temperature conditions, calculated using VE analysis.**

Although scenarios 2 and 3 were evaluated considering a significant difference in surface temperature, the temperature gradient on the BSM base for scenario 3 had the last two 100 mm layers with 25°C and 23°C. Considering the analysis depth was of 305 mm, it explains why the calculated strains for scenario 3 were close to the ones calculated for scenario 2.

The calculated vertical strains during the passage of the load for scenarios 1 to 3, calculated at 55 mm depth (on the top portion of the BSM base, where compression is critical) are presented in Figure 58. As observed for the horizontal strains, the change in vertical strain from scenario 2 to scenario 1 was significant, with an increase of 173% on calculated strains.

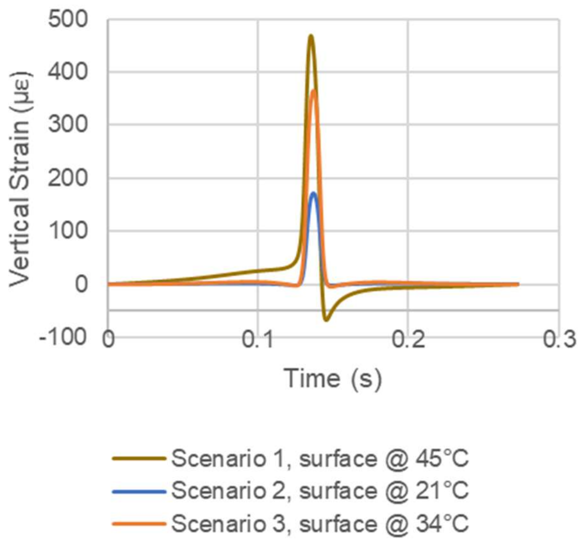


**Figure 58. Vertical strains at 55 mm depth for different pavement temperature conditions, calculated using VE analysis.**

Different than what was observed at 305 mm depth, the evaluation at 55 mm depth resulted in intermediate vertical strains for scenario 3, between scenarios 1 and 2, because of the difference in temperatures at this portion of the pavement for each analysis.

The sensitivity observed in the variation of the strains calculated due to the different temperature conditions is relevant to the design of pavement structures containing foamed asphalt stabilized materials, especially for those containing thick recycled layers such as FDR and CR projects.

The major and minor principal stresses calculated at 55 mm depth during the passage of the loading vehicle are presented in Figure 59. The effect of temperature can be observed in σ1 and σ3, with a decrease in stresses of 9% and 27% when comparing scenarios 1 and 2.

Due to the stiffening of the BSM material with the decrease in temperature, material deformation tends to decrease, and therefore the stress accumulation tends to increase. However, in the evaluated scenarios, much of the decrease in stresses observed between these scenarios can be attributed to the stiffening of the GGWC, which allows for a better dissipation of the acting vertical loads, resulting in lower stresses reaching the underlying layers.

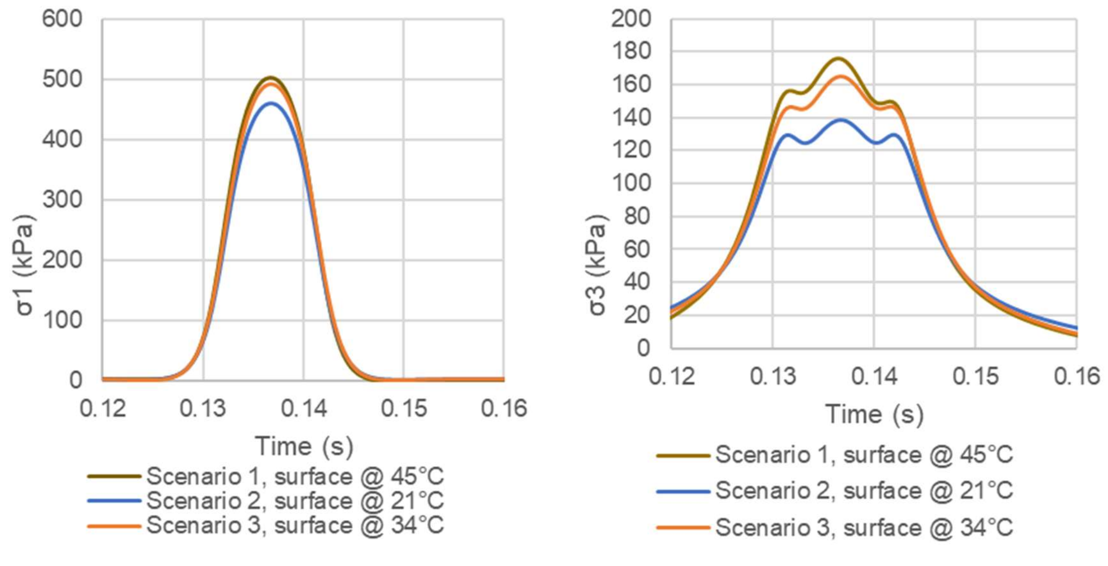


**Figure 59. (a) Major Principal Stress (σ1) and (b) Minor Principal Stress (σ3) Strains at 55 mm depth for different pavement temperature conditions, calculated using VE analysis.**

Although the stresses have decreased with the reduction of temperature, it is important to assess the combination of the calculated stresss, and the result in terms of the DSR, as presented in Figure 60. The proportion to which σ3 decreased was higher than that of σ1 due to the variation of temperature, then the resulting DSR was higher for scenario 2 than scenarios 3 and 1, in decreasing order.

The TG2 performance model presented in equation 6.1 defines that the predicted number of loadings the BSM can withstand is inversely affected by the DSR to the power of three, then the decrease in temperature, and hence the increase in DSR, exponentially reduces the material predicted performance. That prediction however goes against what was observed in the laboratory (Chapter 5), as higher temperatures dramatically reduced the BSM capacity to withstand repeated loads.

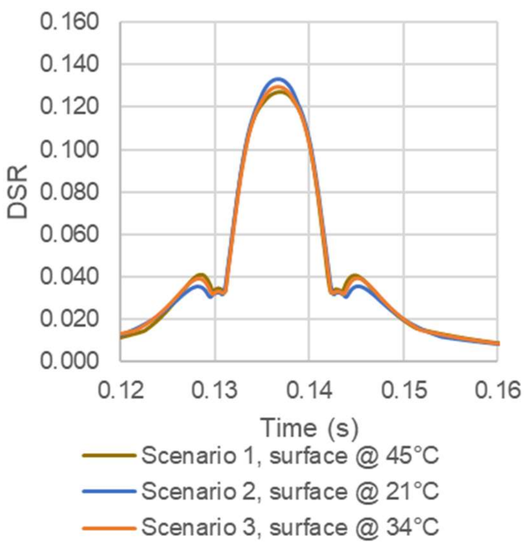


**Figure 60. Calculated values of DSR for three different pavement temperature conditions.**

It can be observed how the influence of temperature on BSM performance is not effectively represented using the DSR in the TG2 transfer function, as higher temperatures may result in lower deviator stresses and inaccurate predicted performance.

The parameter that better described the effect of temperature in the BSM was the vertical strain, that presented peak value at the upper third of the layer, while indicating that an increase in temperature would result in increase of compressive strains, and consequently material deformation.

### 6.3.3 Effect of BSM Constitutive Behaviour

The use of viscoelastic analysis for pavement design is still limited in many countries, with most structural analysis performed considering the linear elastic behaviour, due to its simplicity and overall accessibility. However, pavement response can vary significantly when viscoelastic analysis is applied. In this sense, pavement responses obtained from VE analysis with scenario 3 were compared to outputs from the LE and NLE analysis performed for scenarios 6, 7 and 8.

The comparison of longitudinal strain ($\varepsilon_L$) and transversal strain ($\varepsilon_T$) at the bottom portion of the BSM base, as well as the vertical strain ($\varepsilon_V$), σ1, σ3 and the calculated DSR for the top portion of the layer are shown in Table 20. Scenario 7 presented the higher magnitude values for strains and σ1. This scenario was calculated using LE analysis and a stratified BSM layer, with elastic modulus values based on the Dynamic Modulus test, to simulate the same effect of temperature analysed in scenario 3.

**Table 20. Mechanical responses from the BSM layer considering different calculation scenarios.**

| **Position of Analysis (depth in mm)** | | **305** | **305** | **55** | **55** | **55** | **55** |
|---|---|---|---|---|---|---|---|
| **Analysis** | **Scenario** | **$\varepsilon_L$ (μ)** | **$\varepsilon_T$ (μ)** | **$\varepsilon_V$ (μ)** | **$\sigma_1$ (kPa)** | **$\sigma_3$ (kPa)** | **DSR** |
| VE | 3 | -89.5 | -66.3 | 364.3 | 492.6 | 165.4 | 0.130 |
| NLE | 6 | -106.3 | -71.9 | 222.7 | 512.0 | 269.5 | 0.082 |
| LE | 7 | -111.9 | -74.3 | 432.4 | 515.2 | 221.5 | 0.107 |
| LE | 8 | -101.1 | -68.5 | 239.1 | 513.3 | 263.2 | 0.085 |

The results from scenario 8, which was characterized by a single 300 mm BSM layer with an average modulus based on the TRM test, resulted in lower values than scenario 7, and closer to the NLE analysis of scenario 6. The non-linear characterization of the BSM layer on the NLE analysis was based on the TRM test results and the simplified LE calculation paired with the more complex NLE approach. Since the TRM test was performed at around 25°C, the lower values of $\varepsilon_V$ calculated in scenarios 6 and 8 are influenced by the higher modulus obtained in the test, when compared to scenarios 3 and 7 where the dynamic modulus takes the higher temperatures into consideration.

It is interesting to note that although scenario 3 resulted in the lowest values for principal stresses, the subtraction of σ3 from σ1 resulted in the highest Deviator stress (σd) which ultimately leads to the higher DSR. Even when compared to scenario 7, that resulted in the highest values overall, the DSR from scenario 3 was still the highest, indicating that although the VE analysis may underestimate the pavement responses, it is the most severe when it comes to the DSR, and hence performance prediction.

In terms of stresses, σ3 is the parameter that resulted in the greatest differences between different constitutive behaviour consideration, which directly influenced the DSR values. Since the VE analysis is primarily considered for highly cohesive asphaltic materials, and dynamic modulus tests do not account for the stress dependency, the calculation of the stress state of a cohesive but still stress dependent material such as BSM may not be fully captured.

The estimated number of Equivalent Standard Axle Loadings (ESAL) that the pavement could withstand according to the TG2 transfer model, calculated for all evaluated scenarios is presented in Table 21, considering 95% reliability level (A), 100% of modified proctor compaction (Pmod), 75% of retained cohesion (RC) and 3% of allowable plastic strain (PS).

**Table 21. Estimated number of Equivalent Standard Axles until BSM layer accumulates 3% of permanent deformation.**

| Analysis | Scenario | $\sigma_1$ (kPa) | $\sigma_3$ (kPa) | DSR | N (ESAL) |
|---|---|---|---|---|---|
| VE | 1 | 501.6 | 175.9 | 0.127 | 7.17E+07 |
| VE | 2 | 460.1 | 138.9 | 0.133 | 6.87E+07 |
| VE | 3 | 492.6 | 165.4 | 0.130 | 7.04E+07 |
| VE | 4 | 497.2 | 168.8 | 0.130 | 7.05E+07 |
| VE | 5 | 490.1 | 163.7 | 0.130 | 7.04E+07 |
| NLE | 6 | 512.0 | 269.5 | 0.082 | 8.74E+07 |
| LE | 7 | 515.2 | 221.5 | 0.107 | 8.01E+07 |
| LE | 8 | 513.3 | 263.2 | 0.085 | 8.66E+07 |

As it can be noted, the scenario expected to accumulate 3% of plastic strain with the least amount of load repetitions is the one calculated using VE analysis for the lowest temperature gradient, which according to laboratory experience would be the one to perform best.

## 6.4 PARTIAL CONCLUSIONS

This chapter evaluated the mechanical responses under loading of pavements containing foamed stabilized asphalt layers using three different approaches in terms of the constitute behaviour of the BSM, comparing individual results, and indicating the benefits and shortcomings of each methodology.

The viscoelastic analysis was conducted in five different scenarios using the 3D-Move software, so that the effect of temperature and load frequency could be assessed. Although the frequency of loading resulted in a coherent variation of strains and stresses, this difference did not produce significant changes to the pavement structural design.

The effect of temperature on material responses was noticeable, resulting in increasing tensile horizontal strains and vertical compressive strains. The TG2 performance model (Eq. 6.1), however, was not effective of translating the decrease in performance identified in Chapter 5 due to temperature variation through the application of DSR values calculated based on the VE analysis. As stresses decreased with the increase in temperature, and hence the decrease in stiffness, the DSR also decreased, resulting in higher pavement life prediction, going against the laboratory performance test results.

One parameter that showed good sensitivity to the variation of temperature was the vertical compressive strain, and it could be further investigated so that the effect of temperature is accounted for in the structural design.

The non-linear elastic analysis (scenario 6) presented similar results to those from the linear elastic analysis of scenario 8, as both used the TRM test as input for the BSM layer modulus. Those results, however differed significantly from the viscoelastic analysis of scenario 3 and the linear elastic analysis of scenario 7, which both used inputs from the dynamic modulus tests to simulate the effect of temperature gradients on the pavement.

The calculated values of σ3 for the different constitutive behaviours considered resulted in significant differences, directly influencing the DSR and performance prediction of the pavement structures.

# 7 CONCLUSIONS AND RECOMMENDATIONS

To analyze the structural behaviour and the material performance of foamed asphalt stabilized mixtures, studies involving: literature review of the mixture and structural design procedures and methods used in different countries; the understanding of the material mechanical response to traffic load and temperature using laboratory tests, field measurements, and structural analysis. The next items provide a summary of the conclusions obtained during this dissertation and recommendations for further research.

## 7.1 MIXTURE AND STRUCTURAL DESIGN LITERATURE REVIEW

The comparison of different procedures for mixture and structural design of pavement containing foamed asphalt layers was conducted, highlighting the existance of distinctions among the methods adopted in different countries.

The review showed that there is neither consensus on the procedures for mixture design, nor for the approach used for the performance prediction and failure mechanism.

Design procedures such as the ones from Australia, United Kingdom and Italy tend to seek a higher cohesion material, which would result in a enhanced elastic response and life under the optics of fatigue analysis. In this sense, the mixtures produced in this method tend to have more fine particles, with higher contents of asphalt binder and cement yielding higher stiffness and strength.

The methodology implemented in South Africa and adopted in different countries, on the other hand, recommends the use of coarser gradations, and lesser binder content, named BSM in the literature. in the mixtures are less cohesive, with stress dependent mechanical behaviour, as a high-performance granular material. Permanent deformation is considered the primary mode of failure, and the mixture stiffness and strength must be limited to avoid increasing material cohesion to the point where it is no longer stress dependent.

In the light of the dispersion mechanism of foamed asphalt, the bitumen droplets adhere mainly to the fine aggregate particles to create a mortar binding the coarser aggregates. Therefore, the bitumen content effect is limited to the existing availability of fines, which, in practical terms, makes the mixture a non-continuously bound material regardless of the bitumen content added. In this sense, the mixture will always have a mineral phase, susceptible to moisture damage with less cohesion, creating structural weak points that prevent the material from having fatigue cracking.

Although there are specific performance models for either fatigue or permanent deformation, most countries do not have detailed procedures on how to consider foamed asphalt materials in pavement structural design.

The structural design approach is directly related to the mixture design, test protocols and curing procedures considered, as the resulting mixes can be different for each procedure.

## 7.2 FIELD EVALUATION OF FOAMED ASPHALT STRUCTURES

The evaluation of the mechanical behaviour in the field was conducted through the analysis of five different trial sections with foamed asphalt stabilized layers, providing adequate structural capacity to withstand a traffic of almost 100 million ESALs (high level roads).

Although no permanent deformation measurements were performed in the trial sections, FWD data indicated the good performance of the recycled foamed asphalt layers through increasing values of backcalculated resilient modulus.

The field study showed how the loss of moisture during the curing period affected material behaviour in the field, with the stiffness of the foamed asphalt layer slowly increasing with the reduction in moisture, while also standing smaller seasonal variations due to moisture ingress.

Three of the sections studied showed to be performing better, with one of them having already been monitored for 9 years, showing structural integrity, with stable deflections and increasing backcalculated resilient modulus from the FWD analysis.

The data obtained from the FWD tests in the field also presented good correlation to the resilient modulus obtained in the laboratory. The Triaxial Resilient Modulus showed the materials’ stress dependency, creating a non-linear elastic effect for the layer. It was also observed how the increase in both foamed asphalt binder and Portland cement addition tend to flatten the curve of resilient modulus as a function of confining stress.

The backcalculated moduli for the foamed asphalt base layer of the trial sections show how mixtures with different material composition but similar binder contents can have distinct stiffness, even if taken into the consideration the different stages of curing verified.

The Gap Graded overlay immediately after the laying of the stabilized layer (commonly used in Brazil) was proved efficient for the curing of the foamed asphalt base, with the curing achievement and stable performance. This fact is highlighted by the reduction in pavement deflection from close to 1,000 microns right after rehabilitation to around 300 microns after curing in two of the trial sections monitored. However, pavement deformability and how fast curing takes place influence directly on the surfacing service life, requiring specific consideration during the structural design of the pavement structure.

## 7.3 FOAMED ASPHALT IN SITU TEMPERATURE SENSITIVTY

The viscoelastic behaviour was observed through the assessment of the in situ temperature sensitivity of a foam stabilized section. It was observed a significant variation on the results of FWD surveys, on the the backcalculated resilient modulus and on the temperature sensitivity coefficients calculated, which was mostly associated to the material heterogeneity, layer density in different points of the trial sections, and moisture conditions. The curing of the trial section and consolidation of the pavement proved determinant to the reduction of the deflection variability and normalization of pavement responses. This indicates that changes in material density, the void distribution and moisture within those voids can produce significant impacts on material temperature sensitivity. It also may have significant effect on the material's thermal conductivity, as it changes how heat propagates through the medium. The evaluation of the effect of void distribution on BSMs should be investigated further, as it may be a controlled variable during mixture design phase to influence material sensitivity as desired.

The analysis of deflection bowls showed how temperature changes affected the contribution of the foamed asphalt base and asphalt wearing course for the overall deflection, especially close to the load application point. The impact of temperature variation was also verified on the backcalculed resilient modulus of the different layers during the day for both the Gap graded wearing course and the foamed asphalt base layer.

The temperature sensitivity of foamed asphalt pavements was considered through the correction procedure used by the Asphalt Institute for HMA, with good agreement to the results obtained from literature, verifying that foamed stabilized mixtures have less sensitivity to temperature variation than HMA.

The analysis allowed for the determination of a temperature sensitivity coefficient that can be applied as a parameter for backcalculated moduli correction using temperature data. The application of the calculated coefficient of $0.65 \times 10^{-4}$ presents a good estimate value for analysis, even though it should not precisely describe the behaviour of any foamed stabilized mixture.

## 7.4 LABORATORY EVALUATION OF THE EFFECT OF TEMPERATURE ON FOAMED ASPHALT MIXTURE

The effect of temperature on foamed asphalt materials was also evaluated in the laboratory, providing evidence on how temperature significantly affected the material performance, and should, therefore, be considered for pavement design. This effect is particularly important for pavements in warm climates, where surface and upper layers temperature can go beyond 30°C.

Different tests were performed to fully characterize the material behaviour, including triaxial resilient modulus, dynamic modulus and monotonic triaxial compressive tests. The material performance was also evaluated through permanent deformation tests in different temperatures and stress state conditions.

The TRM tests showed how dependent on the stress state the foamed asphalt material is, with considerable dependency of both the confining and deviatoric stresses. The results showed an increase of 50% on material stiffness depending on the stress state it was subject to, which is significant and should be accounted for during pavement design phase. The DM showed a clear correlation between stiffness and test temperature, with decreasing modulus as temperatures increased.

The permanent deformation tests showed great influence of both the stress state and the effect of temperature. Although different mixtures compositions may result in different degrees of influence, it was significant to observe how small variations in temperature produced exponential impact on the rate of permanent strain accumulation. For the studied mix, composed of 85% RAP, an increase in 5°C was sufficient to reduce by 10 times the number of load cycles to permanent deformation failure. That trend was confirmed for different test conditions, with varying temperatures and stress conditions.

The effect of the stress state on the rate of strain accumulation was also observed, with comparable magnitude of its impact to the observed effect of temperature, further highlighting the importance of temperature and non-linearity consideration during pavement design phase.

The reduction of the deviatoric stress was observed as a possibility to reduce the effect of temperature on the rate of permanent deformation accumulation. The reduction of the deviatoric stresses allow the mixture to rely more on the internal friction of its aggregates, diminishing its dependence to the binder contribution. It is therefore desirable to achieve lower stresses on the BSM layer, with another possible mitigation strategy being to seek for mixtures with higher friction angle, providing better responses at high temperatures, when asphalt binder structural contribution is diminished.

## 7.5 EFFECT OF TEMPERATURE ON MECHANISTIC-EMPIRICAL DESIGN

After the evaluation of the effect of temperature on material behaviour and performance in the field and in the laboratory, the structural behaviour of foamed asphalt pavements was evaluated with different constitutive behaviour models to determine how its service live performance is affected by different temperature conditions.

The viscoelastic analysis was conducted in five different scenarios using the 3D-Move software, assessing the effect of temperature and load frequency on pavement behaviour. It was verified that different frequencies of loading did not result in significant changes to the pavement responses and therefore to its structural design.

The effect of temperature on material responses was noticeable, considering temperatures from 20°C to 45°C, resulting in increasing tensile horizontal strains and vertical compressive strains. The effect on internal stresses, however, due to the reduction in material stiffness associated with the increase in temperature resulted in lower values of DSR, which in turn increases the predicted life under loading. These results demonstrated that the application of DSR values calculated based on the VE analysis may induce the designer into thinner structures than necessary, going against the laboratory performance results.

The vertical compressive strain, however, showed good sensitivity to the variation of temperature, and further investigation is recommended to properly account for the effect of temperature through its association to the DSR parameter.

A linear elastic analysis was performed using ELSYM5, as the most common approach for structural design. It presented good correlation to the viscoelastic analysis when layer modulus for the stratified base was defined based on DM test results. However, if the analysis was conducted considering the BSM base as a single layer, with the average modulus of the TRM test, the results of the analysis presented good correlation to the non-linear elastic analysis performed using the KENLAYER software.

Although the non-linear elastic analysis produced coherent results, it proved to be less practical to assess the effect of temperature, as multiple laboratory tests would be needed. In this sense, the use of viscoelastic analysis was considered as an adequate tool for comprehensive analysis of pavement structures subject to different temperature conditions, although the performance prediction should be carefully considered to avoid inadequate interpretation of the mechanic responses calculated.

## 7.6 RECOMMENDATIONS FOR FUTURE RESEARCH

As the new Brazilian asphalt pavement design method (MeDiNa) is being implemented by the National Department of Transportation Infrastructure (Departamento Nacional de Infraestrutura de Transportes, DNIT), a protocol to adequately characterize foamed asphalt mixture and predict material performance should be able to assess its stiffness, stress dependency and temperature sensitivity, while also considering the potential plastic strain accumulation for usual in-service pavement stress conditions. The association of monotonic triaxial and dynamic modulus tests of the stabilized mixture would be able to provide this information, giving information for pavement structural design and allowing for critical climate conditions to be considered for risk assessment.

In this sense, it is recommended that further research is carried on different compositions of foamed asphalt stabilized mixtures. New characterizations and permanent deformation tests are required to evaluate the effect of material composition and temperature sensitivity, as different RAP percentages, gradations, degree of binder oxidation, material density and other factors may be significant factors.

As much as DSR provides a proper parameter to describe the material stress state, and therefore predict pavement performance, it was not efficient describing the effect of temperature based on laboratory performance tests. In this sense, it is recommended that future research is conducted associating a deformation parameter, such as vertical strain, to the existing DSR model from TG2, allowing the effect of temperature to be accounted for in structural design.

It is also important that rehabilitated sections, where foamed asphalt solutions were applied, are continuously monitored so that pavement performance is verified, allowing for the success and failure experiences to serve as points of improvement for future works.

# 8 REFERENCES


AASHTO, American Association of State Highway and Transportation Officials. **Guide for Pavement Structures**. AASHTO, Washington, D.C., 1993.

ALABASTER, D., PATRICK, J., ARAMPAMOORTHY, H., GONZALEZ, A., **The design of stabilized pavements in New Zealand**, New Zealand Transport Agency research report 498, Wellington, New Zealand. 2013.

ANAS, Gruppo FS Italiane, **Capitolato Speciale di Appalto, Norme Techniche per l'esecuxione del contratto – Parte 2**, IT.PRL.05.21 - Rev. 3.0, Italy. 2021.

ANDRADE, L. R. VASCONCELOS, K. L., BERNUCCI, L. L. B. **Avaliação do comportamento estrutural de pavimentos por meio de adoção de parâmetros de bacia deflectométrica**. Associação Nacional de Pesquisa e Ensino em Transportes AN-PET, Rio de Janeiro, 2016

APEAGYEI, A.K., DIEFENDERFER, B.K., 2013. **Evaluation of Cold In-Place and Cold Central-Plant Recycling Methods Using Laboratory Testing of Field-Cored Specimens**. J. Mater. Civ. Eng. 25, 1712–1720. https://doi.org/10.1061/(ASCE)MT.1943-5533.0000717

ARRA. Asphalt Reclaiming and Recycling Association – **Basic Asphalt Recycling Manual**. 2001.

ASPHALT ACADEMY, **Interim Technical Guideline: The Design and Use of Foamed Bitumen Treated Materials**, TG2, Pretoria, South Africa, 2002.

ASPHALT ACADEMY, **Technical Guideline: Bitumen Stabilized Materials, A Guideline for Design and Construction of Bitumen Emulsion and Foamed Bitumen Stabilized Materials**. TG-2, Pretoria, South Africa, 2009.

AUCKLAND TRANSPORT, **Auckland Transport Code of Practice (ATCOP)**, Chapter 16, Road Pavements and Surfacings, New Zealand. 2013.

AUSTROADS, **Review of Structural Design Procedures for Foamed Bitumen Design**, Austroads Technical Report - AP-T188/11, Sidney, Australia, 2011.

AUSTROADS, **Design and Performance of Foamed Bitumen Stabilised Pavements**, Technical Report AP-T336-18, Sidney, Australia. 2018

AUSTROADS, **Guide to Pavement Technology Part 4D: Stabilised Materials**, Publication No. AGPT04D-19, Sidney, Australia. 2019

BALBO J.T. **Pavimentação Asfáltica: materiais projeto e restauração**. São Paulo: Oficina de Textos. 2007.

BANG, S., LEIN, W., COMES, B., NEHL, L., ANDERSON, J., KRAFT, P., DESTIGTER, M., LEIBROCK, C., ROBERTS, L., SEBAALY, P. and others, **Quality Base Material Produced Using Full Depth Reclamation on Existing Asphalt Pavement Structure--Task 4: Development of FDR Mix Design Guide**. FHWA Report No. FHWA-HIF-12-015, 2011.

BANG, S., KRAFT, P., LEIBROCK, C., LEIN, W., ROBERTS, L., SEBAALY, P., JOHNSTON, D., HUFT, D., **Quality Base Material Produced Using Full Depth Reclamation on Existing Asphalt Pavement Structure – Task 5: Development of Standardized Laboratory Testing Method - Final Report**. FHWA Report No. FHWA-HIF-12-032, 2012

BETTI, G., AIREY, G., JENKINS, K., MARRADI, A., TEBALDI, G., **Active filler's effect on in-situ performances of foam bitumen recycled mixtures**. Road Materials and Pavement Design. Published online on August 31st, 2016.

BIERMAN, C. R., **A design function for Bitumen Stabilised Material performance based on laboratory and field evaluation**. Master of Engineering Thesis, Stellenbosch University, South Africa, 2018.

BONFIM, V. **Fresagem de pavimentos asfálticos**. 3ª Edição. Ed Exceção. São Paulo 2011.

BREDENHANN, S. J., JENKINS, K. J., **Bitumen Stabilised Materials: Real Performance Models for BSM-foam Bases**. 11th Conference on Asphalt Pavements for Southern Africa. Sun City, South Africa 2015.

BROVELLI, C., CRISPINNO, M., **Bitumen emulsion and foam bitumen for cold recycled and bitumen stabilized materials: a comparison based on performances, costs and safety**. 8th International Conference on Managing Pavement Assets. Paper ICMPA068. Santiago, Chile. 2011.

BUCZYŃSKI, P., IWAŃSKI, M., **Complex modulus change within the linear viscoelastic region of the mineral-cement mixture with foamed bitumen**. Construction and Building Materials 172, 52–62. 2018.

C-SHRP, Canadian Strategic Highway Research Program, **Pavement Structural Design Practices Across Canada**. C-SHRP Technical Brief # 23, 2002.

CALTRANS, California Department of Transportation, **Full Depth Reclamation Using Foamed Asphalt**, Caltrans Division of Maintenance. June 2012

CALTRANS, California Department of Transportation, **Highway Design Manual**, Chapters 600-660, California, United States of America, 2017.

CAMPHER, L., **Shrinkage and Flexibility Behaviour of Bitumen Stabilised Materials**. Master of Engineering Thesis, Stellenbosch University, South Africa, 2015.

CASALI, M., GRILLI, A., **Capitolato Speciale D'appalto per la Manutenzione Straordinaria di Pavimentazioni Stradali, Università degli Studi della Repubblica di San Marino**, San Marino, 2021.

CARDONE, F., GRILLI, A., BOCCI, M., GRAZIANI, A., **Curing and temperature sensitivity of cement–bitumen treated materials**. International Journal of Pavement Engineering, Vol. 16, No. 10, 868–880. 2015.

CARTER, A., BUECHE, N., PERRATON, D., 2013. **Laboratory characterization of CIR and FDR materials**. Presented at the 3rd Specialty Conference on Material Engineering & Applied Mechanics, Montréal (Canada), p. 10.

CASTRO, L. N. **Reciclagem a frio “in situ” com espuma de asfalto**. Master of Engineering Degree Thesis, COPPE/UFRJ, Rio de Janeiro. 2003.

CITY OF EDMONTON, **Design standards and construction specifications**, Volume 2, Roadways. Edmonton, Alberta, Canada, 2015.

CHOMICZ-KOWALSKA, A., RAMIĄCZEK, P., **Comparative Evaluation and Modification of Laboratory Compaction Methods of Road Base Mixtures Manufactured in Low-emission CIR Technology with Foamed Bitumen and Bitumen Emulsion.** Procedia Engineering 172, 560–569. 2017.

COLLINGS, D., LINDSAY, R., SHUNMUGAM, R., **LTPP Exercise on a Foamed Bitumen Treated Base – Evaluation of almost 10 years of heavy trafficking on MR504 in KwaZulu-Natal**, Conference on Asphalt Pavements for South Africa (CAPSA04), Sun City, South Africa, 2004.

COLLINGS, D., JENKINS, K. J., **The Long-term behavior of Bitumen Stabilised Materials (BSMs)**, 10th Conference on Asphalt Pavements for South Africa (CAPSA11), KwaZulu-Natal, South Africa, 2011.

COLLINGS, D. JENKINS, K. J., SOUZA, E., **Utilising Recycled Material Stabilised With Bitumen to Rehabilitate a Major Highway Within Stringent Time Constraints**, 11th Conference on Asphalt Pavements for southern Africa (CAPSA), Sun City, South Africa, 2015.

COSTA, M.O. da, 2016. **Considerações sobre os métodos de dimensionamento estrutural de pavimentos com camadas recicladas a frio com espuma de asfalto**. (Mestrado em Engenharia de Transportes). Universidade de São Paulo, São Paulo. 2016.

CRISPINO, M., BROVELLI, C., **Bitumen emulsion and foam bitumen for cold recycled and bitumen stabilized materials: a comparison based on performances, costs and safety**. 8th International Conference on Managing Pavement Assets. Paper ICMPA068. Santiago, Chile. 2011.

CSRA Committee of State Road Authorities, **Technical Recommendations for Highways (TRH) 14, Guidelines for Road Construction Materials**, from the Committee of State Road Authorities. Pretoria, South Africa, 1985.

DAL BEN, M., **Resilient Response and Performance of Bitumen Stabilized Materials with Foam incorporating Reclaimed Asphalt**. PhD Dissertation. Stellenbosch University, South Africa, 2014.

DER/PR, Departamento de Estradas de Rodagem do estado do Paraná, Pavimentação: **Reciclagem de Pavimento a frio “in-situ” com Espuma de Asfalto**, Especificação de Serviço ES-P 32/05, Curitiba, Brazil, 2005.

DER/SP, Departamento de Estradas de Rodagem do estado de São Paulo, **Reciclagem in situ a frio com espuma de asfalto**, Especificação Técnica ET-DE-P00/033, São Paulo, Brazil, 2006.

DER/SP, Departamento de Estradas de Rodagem do estado de São Paulo, **Projeto de Pavimentação**, Instrução de Projeto IP-DE-P00/001, São Paulo, Brazil, 2006.

DIAS, C. R. C., NÚÑEZ, W. P., BRITO, L. A. T., JOHNSTON, M. G., CERATTI, J. A. P., WAGNER, L. L., FEDRIGO W., **Bitumen stabilized materials as pavement overlay: Laboratory and field study**, Construction and Building Materials, Volume 369, 130562, ISSN 0950-0618, 2023.

DÍAZ-SÁNCHEZ, M.A., TIMM, D.H., DIEFENDERFER, B.K., **Structural Coefficients of Cold Central-Plant Recycled Asphalt Mixtures**. J. Transp. Eng. Part Syst. 143, 04017019. 2017.

DIEFENDERFER, B.K., APEAGYEI, A.K., 2011. **Time-Dependent Structural Response of Full-Depth Reclamation**. Transp. Res. Rec. J. Transp. Res. Board 2253, 3–9. 2011.

DIEFENDERFER, B., LINK, S., **Temperature and confinement effects on the stiffness of a Cold Central-Plant Recycled mixture**, in: Asphalt Pavements. CRC Press, pp. 1641–1650. 2014.

DIEFENDERFER, B.K., BOWERS, B.F., SCHWARTZ, C.W., FARZANEH, A., ZHANG, Z., **Dynamic Modulus of Recycled Pavement Mixtures**. Transportation Research Record 2575, 19–26. 2016.

DNIT, Departamento Nacional de Infra-Estrutura de Transportes, IS-247, **Estudos para Elaboração de Projetos de Implantação usando o Método de Dimensionamento Nacional – MeDiNa**, Nota Informativa, 2021.

DNIT, Departamento Nacional de Infra-Estrutura de Transportes, **Manual de Pavimentação**, IPR-719, 3rd edition, Rio de Janeiro, Brazil. 2006.

DNIT, Departamento Nacional de Infra-Estrutura de Transportes, **Reciclagem de pavimento "in situ" com espuma de asfalto** - Especificação de Serviço ES 166/2013, Instituto de Pesquisas Rodoviárias, Rio de Janeiro, 2014.

DNIT, Departamento Nacional de Infra-Estrutura de Transportes, **Reciclagem de pavimento em usina com espuma de asfalto** - Especificação de Serviço ES 169/2014, Instituto de Pesquisas Rodoviárias, Rio de Janeiro, 2014.

EBELS, L. J., **Characterization of Material Properties and behavior of Cold Bituminous Mixtures for Road Pavements**. PhD Dissertation. Stellenbosch University, South Africa, 2008.

EVANGELISTA, F. J., PARENTE, E. J., SOARES, J. B., **Viscoelastic and Elastic Structural Analysis of Flexible Pavements**. Proceedings of the XXVI Ibero-Latin American Conference on Computational Methods in Engineering CILAMCE 2005 – ABMEC & AMC, Guarapari, Espírito Santo, Brazil, 19th – 21st October 2005.

FERNANDO, E. G., LIU, W. **Users Guide for the Modulus Temperature Correction Program (MTCP)**. Report No. FHWA-TX-01;1863-2. Federal Highway Administration. 2001.

FEISTHAUER, B., LACROIX, D., CARTER, A., PERRATON, D., **Simulation and influence of Early-Life traffic curing for cold in-place recycling and full-depth reclamation materials**, 3rd Specialty Conference on Material Engineering & Applied Mechanics, Montréal, Québec May 29 to June 1, 2013

FU, P., HARVEY, J. T., **Temperature sensitivity of foamed asphalt mix stiffness: field and lab study**. International Journal of Pavement Engineering, Vol. 8, No. 2, 137-145, 2007.

FU, P., JONES, D., HARVEY, J. T., **The effects of asphalt binder and granular material characteristics on foamed asphalt mix strength**, Construction and Building Materials, Volume 25, Issue 2, February 2011, 1093-1101, 2011.

FU, P., JONES, D., HARVEY, J.T., BUKHARI, S.A.,. **Laboratory Test Methods for Foamed Asphalt Mix Resilient Modulus**, Volume 10, 27. 2009a

FU, P., STEVEN, B.D., JONES, D., HARVEY, J.T., **Relating Laboratory Foamed Asphalt Mix Resilient Modulus Tests to Field Measurements**. Road Materials and Pavement Design Volume 10, 31. 2009b

FU, P., HARVEY, J. T., JONES, D., CHAO, Y. **Understanding internal structure characteristics of foamed asphalt mixes with Fracture Face Image Analyses**. Transportation Research Record: Journal of the Transportation Research Board, No 2057. Transportation Research Board of National Academies. Washington. D.C., 2008.

GODENZONI, C., GRAZIANI, A., BOCCI, E., BOCCI, M., **The evolution of the mechanical behaviour of cold recycled mixtures stabilised with cement and bitumen: field and laboratory study**, Road Materials and Pavement Design, 19:4, 856-877, 2018.

GONZALES, A., JONES, A., Austroads, **Review of structural design procedures for foamed bitumen pavements**. Austroads Ltd., Sydney, Australia, 2011

GOUVEIA, B.C.S., PRETI, F., ROMEO, E., JENKINS, K., TEBALDI, G., **Use of calcium oxide as active filler for bituminous stabilised materials**. Road Materials and Pavement Design. 22, 2131–2144. 2021

GOUVEIA, B.C.S., PRETI, F., CATTANI, L., BOZZOLI, F., ROBERTO, A., ROMEO, E., TEBALDI, G., **Numerical and Experimental Analysis of the**

**Raise-Temperature Effect of Quicklime in Cold Recycled Mixtures**. Journal of Materials in Civil Engineering. 34, 04022283. 2022.

GRILLI, A., MIGNINI, C., GRAZIANI, A., 2019. **Field behaviour of cold-recycled asphalt mixtures for binder courses**, International Conference on Sustainable Materials, Systems and Structures, Rovinj, Croatia 2019.

GRAZIANI, A.; IAFELICE, C.; RASCHIA, S.; PERRATON, D.; CARTER, A. **A procedure for characterizing the curing process of cold recycled bitumen emulsion mixtures**. Construction and Building Materials, v. 173, p. 754–762, 2018a.

GRAZIANI, A., MIGNINI, C., BOCCI, E., BOCCI, M., **Complex Modulus of Cold Recycled Mixtures: measurement and modelling**. International Society for Asphalt Pavements Conference, Fortaleza, Brazil, 2018b

GRILLI, A.; GRAZIANI, A.; BOCCI, M. **Compactability and thermal sensitivity of cement-bitumen-treated materials**. Road Materials and Pavement Design, v. 13, n. 4, p. 599–617, 2012.

GU, F., MA, W., WEST, R.C., TAYLOR, A.J., ZHANG, Y., **Structural performance and sustainability assessment of cold central-plant and in-place recycled asphalt pavements: A case study**. Journal of Cleaner Production 208, 1513–1523. 2019.

GUATIMOSIM, F. V., VASCONCELOS, K. L., BERNUCCI, L. L. B., JENKINS, K. J., **Laboratory and field evaluation of cold recycling mixture with foamed asphalt**, Road Materials and Pavement Design, 19:2, 385-399, 2018.

GUATIMOSIM, F. V., **Mechanical behaviour and structural performance of recycled foamed bitumen stabilized materials**. Master Thesis, Escola Politécnica, Universidade de São Paulo, São Paulo. 2015.

GUTIERREZ. L. M. K., GUATIMOSIM, F. V., VASCONCELOS, K., DE FARIA, V. S., **Construcción de un trecho experimental con fresado asfáltico reciclado con espuma de asfalto**, In: XX CILA - Congreso Ibero Latinoamericanodel Asfalto, 2019, Guadalajara. XX CILA, 2019.

HARICHANDRAN, R. S., RAMON, C. M., BALADI, G. Y., **Michback User's Manual (Version 1.0 for DOS)**, Department of Civil and Environmental Engineering Michigan State University, March 2000.

HE, G., WONG, W., **Laboratory study on permanent deformation of foamed asphalt mix incorporating reclaimed asphalt pavement materials**. Construction and Building Materials 21, 1809–1819. 2007

HE, G.-P., WONG, W.-G., 2008. **Effects of moisture on strength and permanent deformation of foamed asphalt mix incorporating RAP materials**. Construction and Building Materials 22, 30–40. https://doi.org/10.1016/j.conbuildmat.2006.06.033

HUANG, Y.H., **Pavement Analysis and Design**. 2nd Edn., Prentice Hall, Englewood Cliffs, New Jersey, USA., ISBN-10:0131424734, pp: 762. 2003.

HUAN, Y., SIRIPUN, K., JITSANGIAM, P., NIKRAZ, H., **A preliminary study on foamed bitumen stabilization for Western Australian pavements**. Scientific Research and Essays Vol. 5 (23), Perth, Australia. 2010.

IBGE, Instituto Brasileiro de Geografia e Estatística, **IBGE divulga as Estimativas de População dos municípios para 2018**, Agencia de Notícias, found online on March 10th 2019, at (https://agenciadenoticias.ibge.gov.br/agencia-sala-de-imprensa/2013-agencia-de-noticias/releases/22374-ibge-divulga-as-estimativas-de-populacao-dos-municipios-para-2018).

JENKINS, K., J., **Mix Design Considerations for cold and half-warm bituminous mixes with emphasis on foamed bitumen**. PhD Dissertation, Stellenbosch University. South Africa, 2000.

JENKINS, K. J., **Cracking Behaviour of Bitumen Stabilised Materials (BSMs): Is there such a thing?** 7th RILEM International Conference on Cracking in Pavements.Volume 4 of the series RILEM Book series pp1007-1015. 2012.

JENKINS, K. J., KELFKENS, R. W. C., **Technical Memorandum - Updating Bituminous Stabilized Materials Guidelines: Mix Design Report**, Phase II, Task 12: Laboratory Compaction, South Africa, 2008.

JONES, D., FU, P., HARVEY, J., MINE T., **Full-Depth Recycling with Foamed Asphalt in California: Guidelines for Project Selection, Design, and Construction**. Institute of Transportation Studies, University of California, Davis, Research Report UCD-ITS-RR-09-50. 2009.

JONES, D., WU, R., LOUW, S., **Comparison of Full Depth Reclamation with Foamed Asphalt and Full Depth Reclamation with No Stabilizer in an Accelerated Loading Test**, 93rd Transportation Research Board Annual Meeting, Paper 14-15144, Washington, 2014.

JOOSTE, F., LONG, F., **A Knowledge Based Structural Design Method for Pavements Incorporating Bituminous Stabilized Materials**. Technical Memorandum. Gauteng Department of Public Transport, Roads and Works and South Africa Bitumen Association (SABITA), Pinelands, South Africa. 2007.

KAVUSSI, A., MODARRES, A., 2010. **Laboratory fatigue models for recycled mixes with bitumen emulsion and cement**. Construction and Building Materials 24, 1920–1927.

KHOSRAVIFAR, S., SCHWARTZ, C. W., GOULIAS, D. G., **Mechanistic structural properties of foamed asphalt stabilised base materials**. International Journal of Pavement Engineering. Vol. 16, No. 1, 27–38. 2015.

Kuchiishi, A.K., **Mechanical behavior of cold recycled asphalt mixtures** (Masters Thesis). Universidade de São Paulo. 2019.

KUCHIISHI A. K., VASCONCELOS, K., BERNUCCI, L. L. B., **Influence of Viscoelastic properties of cold recycled asphalt mixtures on pavement response**. International Society for Asphalt Pavements Conference, Fortaleza, Ceará, Brazil. 2018a

KUCHIISHI A. K., ANTÃO, C. C. S. A., VASCONCELOS, K., PIRES, J., ARAÚJO, O. M. O., BERNUCCI, L. L. B., LOPES, R. T., **Investigation of the Matric**

**suction role on the curing mechanism of foamed asphalt stabilized mixtures**. Submitted for presentation and publication on the 8th European Asphalt Technology Association, Granada, Spain. 2018b

KUCHIISHI, A.K., VASCONCELOS, K., BARIANI BERNUCCI, L.L., **Effect of mixture composition on the mechanical behaviour of cold recycled asphalt mixtures**. International Journal of Pavement Engineering 22, 984–994. 2021.

KUNA, K.K., 2015. **Mix Design Considerations and Performance Characteristics of Foamed Bitumen Mixtures (FBMs)** (Ph.D. Thesis). University of Nottingham.

LEANDRI, P., LOSA, M., DI NATALE, A., **Field validation of recycled cold mixes viscoelastic properties**. Construction and Building Materials 75, 275–282. 2015.

LEEK, C., **In-situ Foamed Bitumen Stabilisation: The City Of Canning Experience**, ARRB Transport Research Ltd Conference, 20th, Melbourne, Victoria, Australia 2001

LEEK, C., **Review of the performance of in situ foamed bitumen stabilised pavements in the City of Canning**, 5thAustralian Road Engineering and Maintenance Conference, Melbourne, Victoria, Australia, 2010.

LEWIS, A., J., N., COLLINGS, D. C., **Cold in place recycling: a relevant process for road rehabilitation and upgrading,** 7th Conference on Asphalt Pavements for South Africa, CAPSA’99, Victoria Falls, Zimbabwe, August 29, 1999.

LING, M., LUO, X., GU, F., LYTTON, R.L., **Time-temperature-aging-depth shift functions for dynamic modulus master curves of asphalt mixtures**. Construction and Building Materials 157, 943–951. 2017

LIU, P., XING, Q., DONG, Y., WANG, D., OESER, M., YUAN, S., **Application of Finite Layer Method in Pavement Structural Analysis**, Applied Sciences. 2017; 7(6):611. 2017.

LLEWELLYN, G.B., 2015. **Flexibility Behaviour of Bitumen Stabilised Materials** (Masters Thesis). University of Stellenbosch.

LOIZOS AND V. PAPAVASILIOU, **In situ characterization of pavement materials stabilized with foamed asphalt and cement,** in Proceedings of International Conference on Advanced Characterization of Pavement and Soil Engineering Materials, pp. 875–882, Athens, Greece, June 2007

LOIZOS, A., PAPAVASILIOU, V., PLATI, C., **Investigating In-situ Stress-Dependent Behaviour of Foamed Asphalt Treated Pavement Materials**, Road Materials and Pavements Design, Volume 13, Issue 4, 678-690, 2012.

LYNCH, A. G., **Trends in Back-calculated Stiffness of in-situ Recycled and Stabilized Road Pavement Materials**. Master of Engineering Degree Thesis. Stellenbosch University, South Africa, 2013.

MACCARRONE, S., HOLLERAN, G, LEONARD, D.J. **Bitumen Stabilisation - A New Approach to Recycling Pavements**. In: AAPA Members Conference, 1993.

MACCARRONE, S., HOLLERAN, G., LEONARD. D.J. HEY, S. **Pavement Recycling using Foamed Bitumen**. In: 17th ARRB Conference, Proceedings held in Gold Coast, Queensland, 15-19 August 1994, Volume 17, Part 3, pp 349-365. 1994

MARTINEZ, R. M., BONFIM, V., PAIVA, C. E. L de.,**Retroanalisis para Estimar los Módulos de las capas de un Pavimento Reciclado con Espuma de Asfalto**, 01/2013, XVII Congreso Ibero-Latinoamenricano del Asfalto, Vol. único, pp.205-215, Guatemala, Guatemala, 2013.

MERO, Materials Engineering Research Office, **Pavement Design and Rehabilitation Manual**, Second Edition, Ontario Ministry of Transportation, Ontario, Canada, 2013.

MERRIL, D., NUNN, M., CARSWELL, I., **A guide to the use and specification of cold recycled materials for the maintenance of road pavements**. TRL Report TRL 611, 2014.

MILTON, L. J., EARLAND, M., **Design guide and specification for structural maintenance of highway pavements by cold in-situ recycling**, Prepared for CSS, Colas Limited and the Pavement Engineering Group, Highways Agency, TRL, 1999.

MOLOTO, P.K.,. **Accelerated curing protocol for bitumen stabilized materials** (Masters Thesis). University of Stellenbosch. South Africa. 2010.

MONDAL, P.G., GOTTUMUKKALA, B., KUNA, K.K., **Permanent Deformation Behavior of Foamed Bitumen Stabilized Mixes**. J. Mater. Civ. Eng. 33, (ASCE)MT.1943-5533.0003754, 04021146. 2021

MULUSA, W. K., **Development of a Simple Triaxial Test for characterising bitumen stabilized materials**, Master of Engineering Degree Thesis. Stellenbosch University, South Africa, 2009.

NIVEDYA, M., VEERARAGAVAN, A., RAVINDRAN, P. AND KRISHNAN, J. **Investigation on the Influence of Air Voids and Active Filler on the Mechanical Response of Bitumen Stabilized Material**. Journal of Materials in Civil Engineering, 30(3), p.04017293. 2018.

NUNN, M., THOM, N., **Foamix: Pilot scale trials and design considerations**, Viridis Report VR1, Transportation Research Laboratory, United Kingdom, 2002.

OPSS, Ontario Provincial Standard Specifications, **Construction specification for full depth reclamation with expanded asphalt stabilization**, OPSS.PROV 331, Ontario, Canada, 2015

OPSS, Ontario Provincial Standard Specifications, **Construction specification for Cold In-Situ Recycling with expanded asphalt stabilization**, OPSS.PROV 335, Ontario, Canada, 2015

PLATI, C., LOIZOS, A., PAPAVASILIOU, V., KALTSOUNIS, A., **Investigating In Situ Properties of Recycled Asphalt Pavement with Foamed Asphalt as Base Stabilizer**. Advances in Civil Engineering 2010, 1–10. 2010

PMSP, Prefeitura do Município de São Paulo, **Base de Material Fresado com Espuma de Asfalto**, PMSP ETS-02/2009.

PRETI, F., GOUVEIA, B.C.S., ROMEO, E., TEBALDI, G., DAVE, E.V., SIAS, J.E., **Elasto-Plastic Model for Bitumen Stabilized Materials Using Triaxial Testing and Finite Element Modelling**, Proceedings of the RILEM International Symposium on Bituminous Materials, RILEM Book series. Springer International Publishing, Cham, pp. 687–693. 2022.

RAMANUJAM, J. M. ,JONES, J. D., **Characterization of foamed-bitumen stabilization,** International Journal of Pavement Engineering, 8:2, 111-122, 2007.

RASCHIA, S., MOGHADDAM, T.B., PERRATON, D., BAAJ, H., CARTER, A., GRAZIANI, A., **Effect of RAP Source on Compactability and Behavior of Cold-Recycled Mixtures in the Small Strain Domain**. J. Mater. Civ. Eng. 33, 04021030. 2021

RASCHIA, S., PERRATON, D., CARTER, A., GRAZIANI, A., VAILLANCOURT, M., 2018. **Effect of reclaimed asphalt gradation on bitumen emulsion mixtures**. Presented at the 2018 International Society for Asphalt Pavements (ISAP), Fortaleza (Brasil), p. 8.

ROMANOSCHI, S. A., HEITZMAN, M., GISI, A., **Foamed Asphalt Stabilized Reclaimed Asphalt Pavement: A Promising Technology for Mid-Western Roads**, Proceedings of the 2003 Mid-Continent Transportation Research Symposium, Ames, Iowa, August 2003

SABITA, Southern African Bitumen Association, **TECHNICAL GUIDELINE 2: BITUMEN STABILISED MATERIALS,** 221 p. Pretoria, South Africa, 2020

SABOURI, M., DAVE, E., **Cold Reclamation and Recycling Techniques to Achieve Perpetual Pavements,** (No. Task 2 REPORT). Minnesota Department of Transportation. 2023

SANRAL. South African National Roads Agency Ltd. **South African Pavement Engineering Manual**. Second Edition, 2014.

SALEH, M. AND HERRINGTON, P., **Foamed Bitumen Stabilisation for New Zealand roads**, Transfund New Zealand Research Report No. 250, p. 86, 2003

SILVA, V.D. da,. **Avaliação da deformação permanente de misturas estabilizadas com asfalto**. (Mestrado em Engenharia de Transportes). Universidade de São Paulo, São Paulo. 2019

SCHWARTZ, C., W., KHOSRAVIFAR, S., **Research Report: Design and Evaluation of Foamed Asphalt Base Materials**. Project Number SP909B4E. Maryland. 2013.

STROUP-GARDINER; M., **NCHRP Synthesis 421**, Recycling and Reclamation of Asphalt Pavements Using In-Place Methods – A Synthesis of Highway Practice. Washington D.C., 2011.

TEBALDI, G., DAVE, E., CANNONE FALCHETTO, A., HUGENER, M., PERRATON, D., GRILLI, A., LO PRESTI, D., PASETTO, M., LOIZOS, A., JENKINS, K., APEAGYEI, A., GRENFELL, J., BOCCI, M.,. **Recommendation of RILEM TC237-SIB on cohesion test of recycled asphalt**. Materials and Structures, 51, 117. 2018

THE HIGHWAYS AGENCY, Transport Scotland, Welsh Governement Llywodraeth Cynulliad Cymru, The Department for Regional Development of Northern Ireland,. **Manual of Contract Documents for Highway Works** (MCHW) - Volume 1. 2021

THE HIGHWAYS AGENCY, Transport Scotland, Welsh Governement Llywodraeth Cynulliad Cymru, The Department for Regional Development of Northern Ireland, **Design Manual for Roads and Bridges** HD 24/06 Volume 7, Section 2, Part 3. 2006.

THEYSE, H.L., BEER, M.D., RUST, F.C., **Overview of South African Mechanistic Pavement Design Method**. TRANSPORTATION RESEARCH RECORD 12. 1996.

THEYSE, H., L., MUTHEN, M., **Pavement analysis and design software (PADS) based on mechanistic-empirical design method**. South African Transport Conference 'Action in Transport for the New Millenium'. Pretoria. 2000.

THOMPSON, M., R., GARCIA, L., CARPENTER, S., H., **Cold In-place Recycling and Full-Depth Recycling with asphalt products (CIR &FDRwAP)** Research Report ICT-09-036.Illinois Center for Transportation. 2009.

TMR, Transportation and Main Roads, **Pavement Rehabilitation Manual**, Brisbane, Australia, 2012.

TWAGIRA, E. M., **Influence of Durability Properties on Performance of Bitumen Stabilized Materials**. PhD Dissertation, Stellenbosch University. South Africa, 2010.

VIJAYARUBAN, V.N., **Development of Pavement Performance Evaluation Subroutines for 3D-Move Analysis Software**, Master thesis, University of Nevada, Reno, NV. 2011

YAN, J., LENG, Z., LI, F., ZHU, H. BAO, S. **Early-age strength and long-term performance of asphalt emulsion cold recycled mixes with various cement contents**. Construction and Building Materials, 137, pp.153-159. 2017.

WEST. R., C., **Reclaimed Asphalt Pavement management: Best Practices**. National Center for Asphalt Technology, Auburn, AL. 2010

WIRTGEN GmbH, 2012. Wirtgen Cold Recycling Manual.

ZAUMANIS, M., LOETSCHER, D., MAZOR, S., STÖCKLI, F., POULIKAKOS, L., 2021. **Impact of milling machine parameters on the properties of reclaimed asphalt pavement**. Construction and Building Materials 307, 125114. https://doi.org/10.1016/j.conbuildmat.2021.125114

ZBICIAK, A., MICHALCZYK, R., BRZEZIŃSKI, K.,. **Time–temperature superposition for viscoelastic materials with application to asphalt–aggregate mixes**. Int. J. Environ. Sci. Technol. 16, 5059–5064. 2019